Ministry of Higher Education and Scientific Research
Hassiba Benbouali Unversity of Chlef
Faculty of Civil Engineering and Architecture
Department of Hydraulic

THESIS

Presented for obtaining the degree of

DOCTORATE OF SCIENCES

By

NADIA BADNI

Title:

SIMULATION OF THE DRIP IRRIGATION MANAGEMENT PRRACTICES AND THEIR EFFECTS ON THE SOIL PROPERTIES BY USING « HYDRUS » MODEL

Defended on...../...../....., in front of the board of examiners composed of:

EZZIANE Karim	Professor	UHB Chlef	Chairman
RIABI Mohamed	MCA	UHB Chlef	Examiner
REMINI Boualem	Professor	USD Blida1	Examiner
BOUDERBALA Abdelakder	MCA	UDB Khemis Miliana	Examiner
HAMOUDI Saaed	Professor	UHB Chlef	Supervisor
El-NESR Mohammad	Assistant Professor	U. King Saud. Saud Arabia	Assistant -Supervisor
ELMEDDAHI Yamina	MCA	UHB Chlef	Invited

DEDICATION

In the Name of Allah, the Most Merciful, the Most Compassionate

This work is dedicated: to my parents and my husband; to all the members of my family, particularly to my children Afif and Iyad, my brothers and sisters, I thank you all for your endless help and encouragement along my studies.

Special thanks to Dr Mohammed El Nesr who used their knowledge for the good of science, for the wisest man I have ever known in my life. I proudly thank you for your support and guidance. I tell you that your efforts with me were not spent in vain ...

Finally, I wish to express my deep thanks to my friends and colleagues for their fun, sympathy and kindness.

Nadia

A CKNOWLEDGEMENTS

First of all, praise is to Allah for giving me health, strength and spirit to overcome all the difficulties and obstacles of life and to reach the current position.

This work would not have been accomplished without the contribution and endless ssupport of many people, for whom I am sincerely grateful. The greatest debt of gratitude is owed to my supervisor, Dr. Saaed HAMOUDI, who has never hesitated, in all circumstances, to correct my mistakes and to provide me with her invaluable feedback, wise advice and smart guidance throughout this research. I am immensely grateful to my Assistant -supervisor Dr Mohammed El Nesr ,Assistant Professor of Water and Irrigation Systems Engineering, Department of Agricultural Engineering, College of Food and Agricultural Science, King Saud University Saudi Arabia, for his generous encouragement, help ful Ideas, and for his patience in thorough review of the scientific article and present manuscript, for his help in providing the HYDRUS 2D software which was used for the current model validation without which this research would have never been done. Also, I would like to thank all my colleagues at Center of scientific and technical research in physicochemical analyzes (CRAPC), especially Miss. BOUDJEMAA Amel, and many others for helping me and pushing me to success. Also, Special thanks to the private farm Feddel for

their cooperation, and attention during the field experiments. Last but not least I thank Dr YAmina El Medahi who kindly helped me to carry out my research by accepting to revise my scientific article, and all the examiner who kindly accepted to read this dissertation and provide me with valuable comments and remarks.

ملخص

يعد تحسين البنية الرطبة للمنطقة الجذرية تحت الري بالتنقيط احد اهداف باحثي و مصممي الري وهذا لما يتيحه من زيادة في الانتاج و مردودية المحاصيل الزراعية.

أثناء الري بالتنقيط، يرتفع محتوى الرطوبة في المنطقة الجذرية، مما يقلل من قوى الشد الشعري بين المياه وحبيبات التربة، بحيث يسهل علي النبات حصوله علي احتياجاته المائية. و من هنا تعتبر المعلومات المتعلقة بالتطور الزمني لحجم التربة الرطبة مفيدة في تحديد المسافة المثلى بين المنقطات ومدة الري بالنسبة لحجم التربة التي تحوي علي الجذور الفعالة للمحاصيل وهذا ما يعتبر ذو اهمية بالغة لتحقيق الامكانيات الكاملة لادارة تقنية الري بالتنقيط.

المعادلة التي تصف تنقل المياه في التربة أو الأوساط المسامية بشروط محددة هي معادلة ريتشارد. في هذا البحث، أجريت عمليات محاكاة رقمية باستخدام برنامج هيدروس 2D/3D، هذا النموذج يفسر رقميا معادلة ريتشارد لدراسة تأثير مختلف إدارات الري واستراتيجيات التصميم على ديناميكية مياه التربة، يستخدم هيدروس 2D/3D- طريقة العناصر المتناهية (حيث يتم تقسيم منطقة التدفق إلى شبكة مثلثية الأبعاد (2D). تؤخذ رؤوس هذه العناصر على أنها النقاط العقدية. علاوة علي ذلك، تم استخدم برنامج هيدروس لمحاكاة تأثير تطبيق 8 معدلات تصريف مختلفة (1،2،3.....7،8 ل/سا) و لمسافات بين المنقطات 20،30،50 سم وفق ترددات ري تتراوح بين يوم إلي سبعة أيام تحت الظروف المناخية لمنطقة الدراسة من أجل التنبؤ بنمط ترطيب المنطقة الجذرية لنبات الطماطم. وبالإضافة إلى ذلك، لاثبات فعالية البرنامج واختيار أفضل استراتيجية لإدارة الري بالتنقيط، قمنا بمقارنة محتوى المياه الذي تنبأ به من محاكات برنامج هيدروس مع تلك التي تم قياسها حقليا.

أجريت الدراسة التجريبية في مزرعة خاصة في الشلف ، يقع الحقل جغرافيًا على إحداثيات 36° 13' 60" شمالا و 1° 27' 20" شرقا حيث قيست رطوبة التربة في الميدان باستخدام TDR كما اخذت عدة قراءات محصولية ورطوبية علي أعماق مختلفة في منطقة الجذور علي مدار موسم زراعة محصول الطماطم

كان الهدف الأول هو التحقق من توافق هيدروس 2D / 3D- لمنقطين يعملان في آن واحد لمقاد تربة رملية مزيجية . تم استخدام جذر-متوسط-مربع-الخطأ للتحليل الإحصائي لتقييم أداء النموذج هيدروس 2D/3D- ولاختبار دقة الملاءمة بين قيم محتوى الماء الحجمي للتربة التي تمت محاكاتها و القيم التجريبية. تراوحت قيمة جذر-متوسط-مربع-الخطأ بين 0.0057 و0.043 $م^3.م^{-3}$. وقد أعطت هاته النتائج توافقا ممتازا لبرنامج هدروس 2D/3D في محاكاة قيم محتوى المياه الحجمية مقارنة بتلك التي تم قياسها في الحقل.

كان الهدف الثاني هو محاكاة مختلف استراتيجيات الري باستخدام النموذج المصادق عليه لتحسين حركة المياه الافقية و العمودية.

أظهرت النتائج الحاسوبية أن تصريف المنقطات يؤثر علي شكل الابتلال ، حيث يزيد عرض البلل و يقل عمقه كلما زدنا في تصريف المنقط و العكس صحيح.

من نتائج الدراسات علي المحاكي أنه ينصح باستخدام منقط 3ل/سا مع ري كل ثلاثة أيام و ببعد 50سم بين المنقطات للحصول علي توزيع متجانس للرطوبة في منطقة البلل (استراتيجية مثلى) مع تفادي مشاكل التشبع أو نقص الرطوبة في منطقة الجذور الفعالة، اذ لم يتعدى قطر البلل 50سم عموديا. و هذا ما أثبت حقليا بارتفاع مردود الطماطم تحت هذه الاستراتيجية التي سجلت زيادة بنسبة 30٪ مقارنة مع باقي الاستراتيجيات.

مفتاح الكلمات: المحاكاة؛ ممارسات إدارة الري بالتنقيط؛ خصائص التربة؛ النموذج هيدروس ثنائي/ثلاثي الأبعاد ؛مردود محصول الطماطم ؛ شلف الجزائر.

Résumé

L'optimisation de la structure humide de la zone racinaire sous l'irrigation goutte à goutte est l'un des objectifs des concepteurs d'irrigation et des chercheurs afin d'augmenter la production et le rendement des cultures agricoles.

Lors de l'irrigation goutte à goutte, la teneur en humidité de la zone racinaire augmente, réduisant ainsi les forces capillaires entre l'eau et les grains du sol, de sorte qu'il rendre l'extraction racinaire plus facile. L'information sur l'évolution temporelle du volume de sol mouillé peut être utile pour établir l'espacement optimal des émetteurs et la durée de l'irrigation pour le volume de sol où se trouvent les racines actives des cultures, ceci à une grande importance pour exploiter tout le potentiel de la technologie d'irrigation au goutte-à-goutte.

L'équation qui régit le transfert hydrique dans les sols poreux avec des conditions spécifiques est l'équation de Richards, Dans cette recherche, des simulations numériques ont été effectuées avec HYDRUS-2D/3D, ce modèle résout numériquement l'équation de Richards, pour étudier l'influence des différentes stratégies de gestion et de conception de l'irrigation sur la dynamique de l'eau dans le sol, HYDRUS-2D/3D utilise une approche numérique des éléments finis dans un plan (où la région d'écoulement est divisée en un réseau triangulaire (2D). Les coins de ces éléments sont considérés comme les points nodaux. De plus, HYDRUS a été utilisé pour simuler l'impact de l'application de 8 taux de décharge (3,2,1... 8,7 L/h) avec des distances différentes entre les goutteurs (20, 30 ,50cm) selon des fréquence d'arrosage allant d'un à sept jours dans les conditions climatiques de la zone d'étude pour prédire le mode de teneur en eau dans la zone racinaire de la culture de tomates. Par ailleurs, pour valider le program et choisir la meilleure stratégie de gestion de l'irrigation goutte à goutte, nous avons comparé la teneur en eau prédites par le modèle HYDRUS avec ceux mesuré sur terrain.

L'étude expérimentale a été réalisée dans une ferme privée de Chlef, Le champ est géographiquement situé à une coordonnée de 1° 27'20"'E, 36 ° 13'60"'N, l'humidité du sol a été mesurée au champ à l'aide d'un TDR où plusieurs lectures de la teneur en eau à différentes profondeurs dans la zone racinaire ont été effectuées pendant la saison de croissance de la culture de tomates

Le premier objectif était de valider HYDRUS-2D / 3D pour deux goutteurs de surface agissant simultanément avec une texture sablo-limoneuse. On a utilisé l'erreur quadratique moyenne carrée comme analyse statistique pour valider le modèle HYDRUS-2D/3D et pour tester l'adéquation entre les valeurs de teneur en eau volumétrique du sol simulées et observées. La valeur de l'erreur quadratique moyenne carrée se situe entre 0,0057 et 0,043 $m^3.m^{-3}$. Ces résultats démontrent la fiabilité de HYDRUS 2D/3D dans la simulation des valeurs volumétriques de teneur en eau par rapport à celles mesurées sur le terrain.

Le deuxième objectif était de simuler diverses stratégies d'irrigation à l'aide du modèle validé pour optimiser le mouvement latéral et vertical de l'eau.

Selon les études de modèle, les taux de décharge des émetteurs affectent de manière significative la forme du motif de mouillage, avec un taux de décharge élevé, la largeur d'une isoline augmente, tandis que la profondeur diminue, et vice-versa à de faibles débits.

D'après les résultats d'études sur le simulateur, il est recommandé d'utiliser un goutteur de 3 l/h avec irrigation tous les trois jours et à un espacement de 50 cm entre les goutteurs pour obtenir une répartition homogène de l'humidité (stratégie optimale) tout en évitant les problèmes de saturation ou de manque d'humidité dans la zone des racines actives. Ainsi le diamètre humide ne dépasse pas 50 cm verticalement. Cela a été prouvé sur le terrain par le rendement élevé des tomates dans le cadre de cette stratégie qui a enregistré une augmentation de 30% par rapport aux autres stratégies.

Mots clés : simulation; gestion de goutte à goutte; propriétés du sol; modèle HYDRUS 2D/3D; rendement des cultures de tomates; Chlef Algérie.

ABSTRACT

Enhancing the wet characters of the root zone under drip irrigation is one of the objectives of the irrigation designers and researchers, in the goal to increase production and yield of agricultural crops.

During drip irrigation, the moisture content of the root zone rises, thus reducing the capillary forces between the water and the soil particles, so that it makes root extraction easier to obtain its water needs. Information about temporal evolution of the wetted soil volume can be helpful in establishing the optimal emitters spacing and the duration of irrigation, for the volume of soil where the main crop roots are located; it is of great importance in realizing the full potential of drip irrigation technology.

The mathematical equation that governs water transfer in porous soils with specific conditions is the Richards's equation. In this research, numerical simulations were performed with HYDRUS-2D/3D, this model numerically solves Richards equation, to investigate the influence of different irrigation management and design strategies on the soil water dynamics, HYDRUS-2D/3D uses a numerical finite element approach in plan (where the flow region is divided into a triangular (2D) network. The corners of these elements are taken to be the nodal points. In addition, HYDRUS was used to simulate the impact of 8 discharges rate application (1, 2, … 7, 8 L/h) With difference distances between drippers (20, 30 ,50cm) according to a frequency ranging from one to seven days in the climatic conditions of the study area to predict the water content mode in the root zone of tomato crop. Furthermore, to validate the program and choose the best strategy for managing drip irrigation, model accuracy was evaluated against experimental data in the field.

The experimental study was carried out in the private farm in Chlef. The field is geographically located at coordinate of 1° 27' 20" E, 36° 13' 60" N. Soil moisture was measured using a TDR where several water content readings at different depths in the root zone were carried out during the growing season of tomato crop.

The first objective was to validate the HYDRUS-2D / 3D for two simultaneously-working surface drippers with sandy-loam texture. Root-mean-square-error (RMSE) was employed such as statistical analysis to evaluate the performance of the HYDRUS-2D/3D model and to test the goodness of fit between simulated and observed soil volumetric water content values. The RMSE value range between 0.0057 and 0.043 $m^3.m^{-3}$. These results

demonstrate the reliability of HYDRUS2D/3D in the simulation of volumetric water content values (VWC) compared to those measured in the field.

The second objective was to simulate various irrigation strategies using the validated model to optimize lateral and the vertical leaching water movement.

According to the model studies, emitter discharge rates affects significantly the wetting pattern shape, with a large discharge rate, the width of an isoline increases, while the depth of the isoline decreases, while the reverse is true at small flow rates. From the results of studies on the simulator, it is recommended to use a dripper of 3 L / h with irrigation every three days and at 50 cm between drippers to obtain a homogeneous distribution of moisture in the wet area (optimal strategy) while avoiding problems of saturation or lack of moisture in the active roots area, thus the wet diameter does not exceed 50 cm vertically. This has been proven in the field by the high yield of tomatoes under this strategy which has recorded 30% rising compared to other strategies.

Keywords: simulation; drip irrigation management practices; soil properties; HYDRUS 2D/3D Model; Tomato Crop Yield; Chlef Algeria.

TABLE OF CONTENTS

LIST OF TABLES

LIST OF FIGURES

ABBREVIATIONS

Δ : slope vapor pressure curve

γ : psychrometric constant

ρ_a : apparent density

ρ_b : Dry Bulk density

ρ_s : density of the solid

α : Shape parameters (coefficient in the soil water retention function)

$\alpha(h)$: water stress response function

α_1 :inverse of air-entry potential

η : Irrigation yield

θ :volume water content

θ (h) : retention curves

θ_r : residual water content

θ_s : saturated water content

λ : empirical shape parameters

σ : parameter characterize the width of the pore-size distribution

φ : porosity of the soil

2D : Two-dimensional

3D : Three-dimensional

A : Surface area

b : Emitter's runoff length

B : Irrigation water requirement

B_{jl} : Daily needs of localized irrigation

CS : cross section, Soil cover

Cu : Coefficient of uniformity of irrigation

D_{net} net dose

D_{Raw} : Raw dose

e_a : actuel vapor pressure

Eg distance between drip lines

emitter discharge : emitter discharge

E_r: emitter spacing

erfc : complementary error function

$e_s - e_a$: saturation vapor pressure deficit

ET : evapotranspiration

ET0 : Potential evapotranspiration

ET_{CUT} : cultural evapotranspiration

Ev : evaporation

F :frequency of irrigation

FAO : Food and Agricultural Organization, : Food and Agricultural Organization

G : soil heat flux density

h : the matric potential, : pressure head, : duration of insolation

$h_{\phi 50}$: osmotic head associated with water stress

h_{50} : The coefficient in the root water uptake response function associated with water stress

h_a : Hectares, : bubbling pressure

h_f : suction potential/head

H_{fc} Humidity at the field capacity

h_m : matric potential

H_{pw} : Moisture at the point of wilting

Hr : Humidity of the air

Ig : Overall radiation of the month

K *: Hydraulic conductivity,* : Coefficient which is a function of the culture and the climatic zone

K_ij^A : Components of the dimensionless anisotropy tensor KA

Kc : Crop factor

Kr : relative hydraulic conductivity, : Ground cover reduction factor

K_{sat} : saturated hydraulic conductivity

m : Parameter in the soil water retention function

MADR : Ministry of Agriculture, Rural Development and Fisheries Algeria

M_g :mass of the gaseous phase

M_l : mass of the liquid phase

M_s : mass of the solid phase

M_t : total mass

n : Shape parameter (exponent of soil water retention function)

O_i : measured value

P *: Percentage of humidified soil,* : Percentage of the monthly duration of illumination

P_{eff} : The effective rain

P0 : Value of the pressure head below which roots start to extract water from the soil

P2H : Value of the limiting pressure head below which roots no longer extract water at the maximum rate

P_i : predicted value

Popt : Value of the pressure head below which roots extract water at the maximum possible

q : water flux per unit area

Q*d*: Emitter discharge rate

r : radial (horizontal) coordinate

R^2 : Correlation coefficient

r2H : Potential transpiration rate

RFU : easily usable water reserve

RMSE : root-mean-square-error

R_n : net radiation at the crop surface

S : sink term

S(h) : root water uptake

Sp : potential water uptake rate

T : Average monthly temperature in

T': required irrigation duration

T_p : potential transpiration rate

u_2 : wind speed at 2 m height

V_g : volume of the gaseous phase

V_l : volume of the liquid phase

V_s : volume of the soil sample

V_t : total volume

V_v : void volume

VWC volumetric water content

WSA : wetted soil area

WUE : water use efficiency

X : Wetted radius (horizontal direction)

Y : Wetted depth (vertical direction)

Y' : Degree of allowable drying

z : vertical coordinate

Z : Root depth

1 Introduction

1.1 Irrigation techniques in Algeria

The Algerian agriculture is experiencing serious problems: crop production has slightly increased and its weight on economy has considerably decreased, Water resources are limited and gradually decreasing to the detriment of agriculture.

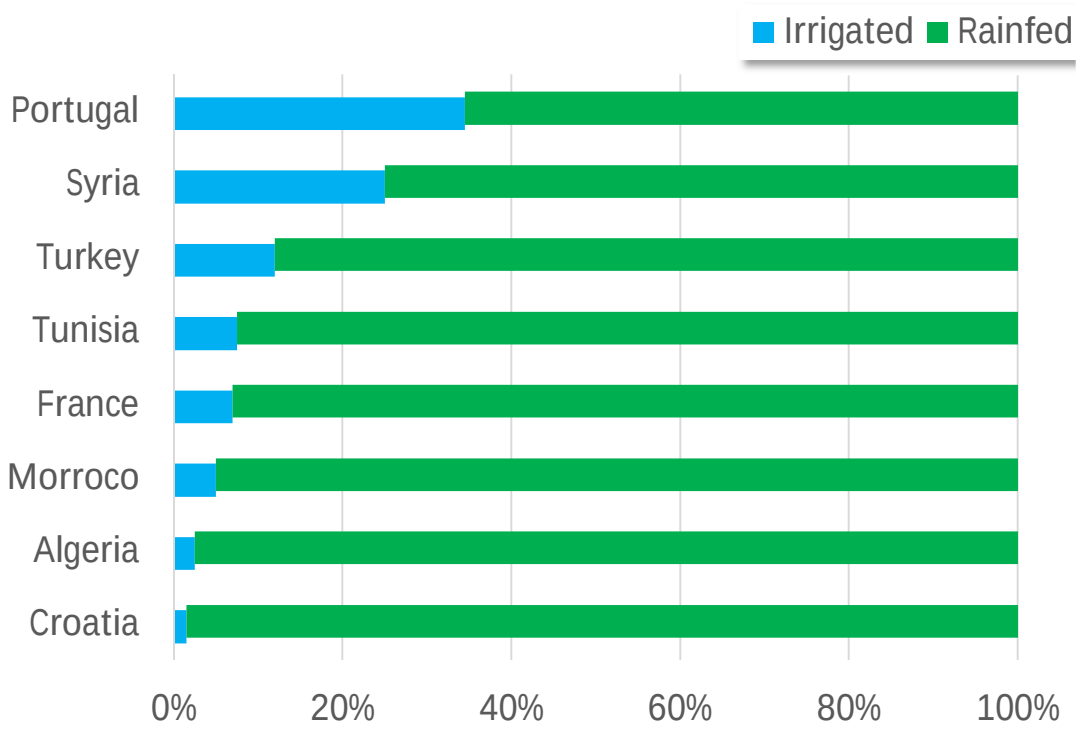

Fig.1. 1: Share of irrigated land in relation to the total area of agricultural land in the Mediterranean basin (Office International de l'Eau, 2009).

The average percentage of irrigated field out of the total agricultural land is about 2.5 % Figure 1.1. (Office International de l'Eau, 2009).

The implementations of the water economy action plan and the investments undertaken by the state have led to a significant increase in the field of irrigation.

The irrigated areas have increased from 350 000 ha in 2000 to 1330 670 ha in 2018 (Table 1) (MADR, 2019).

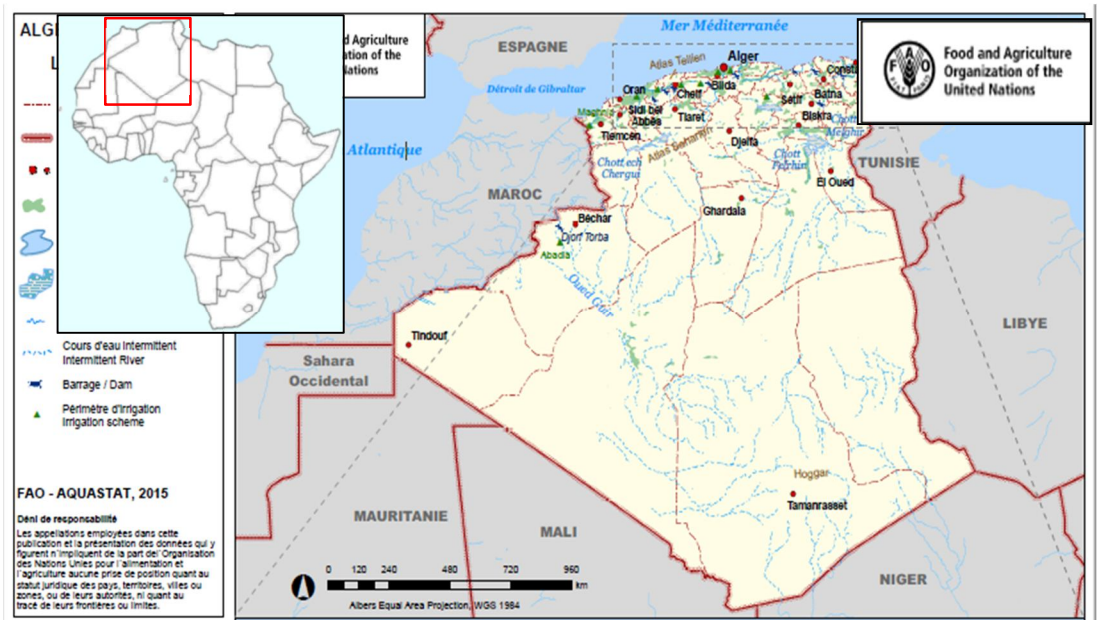

Fig.1. 2: The Water Sector in ALGERIA Food and Agricultural Organization (FAO, 2016).

Figure 1.2 show the water sector in Algeria , the Irrigation and drainage development areas are presented in appendix 1 (FAO, 2016).

T able 1. 1: The irrigated areas in Algeria from 2000 to 2018 (MADR, 2019) .

Years	Total irrigated area (ha)	Irrigation Systems		
		Flood irrigation	Sprinkler irrigation	Drip irrigation
2000/2001	350,000	275,000	70,000	5,000
2001/2002	617,427	449,421	111,978	56,028
2002/2003	644,978	453,531	127,570	63,877
2003/2004	722,320	485,019	138,301	99,000
2004/2005	793,334	518,108	150,739	124,487
2005/2006	825,206	520,503	153,006	151,697
2006/2007	835,590	515,046	162,056	158,488
2007/2008	905,293	512,496	204,859	187,938
2008/2009	906,174	513,012	205,026	188,136
2009/2010	972,862	540,604	230,924	201,334
2010/2011	981,736	545,698	233,854	202,184
2011/2012	1004,530	556,149	241,980	206,401
2012/2013	1053,523	578,846	263,148	211,529
2013/2014	1136,259	617,754	284,321	234,184
2014/2015	1215,261	620,950	344,726	249,585
2015/2016	1260,508	621,457	388,081	250,970
2016/2017	1301,231	622,057	418,473	260,701
2017/2018	1330,670	573,175	444,707	312,788

Of these 1330,670 ha in 2018, 43 percent is irrigated by flood irrigation, 33.5 percent by sprinklers and 23.5 percent by micro-irrigation Figure 1.3(b), flood irrigation is gradually giving way to pressurized irrigation systems (sprinkling and micro irrigation), which in fact rose from 21 % in 2000 to 57% in 2018 Figure 1.3, and the details of the assessment of irrigated areas in Algeria from 2000 to 2018 and in the wilaya of Chlef is given in appendix 1.

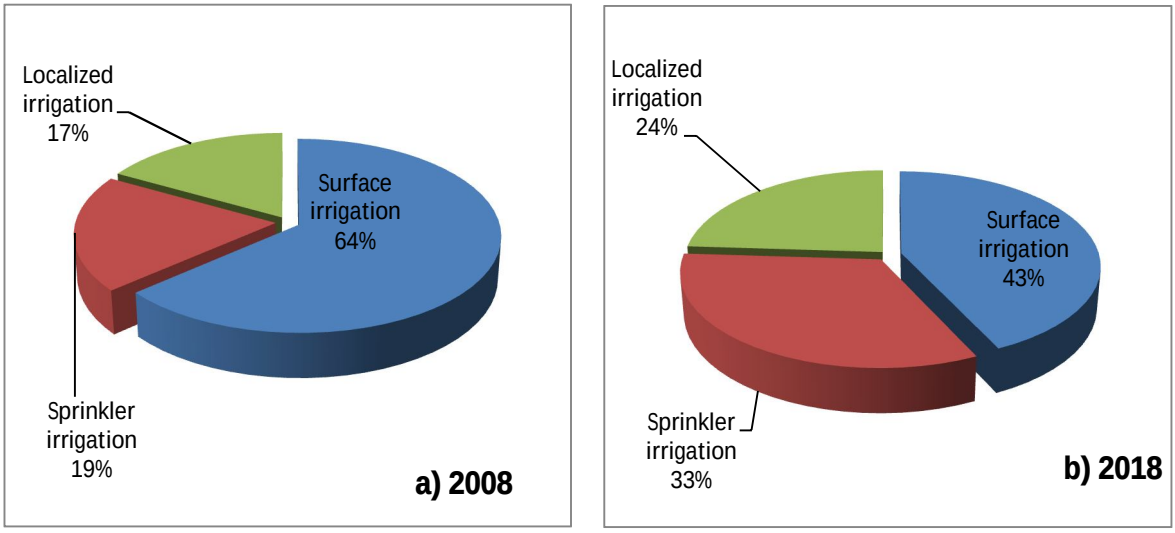

Fig.1. 3: Assessment of irrigation techniques on irrigated areas in Algeria a)2008 b)2018.

For the semi-arid regions such as in Chlef Algeria, their soils suffer from high temperatures for a long time, rainfall lasts for 6 months from November to April of the year, lack of water, and poor plant-nutrients as well. These problems lead to the use of the most efficient irrigation system in conveying water to the plant without wasting any of the scarcely-found water resources.

According to this, the drip irrigation system is the most suitable system to semi-arid's conditions, due to its high conveying efficiency, water conservation, and due to the precise ability to apply fertilizers and chemicals additions through it, so as to enrich the soil's poverty in plant essential nutrients as discussed by (Bruinsma, 2003; Skaggs et al., 2010; Hardie et al., 2018; Ghazouani et al., 2019).

The future improvements in irrigation, as modified irrigation technology or techniques, will play an important role. These improvements can in the future increase the productivity of water used by irrigation and may provide significant adaptation potential under a changing climate. However, Future improvements in drip irrigation as modified irrigation technology will play an important role. These improvements can in the future increase the productivity of water used by irrigation and to increase water productivity. The great potential of drip irrigation lies in improving water management by improving crop yield and quality using less water, and by localizing chemical and fertilizer applications to enhance their efficient use and to reduce the risk

of chemical pollution (Fischer et al., 2007). Under drip irrigation, the soil is moistened by water supplied by the small points of water sources of low flow, whereby only a small portion of the total volume of soil is wetted, but even in this volume the content of soil moisture is uneven. Therefore, the root system of plants developed according to this non-uniform moisture content.. During water infiltration into the soil, the water content changes spatially and temporally. Soil water distribution is strongly dependent on the drip irrigation system design parameters, like emitter discharge rate, spacing between the emitters, system pressure, drip emitter type, soil physical properties, climatic conditions, vegetation properties and root distribution. To design drip irrigation systems effectively, the soil water dynamics needs to be predicted using all the above-mentioned variables. Information about temporal evolution of the wetted soil volume can be helpful in establishing the optimal emitters spacing and the duration of irrigation for the volume of soil where the main crop root (Provenzano, 2007)

There are some guidelines published by several studies e.g. (Keller and Karmeli, 1975; Vermeiren and Jobling, 1984; Keller and Bliesner, 1990; FAO, 2002) to help users to operate surface drip irrigation systems. Unfortunately, there are few, if any, clear guidelines on how to design surface drip irrigation systems by considering the differences in soil hydraulic properties. Some irrigation manuals and guidelines, such as (Vermeiren and Jobling, 1984), proposed excavation of the soil beneath the emitters to visually observe the wetting pattern geometry. In engineering terms, systems are often designed to an economic optimum, which may result in insufficient or excessive irrigation.

On the other hand, models that simulate the dynamics of water in the soil beneath surface drip irrigation can help in predicting soil water content distribution. One such model is the numerical model (Šimůnek et al., 1996, 2006). The model has been used extensively to simulate water distribution under surface and subsurface drip irrigation systems e.g.(Skaggs et al., 2010; Kandelous et al., 2011; Elnesr et al., 2013; Abou-Lila et al., 2013; Hardie et al., 2018; Arraes et al., 2019; Ghazouani et al., 2019; Rasheed, 2020). The use of such models can, in comparison to field experiments, save financial resources and time-demanding laborious work, which would have to be undertaken to examine the dimensions of wetting patterns under different drip irrigation strategies and field/soil conditions. Once all the necessary soil parameters are determined, HYDRUS can simulate distribution of water under drip irrigation systems for a wide range of conditions which include different drip irrigation scheduling options, emitter discharge rates, amount of water applied, pulsing irrigation and different soil water initial conditions.

1.2 Research aims and objectives:

1.2.1 Aims

The aim of this study is to investigate numerically and experimentally the influence of soil texture and hydraulic properties, evapotranspiration, vegetation root distribution and rate of water applied on the size of the wetted area and therefore emitter spacing under surface drip irrigation systems that are appropriate for study area climate conditions. This research addresses the interrelation between all the above-mentioned parameters, which are important for efficient drip irrigation, to maintain/produce water distribution between the emitters uniformly and to achieve sufficient water content at the depth of the root zone, which is important for growing row crops, without losses of water towords the groundwater.

1.2.2 Objectives

These considerations lead to the following specific objectives:

i) To evaluate the effect of different irrigation discharge and frequency of two simultaneously working surface drippers, on the dynamics of the spatial distribution of water in the root zone.
ii) Estimate the depth (Y) and radius (X) distribution of the moisture content in a cultivate soil profile
iii) Test the capability of the HYDRUS-2D/3D model in modeling water movement in the soil which makes it possible to choose the type of drip irrigation strategy and management best adapted to the problematic with time steps varies between the hour and the day during the plant cycle of the tomato crop.

In this thesis, the specific objectives mentioned above have been examined through three major parts depending on the research. In the first part of the research, numerical simulations were carried out for the soil class of the study area. the first part consisted in validating HYDRUS-2D / 3D for two surface emitters working simultaneously with a sandy loam texture under tomato crops, for different water application speeds. The second part involves using HYDRUS- 2D / 3D to simulate the extent of the wetting scheme under irrigation drip for four different flow rates of different emitters and seven irrigation times. This dataset contained the results of the extent of wetting regimes in the X and Y directions for each flux applied at different times throughout the life cycle of our crop. The dataset includes 128 measurements.

Digitally generated data from the first part of the search was used for the second part of the research. Finally, in the third part of this research, numerical simulations have been realized with HYDRUS-2D / 3D to study the influence of these different

Management strategies of tomato irrigation on the water spread of the surface emitter taking into account both realistic plants and weather conditions.

1.3 Research hypotheses

The dissertation examines numerically and experimentally the influence of different drip irrigation system design and management factors on the wetted soil geometry. The hypotheses to evaluate this are:

1. Soil is assumed to have uniform physical properties, homogeneous and isotropic;
2. The initial water content is assumed to be uniform;
3. Darcy's law is applicable to saturated and unsaturated zones;
4. The hydraulic conductivity of the soil, and all its derived functions, are differentiable, continuous, and single-valued functions of moisture content;
5. Root depth was assumed to be 30 cm.

2 Literature Review

2.1 Irrigation Systems, advantages, and disadvantages:

Irrigation is a technique that involves artificially providing crops with water to enable them to grow. This technique is used in farming to enable plants to grow when there is not enough rain, particularly in arid areas. It is also used in less arid regions to provide plants with the water they need when seed setting.

When using irrigation due to the insufficiency of rainfall to allow crop growing, irrigation is said to be supplementary; which is the process of distribution additional water to the crop with the objective of stabilizing and increasing yield, in environments where the given crop is usually grown under rainfall agriculture.

In arid and semi-arid areas, irrigation is used for plants production during the dry season in the absence of rain, irrigation is said full. Related to full irrigation, one can use sometimes deficit irrigation to save water. Indeed deficit irrigation is an optimization strategy in which irrigation is applied during drought-sensitive growth stages of a crop (FAO, 1990). The correct amount of water to apply at each irrigation depends on the amount of soil water used by the plants between irrigations, the water holding capacity of the soil, and the depth of the crop roots. The rate at which water added into the soil varies from one irrigation to the next and from season to season. In general, there are many methods of applying water to the field. However, in irrigation practice there are three basic methods namely: Flood irrigation, Sprinkler irrigation, and Drip irrigation.

2.1.1 Surface irrigation

Flood irrigation is the oldest and most common method of applying water to crops.

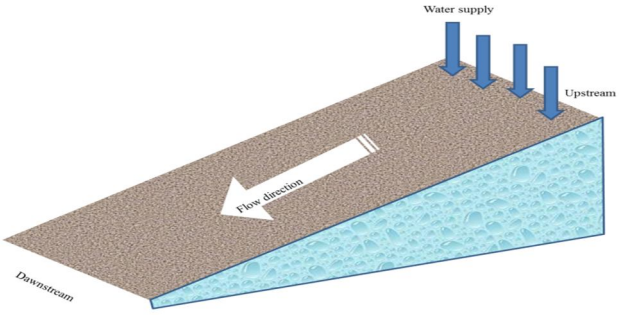

Fig.2. 1: Principle of surface irrigation (Rao et al., 2010).

Is defined as the group of application techniques where water is applied and distributed over the soil surface by gravity Figure 2.1.

In this method of irrigation, water is applied by a channel located at the upper reach of a field.

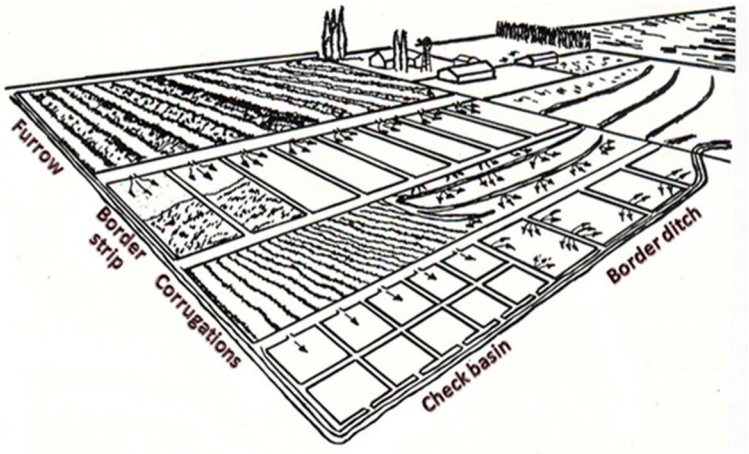

Fig.2. 2: Different methods of irrigation (Rao et al., 2010).

Water may be distributed to the crops in smaller rectangular basins, in long parallel strips or in small channels between crop rows. Two general requirements of prime importance to obtain high efficiency in surface irrigation are, properly constructed water distribution systems and proper land preparation to permit the uniform distribution of water over the field. Surface irrigation is the method generally adopted in all countries. The types of surface irrigation generally include the following (Figure 2.2.).

Furrow irrigation: Furrows are narrow ditches dug on the field between the rows of crops.

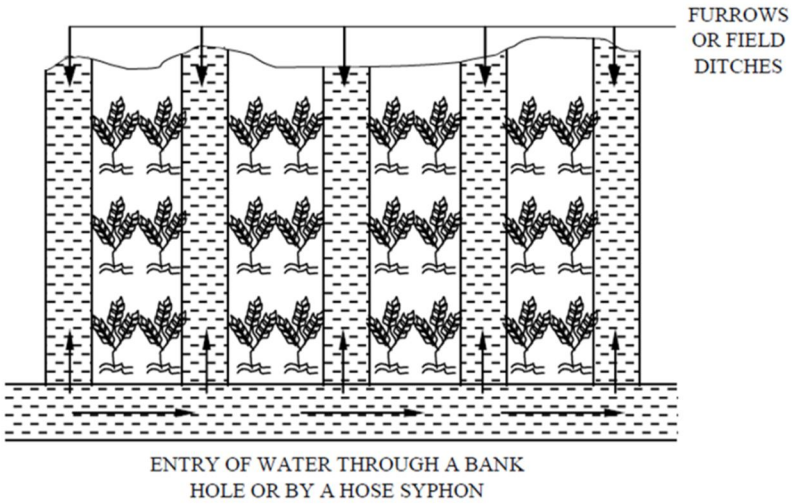

Fig.2. 3: Furrow irrigation method (Rao et al., 2010).

The water runs along them as it moves down the slope of the field. The water flows from the field ditch into the furrows by opening the bank or dike of the ditch or by means of siphons or spiles Figure 2.3.

Basin irrigation: the second type is the most common form of surface irrigation, the field is divided into small units with a level surface and surrounded by bunds or ridges to form basin.

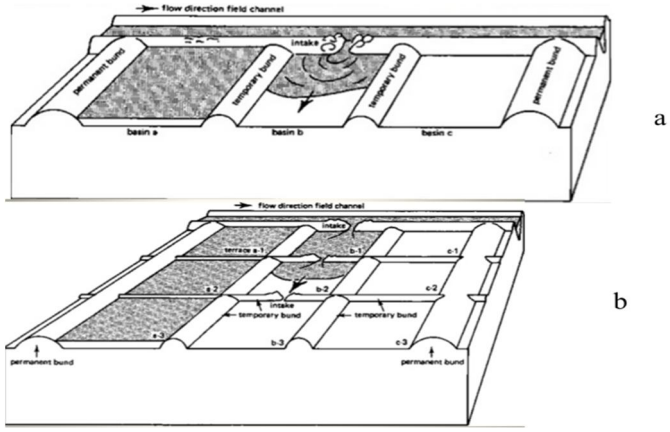

Fig.2. 4 :Water application method a) direct method b) cascade method (Rao et al., 2010).

Two methods of water application are envisaged direct method and cascade method, in the first water is led directly from the field channel into the basin through bund breaks Figure 2.4-a, in the second Figure 2.4-b the water is supplied to the highest terrace (a.1) and is allowed to flow through terrace a.2 until the lowest terrace (a.3) is filled. The intake of terrace a.1 is then closed and the irrigation water is diverted to terrace b.1 until b.1, b.2, and b.3 are filled, and so on.

Border irrigation: this type can be viewed as an extension of basin irrigation to sloping, long rectangular or contoured field shapes, with free-draining conditions at the lower.

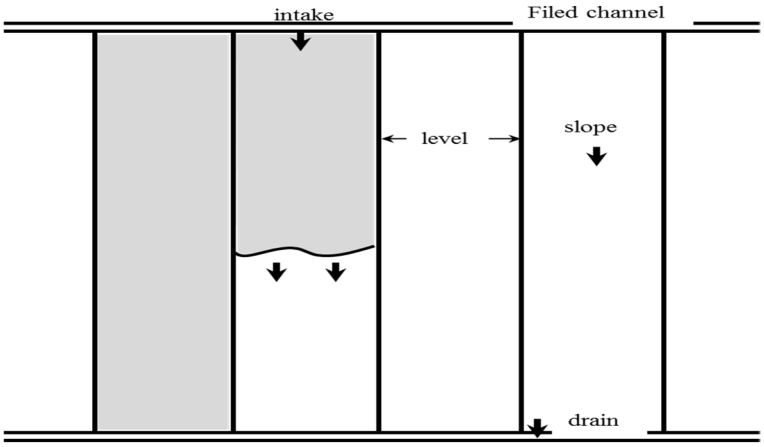

Fig.2. 5 : Border irrigation technique (Rao et al., 2010).

As shown in Figure 2.5, the adoption of one or the other of these two methods depends sometimes upon careful trials, but more often upon custom following the practices. The mean factors determining the choice between flooding and furrowing are:

Nature of the soil: Furrowing is normally preferred for light and erodible soils. On such soils, the soil erosion due to flooding often results in large channels, gullies or eroded soil. On heavier soils, flooding may be practiced safely, as far as erosion is concerned. Many soils, after having been wetted, bake and form a hard crust, which is injurious to the soil and to the plants. On such soils, the furrowing method is advisable, for by that method only a part of the surface is covered with water and that part may be covered with loose earth by cultivation soon after irrigation. Other soils, after having been wetted, as they dry, fall apart, forming natural mulches. On these soils, flooding is safe.

The contour of the land: On relatively level land, either flooding or furrowing may be adopted. Flooding is best done when the slope of the land is not steep, especially in the soil that tends to erode easily. On steeper lands, furrowing must be employed. The heavier the soil, the steeper may be the grade.

Head of the water stream: The "head'' indicates the volume of water supplied to the unit of time. Under some systems of canal management, farmers are given large streams of water for short times; under other systems, small streams are available for longer periods. The total quantity of water at the end of the period may, in either case, be the same. A high head of water moves rapidly over the land. Loose, sandy soils that absorb water rapidly must be irrigated with a high head of water, especially under the flooding method, or the water may all be drawn into the soil, before the lower end of the field is reached. Under the flooding method, a high head of water may be used on nearly all soils, but a low head is suitable only for heavier soils. It follows that the furrowing method is best adapted where the head of water is low; the flooding method where the head is high. This deduction has found practical expression over the whole irrigated area.

The quantity of water available: If irrigation water is abundant, and a high head may consequently be secured, the flooding method is usually employed. If water is scarce, the main consideration is to make the total supply cover the largest area and the furrowing method is ordinarily employed, since, by this method, a small quantity of water may be made to cover much land. It has been shown that the productive power of water decreases, as the total quantity applied to a given area is increased. That is, with each additional centimeter of water, the less dry matter is produced. Consequently, where water is scarce, it is more profitable to spread the small quantity of water over a large area of land. To do this, the

furrow method is indispensable. In irrigation practice, therefore, although the reason is not always understood, the furrowing method is invariably used wherever the supply of water is low.

Nature of the crop: The nature of the crop also determines the method of irrigation. There are certain crops that are sensitive to the inundation of water around their roots. Furrowing is the most suited method for these crops.

In general, in this type of irrigation, more than 75% of the water goes as percolation loss and the fertility in topsoil is washed away and goes as percolation loss, graded, gravity-driven slopes suit food irrigation best. Advantages include a lower initial investment of equipment, lower pumping costs, and minimal labor. A few hoses are all it takes to have functioning furrows between rows. Water stays in the root zone, and the foliage stays dry. Drawbacks to flood irrigation include potential overwatering and wasteful runoff. If the soil lacks proper sloping or does not absorb readily, water cannot move through the garden resulting an accumulation of salinity between furrows. Standing water damages plants and reduces yields for edible crops.

2.1.2 Sprinkler irrigation

The method of applying water to the plant on the ground surface through spraying it overhead, somewhat resembling rainfall, is known as sprinkler irrigation (Keller and Bliesner, 1990).

Fig.2. 6 : Sprinkler irrigation (Rao et al., 2010).

It is a method started in the USA in the immediate post-war period. In this method of irrigation, water is applied above the ground surface as a spray somewhat resembling rainfall

Figure 2.6. The spray is developed by the flow of water under pressure through small orifices or nozzles. The pressure is usually obtained by pumping, although it may be by gravity if the water source is high enough above the area to be irrigated. The irrigation water is distributed to the field through pipelines.

Well-designed sprinklers distribute water better than surface methods. Surface runoff of irrigation water is totally eliminated. The amount of water can be controlled to meet crop needs and light application can be made efficiently on seedlings and young plants. Sprinkler irrigation may be advantageously used under the following conditions:

1. The land is unsuitable or uneconomical for leveling.

2. Soils are too porous and highly erodible.

3. Stream size is too small to distribute water efficiently by surface irrigation methods.

4. Effective control of water application is convenient for applying light and frequent irrigation with higher water application efficiency.

5. Areas located at a higher elevation than the source of water.

6. Labour costs are usually less than those for surface methods.

7. Moreland is available for cropping since field supply channels and bunds or ridges are not required.

8. The irrigation method does not interfere with the movement of farm machinery.

Sprinkler irrigation system, has, however, the following disadvantages:

1. Wind distorts sprinkler patterns and causes uneven distribution of water.

2. Evaporation losses are high when operating under high temperatures. This becomes more harmful when the irrigation water has larger amounts of dissolved salts.

3. Initial investment and continued operating costs are much higher than those in case of surface irrigation methods.

4. Power requirements are usually high since sprinklers operate with a water pressure.

5. Fine-textured soils that have a slow infiltration rate cannot be irrigated efficiently in hot windy areas. If water applied at the low rate required for these soils, the percentage of water lost by evaporation and wind drift increases.

6. Ripening soft fruits are damaged by the spray.

7. A stable and continuous water supply is needed for the most economical use of the equipment. This is not possible in rural areas due to the erratic power supply.

8. The system cannot be used in areas with water containing sand, debris and large amounts of dissolved salts.

2.1.3 Drip irrigation methods (surface and subsurface)

Excessive water intake and deep percolation losses are the major limitations in water application through surface methods of irrigation. Micro-irrigation is defined as the slow application of water on or below the soil surface. It can also be called localized irrigation, in which part of the soil volume is wetted (Aujla et al., 2005; Barragan et al., 2010; Saskia et al., 2013; Arraes et al., 2019). Micro irrigation systems can be classified as a surface drip, subsurface drip, bubbler, and micro sprinklers systems. According to the ASAE, (2007), drip irrigation is, defined as a ″method of micro irrigation wherein water is applied to the soil surface as drops or small streams through emitters. Discharge rates are generally less than 8 L/h for single-outlet emitters and 12 L/h per meter for line-source emitters″.

After the plastic revolution at the end of the Second World War took place the greenhouses in England between 1945-1948 and later in the United States (Dasberg and Or, 1999), drip had been developed in the 1970s. Currently, the irrigated area by micro-irrigation in the world rose from 436,590 ha in 1981 to more than 6,089,534 ha in 2006 (Reinders, 2007).

2.1.3.1 Drip irrigation methods layout

Drip irrigation also referred to as trickle irrigation or micro-irrigation, is one of the latest methods of irrigation which is becoming increasingly popular in areas with water scarcity and salt problems. It is a method of watering plants frequently with a volume of water approaching their consumptive use, thus minimizing losses due to deep percolation, surface runoff and soil surface evaporation.

Fig.2. 7 : Wetting patterns with drip irrigation (Hebei Jinshi Industrial Metal Co., 2020).

This method uses small diameter plastic lateral lines with water outlets called "emitters" or "drippers" at selected spacing to deliver water to the soil surface near the base of the plants Figure 2.7. The system applies water slowly to keep the soil moisture within the desired range for plant growth. Perforations known as emitters are designed to emit water in a trickle rather than a jet of water. The emitters are placed so as to produce a wet strip along the crop row or a wetted bulb of soil at every plant. All the field pipes are left in place for the duration of the growing season of the crop. Fertilizers are usually applied in solution along with the water. The layout of a drip irrigation system is shown in Figure 2.8.

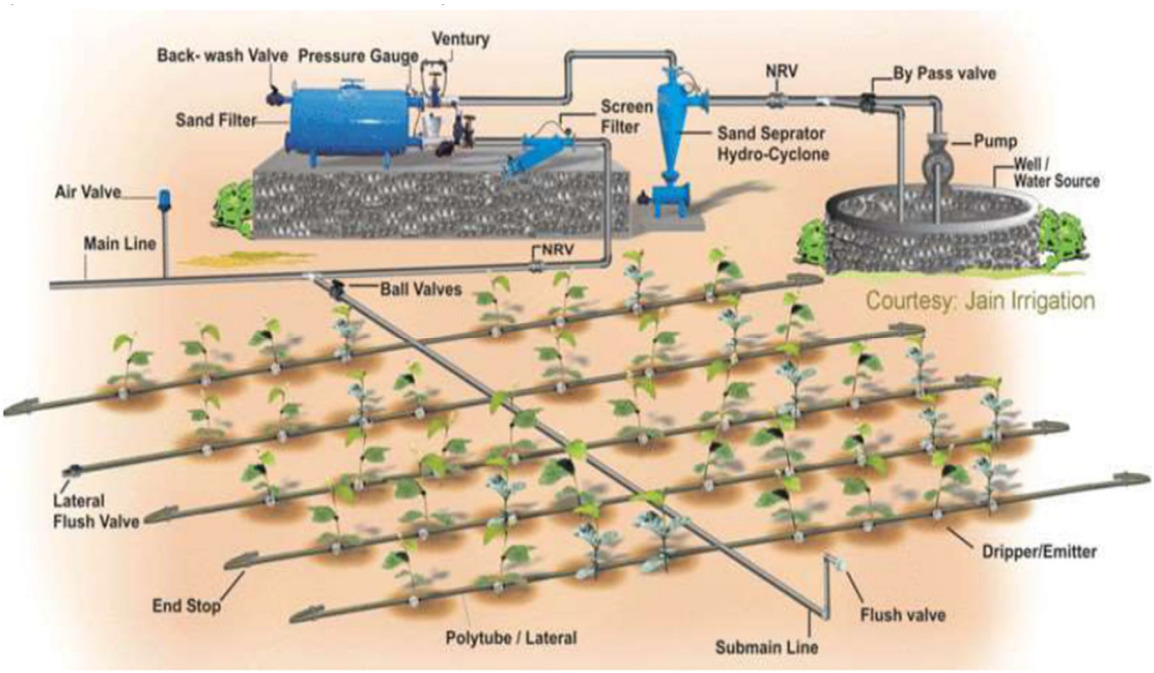

Fig.2. 8 : Lay-out of a drip irrigation system (Lamm et al., 2007)

Drip emitters create different sub-soil wetting patterns in different soil types. The texture of the soil determines the vertical and horizontal distribution of water in it.

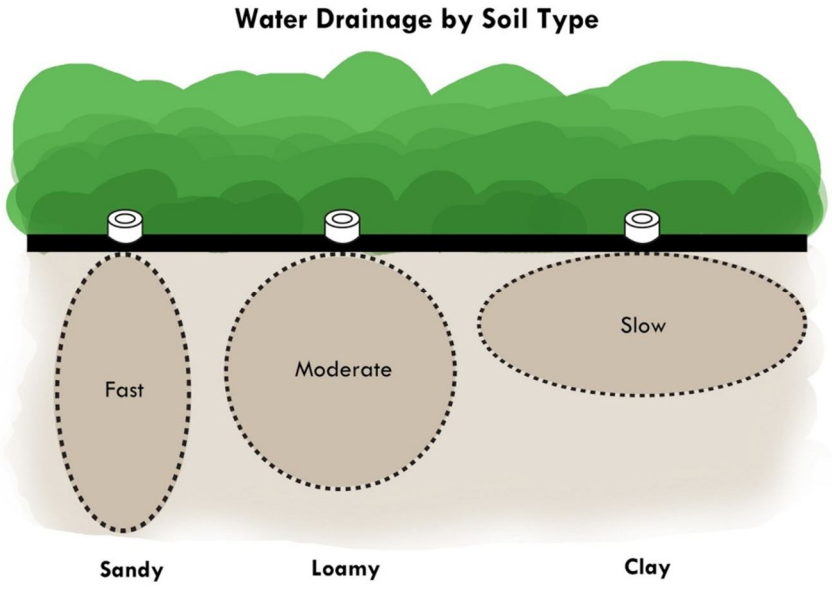

Fig.2. 9 :Different sub-soil wetting patterns in different soil types (Drip Depot, 2014).

In coarse-textured soils (sandy soils) water will tend to spread more vertically, while in fine-textured soils (clay soils) there will be a considerable lateral movement, resulting in a larger radius of the wetted zone Figure 2.9.

Subsurface drip irrigation is a low-pressure, high-efficiency irrigation system in which water and fertilizer are fed directly into the root zone by buried drip tubes to meet to crop water requirements. These technologies have been part of irrigated agriculture since the 1960s, with technology advancing rapidly over the last three decades. An underground system is flexible and can provide frequent light irrigations. This is particularly suitable for arid, semi-arid, warm, and windy areas with limited water supply. Since the water is applied below the soil surface, the effect of surface irrigation characteristics, such as crusting, saturated conditions of ponding water, and potential surface runoff (including soil erosion) are eliminated when using subsurface irrigation.

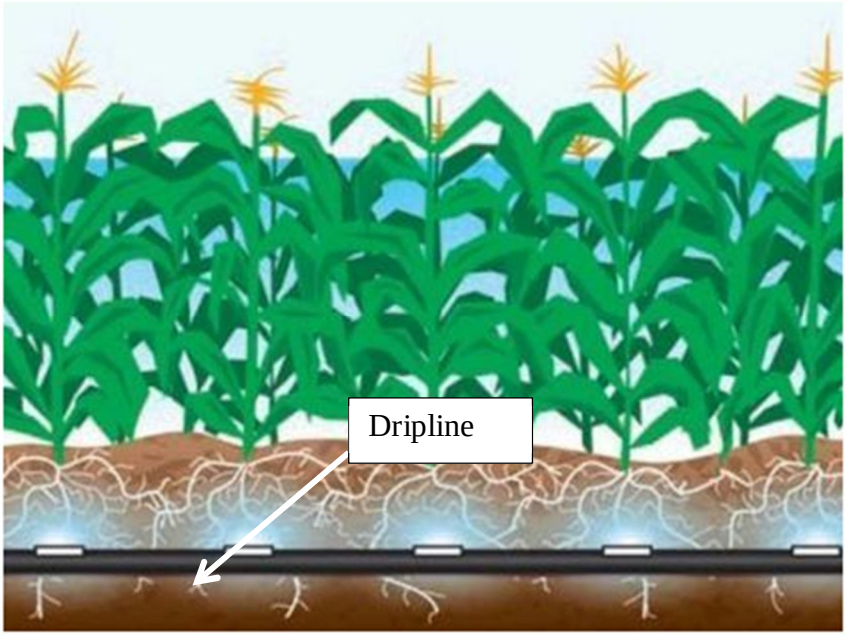

Fig.2. 10 :Wetting around the tube in subsurface drip irrigation (Chamsa, 2020).

With an appropriately sized and well-maintained system, water application is highly uniform and efficient. Wetting occurs around the tube and water typically moves out in all directions Figure 2.10.

This method has the following advantages:

1. Water distribution occurs near the plant roots, resulting in uniform and controlled water distribution.
2. Land leveling for irrigation on steeper slopes is eliminated.
3. No surface flow, no tail water loss or soil erosion occurs.
4. Concurrent application of water and fertilizer is possible.
5. It permits cultural operations during irrigation on trees.
6. It restricts weed growth only to the wetted areas.
7. It results in considerable water saving and increased yields.

The initial cost of the drip irrigation equipment is considered to be its limitation for large-scale adoption. Economic considerations, therefore, limit the use of drip irrigation system to orchards and vegetables in water scarcity areas.

2.2 Drip irrigation system design and planning

In this original process, water is applied separately to each plant, the systems are designed to transport water from the source to a crop, through a delivery network of pipes and emission water devices. The general objective of the design of the drip irrigation system is to provide water efficiently and uniformly to a crop, to help meet evapotranspiration (ET) requirements. At the same time, only the part of soil colonized by the roots of the culture is moistened. Under each dripper, a saturated zone of low volume is formed, from which the majority of the water diffuses in unsaturated flow, the water is diffused radially under the effect of the capillary forces and vertically under the effect of Gravity (FAO, 2002a). For a given flow and duration of irrigation in order to form the humidity bulb, it is essential to control the volume of soil moistened and the quantities of water supplied to each supply, as well as the frequency of The shape and dimensions of the volume of moistened soil (lateral extension and depth of wetting) depend essentially on the hydrodynamic characteristics of the soil and its degree of dryness (Rieul and Ruelle, 2003).

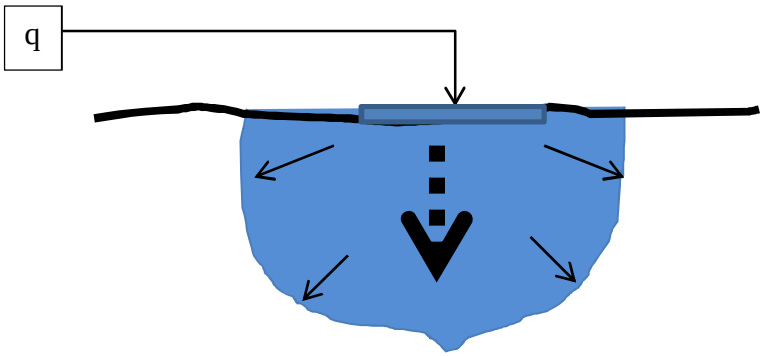

a: Clay soil ⇒ lateral diffusion

Fig.2. 11 : the shape of the moistened soil in a heavy soil texture (clay texture) (Rieul and Ruelle, 2003).

For a given duration and flow rate, the shape and dimensions of the volume of moistened soil (lateral extension and depth of humectation) depend essentially on the hydrodynamic characteristics of the soil (such as large « onion » bulb Clay soil and/or a horizon with high compactness at medium depth Figure 2.11 , and in the form of a narrow bulb in "carrot" Sandy or stony ground With very low clay content and Figure 2.12.

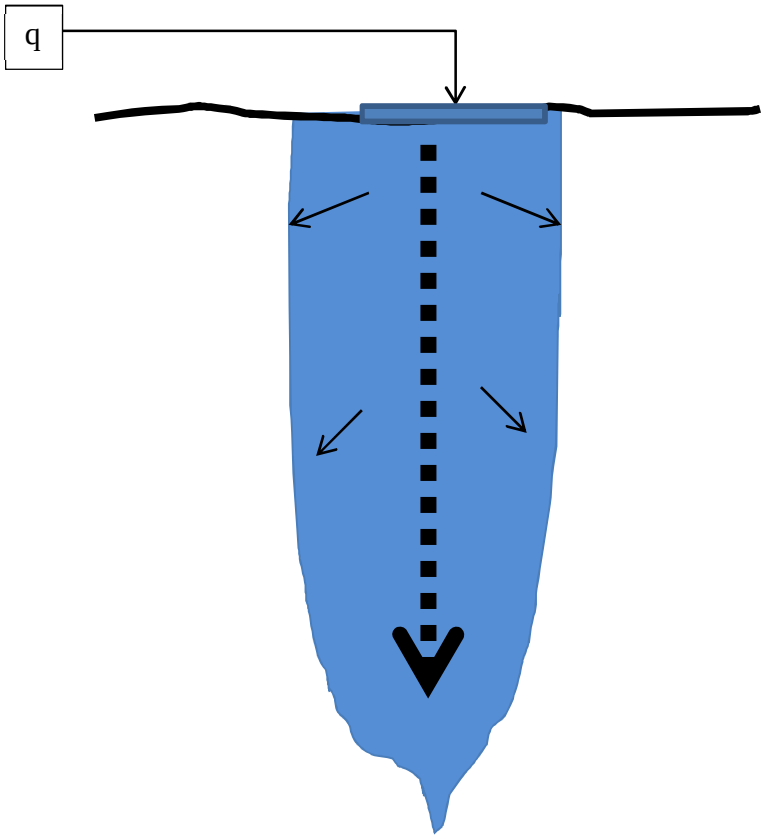

b: Sandy soil ⇒ weak lateral diffusion,
strong percolation

Fig.2. 12 : The shape of the wetted soil according to sundy texture (Rieul and Ruelle, 2003)

Typical layout of a localized irrigation network

A drip irrigation system is comprised of many components, each of which plays an important part in the operation of the system. Figure 2.13-14-15 (Rao et al., 2010).

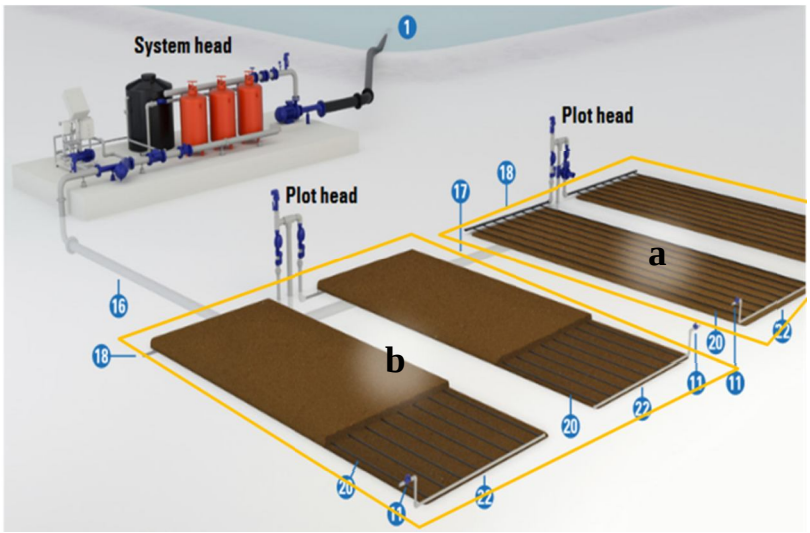

Fig.2. 13 : Typical localized drip irrigation field layout.

a) Surface drip irrigation and b) subsurface drip irrigation.

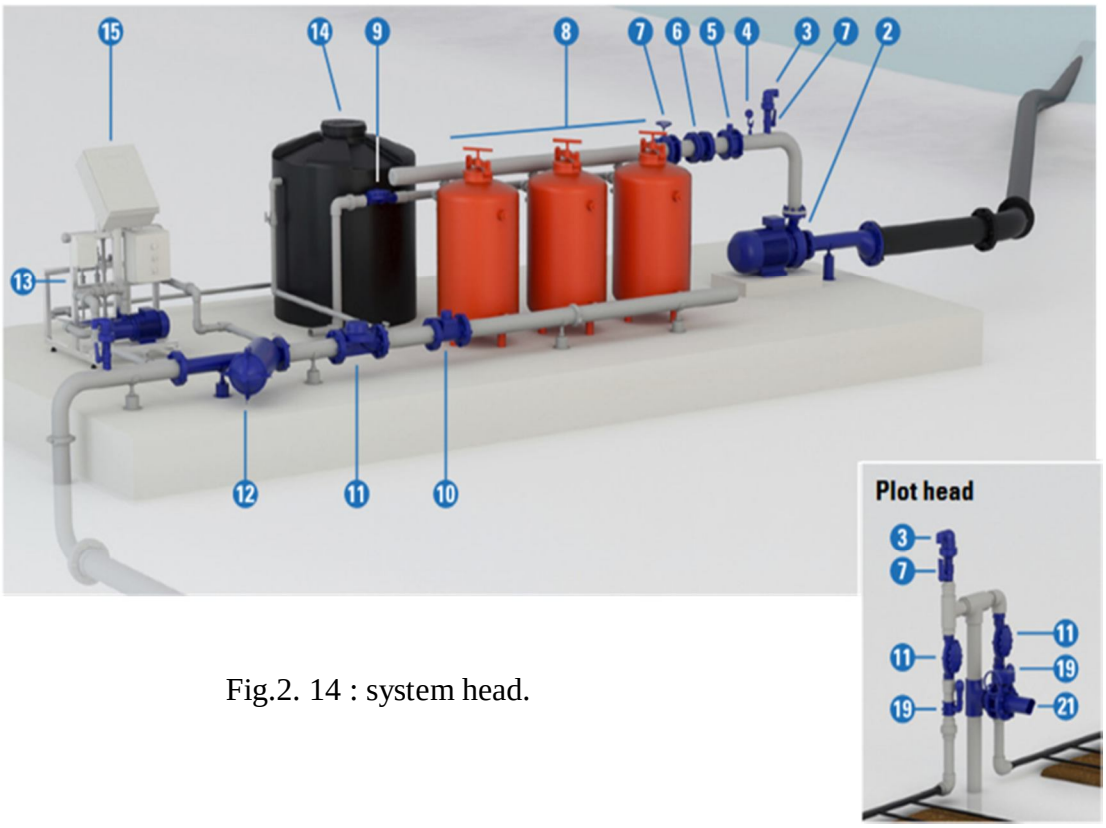

Fig.2. 14 : system head.

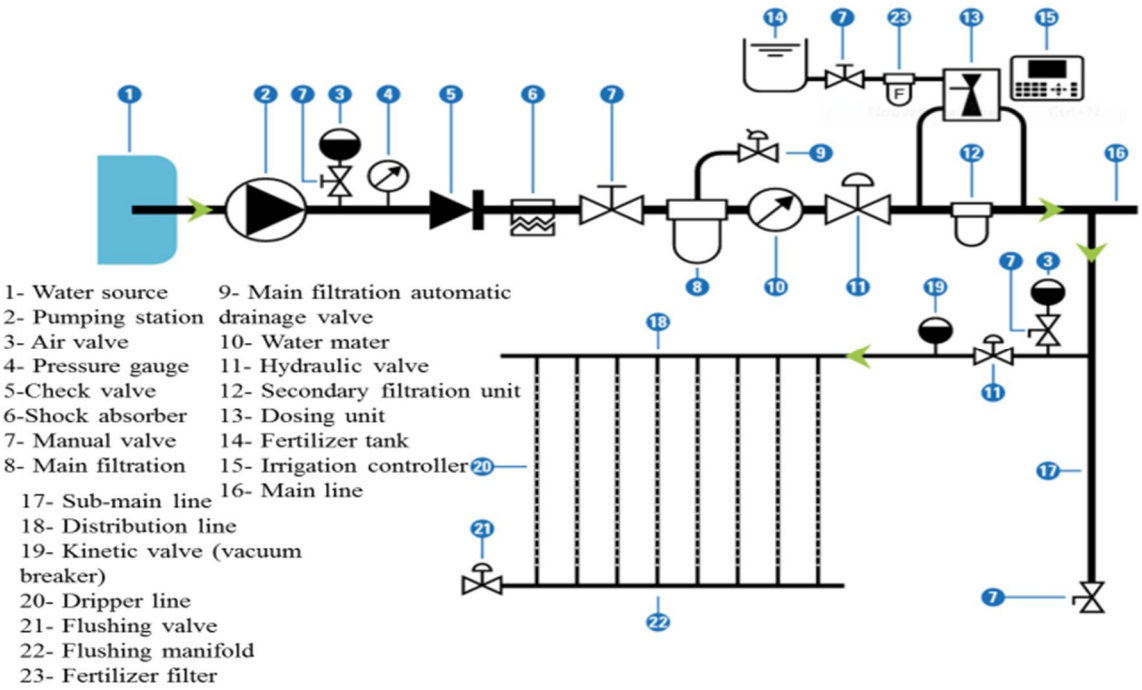

Fig.2. 15: Schematic diagram.

2.3 Drip irrigation management methods

The design of a drip irrigation network depends on the irrigation water needs and crop water requirements which can be defined as a the height of water (or the amount of water) dose delivered to the plant at favorable times, in order to counterbalance water losses by evapotranspiration and put the crop in the best humidity conditions required, to obtain maximum yield.

The water requirements of a crop require knowledge of various parameters, both the plant itself, the climatic and soil data of the region.

- Soil parameters will be used to estimate the useful soil of the water reserve.
- Crop data will specify the readily available water supply from the plant.
- Climate data will provide the necessary information on the water requirements of the crop. For this we define:

Potential evapotranspiration or reference (ETP or ET0):

Evapotranspiration is a complex phenomenon integrating both evaporation of soil water (physical phenomenon) and transpiration of vegetation cover (physiological phenomenon). Evapotranspiration can be evaluated according to several empirical formulas as below:

a) BLANEY-CRIDDLE formula

It has been established and given satisfactory results for the arid and semi-arid regions, it is expressed by the following formula:

$$ET_0 = P \times K \times (0.457 \times T + 8.13) \qquad (2.1)$$

where:

ET0: Potential evapotranspiration in mm / day

P: Percentage of the monthly duration of illumination relative to the annual duration wich depends only on latitude

K: Coefficient which is a function of the culture and the climatic zone.

T: Average monthly temperature in (° c)

b) TURC Formula:

If the relative humidity of the air is greater than 50%, the potential evapotranspiration is given by:

$$ET_0 = 0.40\ (Ig + 50) \times \frac{T}{T+15} \quad \text{en (mm/month)} \qquad (2.2)$$

where:

T: Average temperature of the period considered in ° C

Ig: Overall radiation of the month considered in (cal / cm2 / d), according to TURC, the coefficient 0.40 is reduced to 0.37 for the month of February.

If the relative humidity of the air is less than 50%, the ETP is given by:

$$ET_0 = 0.40\ (I_g + 50) \times \frac{T}{T+15} \times (1+\frac{50-H_r}{70}) \qquad (2.3)$$

where:

Hr: The humidity of the air in%

Ig: Overall radiation in (cal / cm2 / day), where as :

$$Ig = Ig_A \times (0.18 + 0.62 \times \frac{h}{H}) \qquad (2.4)$$

Ig_A :Theoretical maximum radiation

H: Astronomical duration of day in (hour/month)

h :the duration of insolation in (hour/month)

c) Penman-Monteith method: The FAO Penman-Monteith method is selected as the method by which the evapotranspiration can be unambiguously determined, and as the method which provides consistent evapotranspiration values in all regions and climates. it's given by:

$$ET_0 = \frac{0.408\Delta(R_n - G) + \gamma \frac{900}{T+273} u_2 (e_s - e_a)}{\Delta + \gamma(1 + 0.34u_2)} \qquad (2.5)$$

where

ET_o reference evapotranspiration [mm day^{-1}],

R_n net radiation at the crop surface [MJ m^{-2} day^{-1}],

G soil heat flux density [MJ m^{-2} day^{-1}],

T mean daily air temperature at 2 m height [°C],

u_2 wind speed at 2 m height [m s^{-1}],

e_s saturation vapour pressure [kPa],

e_a actuel vapeur pressure [kPa],

e_s - e_a saturation vapor pressure deficit [kPa],

Δ slope vapor pressure curve [kPa $°C^{-1}$],

γ psychrometric constant [kPa $°C^{-1}$].

Taking into account the climatic characteristics of our study area, where a relatively low humidity is recorded during the dry months of the year with a semi-arid climate (Badni, 2012), In our case, we will use the software CROPWAT (Derek et al., 1998), established by the FAO (Derek, 1998), based on the Penman method modified by Monteith, (1965) Better adapts to this type of climate.

Crop water requirements under drip irrigation

Irrigation planning was managed by calculating the daily depletion of soil water that directly affects crop water requirements through the following water balance equation :

$$B_j = ET_{CUT} - (P_{eff} + RFU) \quad (2.6)$$

where:

B: Irrigation water requirement (mm)

ET_{CUT}: cultural evapotranspiration (mm / day)

$$ET_{CUT} = ET_0 \times K_C \times K_r \quad (2.7)$$

$$ET_{CUT} = \text{ETo x Kc x Kr}$$

where:

ETo =Reference crop evapotranspiration using the Penman-Monteith method;

Kc = Crop factor

Kr = Ground cover reduction factor

P_{eff} : The effective rain (mm)

RFU: easily usable water reserve (mm).

The principles and the method of calculation are provided in Appendix 01

2.4 Vadose zone properties

The soil is defined as a porous medium: a solid material enclosing inter-related pore spaces. The percolation of fluids within a porous media is possible through the inter-related pore spaces. Water can flow through the soil porous media under both saturated and unsaturated conditions. The rate and volume of water being displaced through the soil profile are affected by the percentage of moisture saturation in the soil (Lazarovitch et al., 2007).

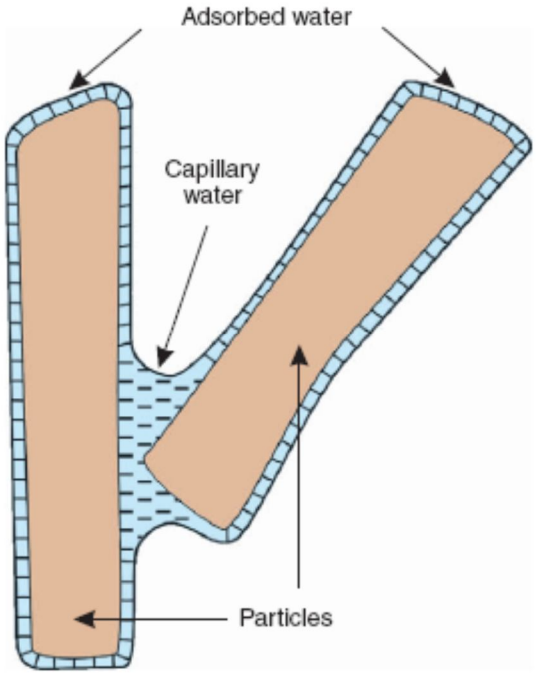

Fig.2. 16 : Water in an unsaturated soil is subject to capillarity and adsorption (Hillel, 2004).

Water content found within these pores can be divided into three categories: drainage or surplus water, plant-available or capillary water, and non-available water Figure 2.16. Non-available water is the hygroscopic water held by the soil at conditions below the permanent wilting point (less than -15 bars). Drainable water is the amount of water that is able to drain due to gravity (greater than -1/3 bar).

The plant-available water lies in between the permanent wilting point and field capacity; the water retained by the soil due to capillary forces.

The vadose zone of the soil is the shallow, unsaturated zone above the water table, the layer in which the poral space is not completely filled with water. When the poral space is open and continuous (which is often the case), water is retained in the pores by surface tension forces. The unsaturated zone is then equivalent to the soil layer in which the water pressure is below atmospheric pressure. This "negative pressure" is usually converted to positive "sucking "

2.4.1 Physical properties

The soil is a complex and dynamic medium with three phases: solid, liquid and gaseous. The solid phase is composed of mineral particles and organic particles, the liquid phase is composed of water and solutes, the gaseous phase is the air of the soil. Particles of the solid phase are of various sizes and irregular shapes. Two concepts are important to consider in characterizing solid particles and their arrangement: soil texture and soil structure.

Soil texture represents the distribution of elementary particles as a function of their diameter. For particles with a diameter of less than 2 mm, three types of particles are distinguished according to the USDA (United States Department of Agriculture) classification: sands (0.05-2 mm), silts (0.002-0.05 mm) and clays (less than 0.002 mm)(Hillel, 2004). Particles larger than 2 mm in diameter are called coarse elements. The distribution is usually represented by a ternary graph or texture triangle at the international level, the most used classification is that of the USDA.

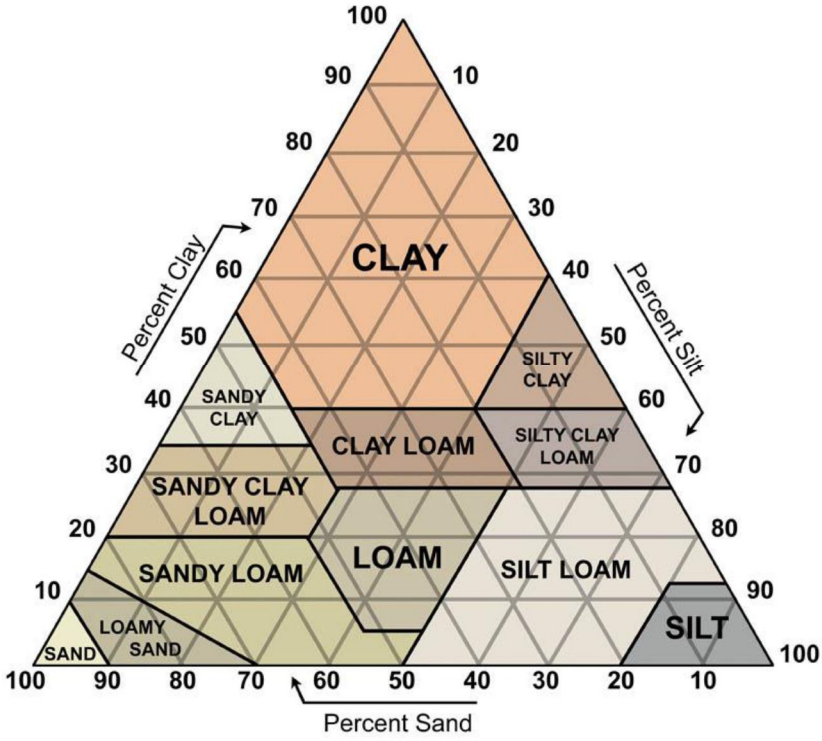

Fig.2. 17 : Texture triangle proposed by (USDA, 2020).

This triangle classifies soils according to 12 classes of texture Figure 2.17. Particle size in soil affects density, porosity, water and air circulation, and water retention among other properties. This distribution of pore size is very little influenced by tillage and evolves little over time. Thus, most soil classification systems are based on texture, which is then considered as the basic criterion of classification.

The soil structure is a dynamic characteristic that refers to the arrangement of solid particles. It defines the porosity of the soil, the poral space that can be filled with water and air. The pore volume varies in space and time depending on agro-environmental conditions and soil properties.

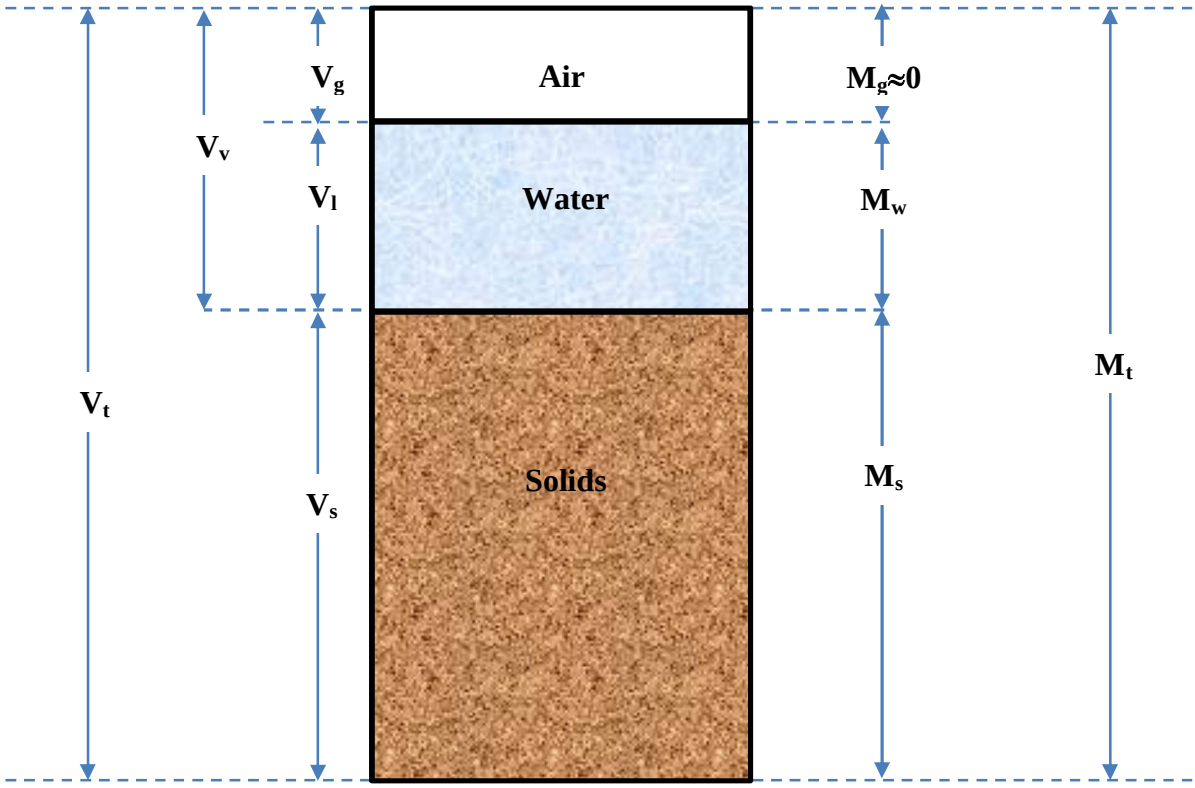

Fig.2. 18 : Schematic representation of the constitution of a soil volume (Hillel, 2004).

The characterization of the soil structure is essential for the study of the transfer of water in the soil because it determines the hydrodynamic properties of the soil.

The important variables to be known about the physical and hydrodynamic properties of the soil are as shown in Figure 2.18.

The density of the solid ρ_s:

$$\rho_s = \frac{M_s}{V_s} \qquad (2.8)$$

The bulk density of the soil: The apparent density ρ_a, [M L^{-3}]) corresponds to the ratio between the mass of the dry sample (M_s) and the apparent volume occupied by the soil sample (V_s),

$$\rho_a = \frac{M_s}{V_t} \qquad (2.9)$$

Total porosity: The porosity is expressed by the ratio between the void volume (V_v in [L^3]) and the total volume of the soil (V_t in [L^3]).

$$\varphi = \frac{V_g + V_l}{V_t} \qquad (2.10)$$

The volume water content is given by :

$$\theta = \frac{V_l}{V_t} \qquad (2.11)$$

Where:

V_s represents the volume of the solid phase m^3

V_l represents the volume of the liquid phase m^3

V_g represents the volume of the gaseous phase m^3

V_t represents the total volume of m^3 soil

M_s represents the mass of the solid phase kg

M_l represents the mass of the liquid phase kg

M_g represents the mass of the gaseous phase kg

M_t is the total mass of soil kg

ρ_s represents the density of the solid kg m^{-3}

ρ_d represents the density of the soil kg m^{-3}

φ represents the porosity of the soil m^3 m^{-3}

θ represents the volume water content m^3 m^{-3}

2.4.2 Hydraulic properties of soil

Knowledge of the hydrodynamic properties of the soil, particularly its water retention properties, is involved in many important agricultural control processes and will be recognized as a key factor in good soil management. In agriculture, accurate knowledge of soil moisture content is essential for the proper management of water resources and well-planned tillage operations. The retention curve and the hydraulic conductivity curve are the most important hydrodynamic properties of a soil. The retention curve represents the relationship between the matrix potential and the soil moisture content. It indicates how much water the soil can hold at a given potential. This property is influenced by both texture and soil structure. In addition, fine textures, such as clay soils, retain more water than those with a coarse texture, sandy soil for example. The characterization of this curve is essential for modeling the transfer of water and solutes into the soil.

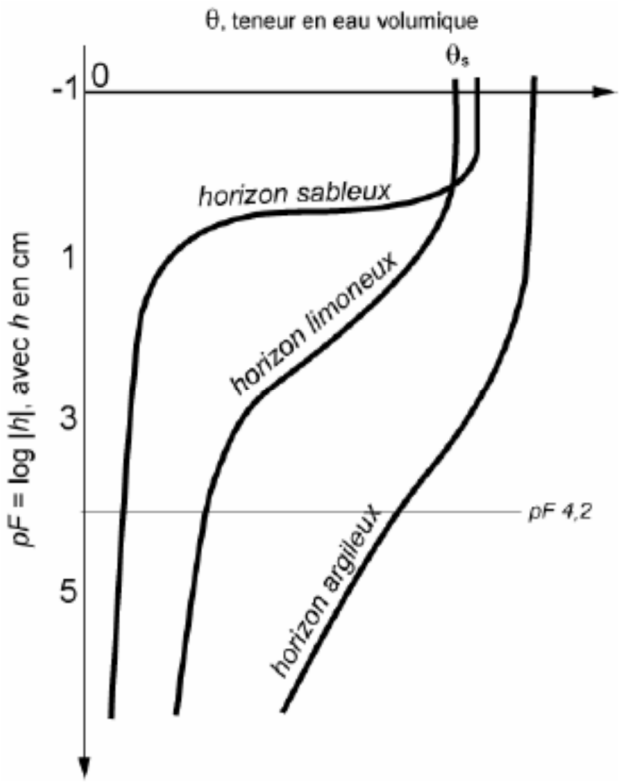

Fig.2. 19 : Typical retention curves of clay, loamy and sandy soils (Bruand and Coquet, 2005).

Figure2.19 shows the retention curves corresponding to the 3 major classes of soil texture. Hydraulic conductivity (K) characterizes the capacity of a soil to transmit water; it is a function of the distribution of pores in the soil profile (volume and pore continuity) and saturated hydraulic conductivity (K_{sat}). According to Darcy's Law, under laminar flow conditions in a saturated homogenous pore system, the velocity of water flowing within the soil particles is a function of hydraulic conductivity, porosity, and pore hydraulic gradient.

2.5 Modeling water movement in soil

Knowledge of water movement in the variably saturated soil near the soil surface is essential to understand man's impact on the environment. Movement in the upper soil determines the rate of plant transpiration, soil evaporation, runoff and recharge to the groundwater. In this way, unsaturated soil water flow is a key factor in the hydrological cycle. Due to the high solubility of water, soil water transports large amounts of solutes, ranging from nutrients to all kind of contaminations. Therefore an accurate description of unsaturated soil water movement is essential to derive proper management conditions for vegetation growth and environmental protection in agricultural and natural systems.

2.5.1 Governing equations

2.5.1.1 . Water flow modeling

Soil water retention is the key of soil property used in many applications in the fields of irrigation. The modeling of flows in unsaturated soils requires the determination of the retention curves θ (h) and hydraulic conductivity K (θ). Quite number models have been proposed over the years to describe the expressions of the retention curve θ (h). Some of these models are new while others are a modification of the existing models. Some of these models are discussed below.

2.5.1.2 Water Retention Models θ (h)

2.5.1.2.1 Van Genuchten Water Retention Model

A commonly used retention model is the van Genuchten (1980) closed form analytical expression. The closed form equation consists of four independent parameters which have to be estimated from observed soil water retention data. Many curve fitting and parameter optimization codes such as RETC software (van Genuchten et al., 1991) are widely used today.

These types of relationships are empirical in nature with a physical basis. The van Genuchten equation is expressed

as:

$$\theta(h) = \theta_r + (\theta_s - \theta_r)[1 + (\alpha h)^n]^{-m} \qquad (2.12)$$

Where, θ is the volumetric water content [$L^3.L^{-3}$]; h is the pressure head [L]; θ_s and θ_r represent the saturated and residual water contents[$L^3.L^{-3}$]; respectively; α, n and m are empirical shape parameters.

2.5.1.2.2 Brooks-Corey Water Retention Model

Another well-established parametric model was proposed by Brooks and Corey (1964). This is a four-parameter water retention model. A Brooks-Corey model is a type of nonlinear curve fitting model for fitting water retention characteristics using experimental data. The Brooks-Corey functions can be defined as:

$$\theta(h) = \theta_r + (\theta_s - \theta_r)(\alpha h)^{-\lambda} \qquad (2.13)$$

Where, θr is the residual water content [$L^3.L^{-3}$]; θs is the saturated water content [$L^3.L^{-3}$]; h is the matric potential [L], λ and α are empirical shape parameters.

2.5.1.2.3 Fredlund-Xing Water Retention Model

This is a five-parameter water retention model (Fredlund and Xing, 1994).

$$\theta = \theta_r + \frac{\theta_s - \theta_r}{\left\{ln\left[e + \left(h_f/\alpha\right)^n\right]\right\}^m} \qquad (2.14)$$

Where θ_r is the residual water content [cm^3cm^{-3}], θ_s is the saturated water content [$L^3.L^{-3}$]; h_f is the suction [L], α, n, and m are empirical shape parameters.

The Fredlund-Xing water retention model was developed based on pore size distribution of the soil. If the pore size distribution of a soil can be obtained or predicted, then the soil water characteristic curve is uniquely determined from the equation above.

2.5.1.2.4 Gardner Water Retention Model

This is a four-parameter water retention model by Gardner (Gardner, 1958).

$$\theta(h) = \theta_r + (\theta_s - \theta_r)[1 + (\alpha h)^n]^{-1} \qquad (2.15)$$

2.5.1.2.5 Bi-exponential Water Retention Model

Biexponential water retention model was developed by Omuto. This is a five-parameter water retention model contained in a bimodal pore-size distribution. The parameters are for the first and second compartments (Omuto, 2009).

$$\theta(h) = \theta_r + \theta_1 e^{-\alpha_1 h} + \theta_2 e^{-\alpha_2 h} \qquad (2.16)$$

Where, θ_1 represents the difference between saturated moisture (θ_{s1}) and residual moisture contents (θ_{r1}) in the structural pore-space; θ_2 represents the difference between saturated moisture (θ_{s2}) and residual moisture contents (θ_{r2}) in the textural pore-space; $\alpha_1$represents the inverse of air-entry potential in the structural pore-space; α_2 represents the inverse of air-entry potential in the soil textural pore-space; θ_r is the sum of residual moisture contents in the structural pore-space (θ_{r1}) and textural pore-space (θ_{r2}).

2.5.1.2.6 Campbell Water Retention Model

This is a three-parameter water retention model (Omuto, 2009).

$$\theta(h) = \theta_s(\alpha h_f)^{\lambda} \qquad (2.17)$$

Where h_f is suction potential/head; θ_s is the saturated moisture content. It's the moisture content when suction potential is very low (almost at the saturation point); α is the inverse of h_a air-entry potential or bubbling pressure, λ is a parameter or index for the pore-size distribution.

2.5.1.2.7 Tani Water Retention Model

This is a three-parameter water retention model developed by Tani (1982); (Omuto, 2009)

$$\theta = \theta_r + (\theta_s - \theta_r)[1 + (\alpha h)e^{-\alpha h}] \qquad (2.18)$$

Where, h Suction potential/head; θ_r is the residual moisture content. It's the moisture content when suction potential is very high (almost at the drying point); θ_s is the saturated moisture content. It's the moisture content when suction potential is very low (almost at the saturation point); α is the inverse of air-entry potential or bubbling pressure.

2.5.1.2.8 Kosugi Water Retention Model

This is a four-parameter water retention model developed by Kosugi (1999); (Omuto, 2009)

$$\theta(h) = \theta_r + \frac{1}{2}(\theta_s - \theta_r)erfc\left[\frac{\ln(h/h_m)}{\sigma\sqrt{2}}\right] \qquad (2.19)$$

where, θ_s is the saturated soil water content; θ_r is the residual soil water content; h_m is the matric potential corresponding to the median pore radius; σ is a dimensionless parameter to characterize the width of the pore-size distribution; *erfc* denotes the complementary error function.

2.5.1.2.9 Ruso Water Retention Model

Ruso water retention model is a four-parameter function. This is a type of nonlinear curve fitting model for fitting water retention characteristics using experimental data (Russo et al., 1998; Omuto, 2007).

$$\theta(h) = \theta_r + (\theta_s - \theta_r)[(1 + 0.5\alpha h)e^{0.5\alpha h}]^{2/n+2} \qquad (2.20)$$

where, h is suction potential/head as contained in the x-column of the xy water retention table or data; θ_r is the residual moisture content. It's the moisture content when suction potential is very high (almost at the drying point); θ_s is the saturated moisture content. It's the moisture content when suction potential is very low (almost at the saturation point); α is the inverse of air-entry potential or bubbling pressure; n is a parameter or index for the pore-size distribution.

2.5.1.2.10 Exponential Model

This is a three-parameter water retention model (Omuto, 2007).

$$\theta(h) = (\theta_r + \theta_s)e^{-\alpha h} \qquad (2.21)$$

Where, h is suction potential/head as contained in the x-column of the xy water retention table or data; θ_r is the residual moisture content; θ_s is the saturated moisture content; α is the inverse of air-entry potential or bubbling pressure.

The following summary table 2.1 presents a list of the most used models of θ (h) with their parameters

Table 2. 1 : summary table of most used water retention models.

authors	Model θ(h)	Parameters
(Campbell, 1974)	$\theta(h) = \theta_s(\alpha h)^{\lambda}$	$\theta_s, \alpha, \lambda$
(Tani, 1982)	$\theta(\mathrm{h}) = \theta_r + (\theta_s - \theta_r)[1 + (\alpha h)e^{-\alpha h}]$	$\theta_r, \theta_s, \alpha$
Exponential (Omuto, 2007)	$\theta(h) = (\theta_r + \theta_s)e^{-\alpha h}$	$\theta_r, \theta_s, \alpha$
(van Genuchten, 1980)	$\theta(h) = \theta_r + (\theta_s - \theta_r)[1 + (\alpha h)^n]^{-(1-\frac{1}{n})}$	$\theta_r, \theta_s, \alpha, n$
(Gardner, 1958)	$\theta(h) = \theta_r + (\theta_s - \theta_r)[1 + (\alpha h)^n]^{-1}$	$\theta_r, \theta_s, \alpha, n$
(Russo et al., 1998)	$\theta(h) = \theta_r + (\theta_s - \theta_r)[(1 + 0.5\alpha h)e^{0.5\alpha h}]^{2/n+2}$	$\theta_r, \theta_s, \alpha, n$
(Brooks and Corey, 1964)	$\theta(h) = \theta_r + (\theta_s - \theta_r)(\alpha h)^{-\lambda}$	$\theta_r, \theta_s, \alpha, \lambda$
(Kosugi, 1999)	$\theta(h) = \theta_r + \frac{1}{2}(\theta_s - \theta_r)erfc\left[\frac{\ln(h/h_m)}{\sigma\sqrt{2}}\right]$	$\theta_r, \theta_s, \sigma, h_m$
(Fredlund and Xing, 1994)	$\theta(h) = \theta_r + \frac{\theta_s - \theta_r}{\{ln[2.7183 + (h/\alpha)^n]\}^m}$	$\theta_r, \theta_s, \alpha, n, m$
(van Genuchten, 1980)	$\theta(h) = \theta_r + (\theta_s - \theta_r)[1 + (\alpha h)^n]^{-m}$	$\theta_r, \theta_s, \alpha, n, m$
Biexponential (Omuto, 2009)	$\theta(h) = \theta_r + \theta_{s1}e^{-\alpha_1 h} + \theta_{s2}e^{-\alpha_2 h}$	$\theta_r, \theta_{s1}, \theta_{s2}, \alpha_1, \alpha$

2.5.1.3 Hydraulic conductivity models K (θ(h))

Due to the complexity of the forces governing hydraulic conductivity, many approximate solutions have been developed to obtain closed form solutions for infiltration rates.

Among the models of K_r (h), we can cite the Childs and Collis-model (Childs and Collis-George, 1950) equation [2.27], the Burdine model (Burdine, 1953) equation [2.28], and the model from (Mualem, 1976) equation [2.29].

$$K_r(S_e) = S_e^{n_{CCG}} \left[\int_0^{S_e} \frac{[S_e - S_e]dS_e}{h(S_e)^2}\right]\left[\int_0^{1} \frac{[1 - S_e]dS_e}{h(S_e)^2}\right]^{-1} \qquad (2.22)$$

$$K_r(S_e) = S_e^{n_s+1} \left[\int_0^{S_e} \frac{dS_e}{h(S_e)^2}\right]\left[\int_0^{1} \frac{dS_e}{h(S_e)^2}\right]^{-1} \qquad (2.23)$$

$$K_r(S_e) = S_e^{n_m} \left[\int_0^{S_e} \frac{dS_e}{h(S_e)}\right]\left[\int_0^{1} \frac{dS_e}{h(S_e)}\right]^{-2} \qquad (2.24)$$

The model K (Se) of Mualem, (1976) associated with the model Se (h) of van Genuchten, (1980) gives:

$$K_r(h) = \frac{[1 - (-\alpha h)^{n-1}[1 + (-\alpha h)^n]^{-m}]^2}{[1 + (-\alpha h)^n]^{m/2}} \qquad (2.25)$$

with the relation: m = 1 - 1 / n.

The same model of K (Se) (Mualem, 1976) associated this time with the model Se (h) of Brooks and Corey, (1964) gives:

$$K_r(h) = \left(\frac{h_b}{h}\right)^{2+2,5/b} \qquad (2.26)$$

2.5.2 Solute transport modeling

The usual approach to physically-based modeling of solute movement through saturated and unsaturated soils has been through the use of the advection-dispersion equation Cassel and Nielsen (1986). More general approaches to solute transport define the system as a transfer function model consisting of an input, output, and an appropriate probability density function, such a general formulation allows treatment of systems for which the exact mechanisms are too complex for a detailed description, and/or statistical random processes in heterogeneous soils (Warrick, 1974)

When the soil is homogeneous, or at least homogeneous within layers, and flow processes are approximately Darcian, the assumptions governing the advection-dispersion equation generally provide a good approximation to solute transport within the soil, although the higher-order statistics of the solute transport may not be well-reproduced.Mass conservation laws are used to describe and constrain fluxes of solutes. This follows similar principles to those outlined in the Richards' equation derivation, with the continuity equation applied to solute mass and fluxes rather than water. The physical processes that control the flux into and out of elemental volumes are advection and hydrodynamic dispersion (Freeze and Cherry, 1979). Adsorption of chemicals onto the soil solids must also be considered, and plant uptake.

2.5.3 Analytical and Numerical solutions

2.5.3.1 Analytical solutions

Models can be solved by either analytical or numerical techniques. Analytical models are ones in which all relationships are expressed in closed form so that the equations can be solved by the classical methods of analytical mathematics. Numerical models are ones in which the governing equations are solved by means of step-by-step numerical calculations.
Analytical models used for a surface point source, usually solve the governing water flow equation under specific conditions. Analytical models rely on assumptions, such as soil homogeneity, and they do not take into account root water uptake.

Cote et al. (2003) developed a user friendly Microsoft Windows-based software program, WetUp, that provides visualization of the wetting patterns.

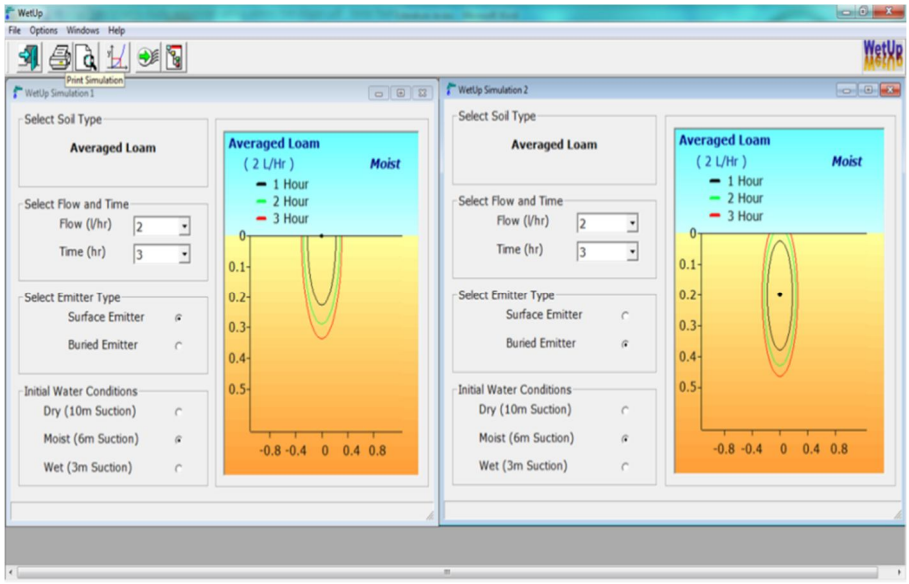

Fig.2. 20 : WetUp window showing wetting perimeters at different times for different flow rates from a surface emitter (panel 1) and buried emitter (panel 2) (Cook et al., 2003).

The program estimates dimensions of the wetting patterns, in different soil textures, with different soil hydraulic characteristics, for surface or subsurface point sources (emitters) (Figure 2.20). WetUp contains a database of predefined soil types, emitter flow rates (from 0.503 to 2.7 L/h), application times (1 – 24 h), initial soil moisture conditions (3, 6 and 10 m of suction) and emitter position (surface or subsurface).

WetUp uses Philip's solution (Philip, 1984) for flow from a surface and subsurface point source. The solution determines the travel time of water and is based on a quasi-linear analysis of steady three-dimensional unsaturated water flow.

Kandelous and Šimůnek, (2010) compared WetUp to other empirical and numerical solutions, for estimating the size of the wetting pattern. The result show that WetUp predictions of the geometry of the wetting pattern were less precise compared to numerical model HYDRUS-2D (Šimůnek et al., 2006), this observation are mentioned by (Cote et al., 2003; Šimůnek et al., 1996). Also reported that WetUp tends to underestimate horizontal wetting at large volumes of water applied for coarse-textured soils.

Other analytical solutions have been derived for steady infiltration from a buried point source and from cavities (Philip, 1968, 1984), from a surface point (Warrick, 1974), and, from shallow circular (Wooding, 1968). (Mmolawa and Or, 2000) presented a semi-analytical model for calculating water flow and non-reactive solute transport with and without plant uptake for a buried or surface point source.

Application of analytical models in trickle irrigation management is limited because the solutions are based on limiting assumptions with regards to source configurations, the linearization of the flow equation and homogeneous soil hydraulic properties. Most of them also do not take into account root water uptake.

2.5.3.2 Numerical 2D/3D modeling

There are several numerical models developed with the purpose of simulating the surface and subsurface point source water infiltration. Brandt et al. (1971) developed a model to analyze multidimensional transient infiltration from a trickle source. Bresler et al. (1971) compared the theory, discussed by Brandt et al. (1971), with experimental results. Calculated and measured locations of wetting fronts and soil water content distribution were examined. They concluded that, despite the dissimilarity between the theoretical and experimental results, the agreement is sufficient for the practical implementation of the theory.

In 1975 Bresler (Bresler, 1975) reported a study about numerical model simulations for analysis of multidimensional simultaneous transfer of a non-interacting water and solute transport, applicable to the infiltration from a trickle source. Mostaghimi et al. (1981) studied water movement in silty clay loam soil under single emitter source. They used the numerical method of Bresler, (1975) and compared it to laboratory experimental results. The study showed that increasing discharge rate of an emitter results in an increase in the vertical direction and decrease in the horizontal direction of the wetted zone. Those results are in contraindication with the results of Bar-Yosef and Sheikholslami, (1976); Li et al. (2003) and Khan et al. (1996). Bresler, (1975) also found quite good agreement between predicted and measured soil water content distribution under drip irrigation.

Šimůnek et al. (1996) developed a software package, HYDRUS-2D, which was updated to provide a third dimension, now called HYDRUS-2D/3D (Šimůnek et al., 2006). The software enables implementation of three-dimensional water flow, solute transport, and root–water and nutrient uptake based on finite-element numerical solutions of the flow and transport equations. For the water flow module.

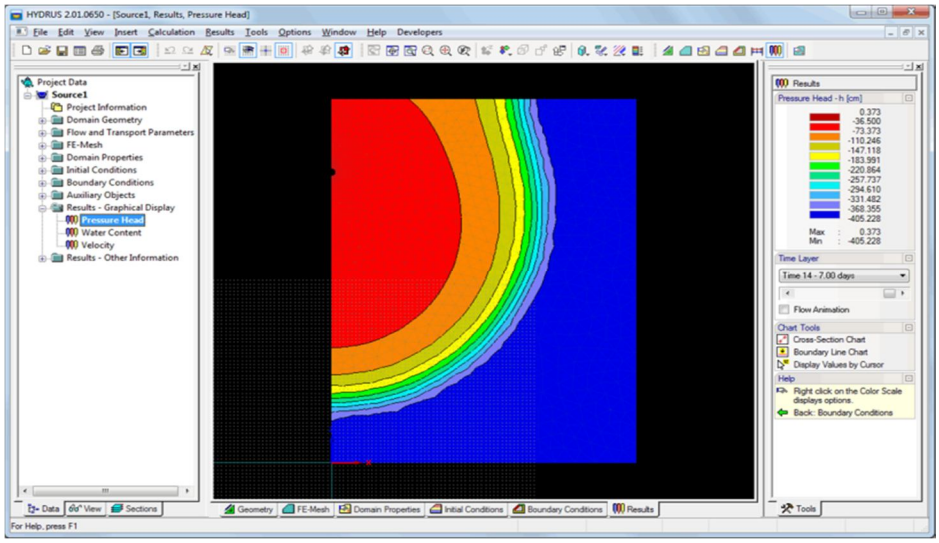

Fig.2. 21: The main window of the HYDRUS GUI, including his main components (*Hydrus 2D/3D V 2.02.0680*, 2012).

The program numerically solves Richards equation (Richards, 1931) for variably saturated flow. The flow equation also incorporates a sink term to simulate water uptake by plant roots. In 2011, version 2.0 of HYDRUS-2D/3D has been released. It includes many new features as compared to version 1.0. The most important ones, which can be used for simulating drip irrigation design and management, are various new boundary conditions (i.e. surface and subsurface drip irrigation) and triggered irrigation (irrigation can be triggered by the program when the pressure head drops below a specified value, Šimůnek et al. (2011). The main unit

of the program is the HYDRUS graphical user interface (GUI) which defines the overall computational environment of the system (Figure 2.21). The availability of computers and their reliability in soil-water flow modeling and solute transport make water resource and environmental management more useful, so the HYDRUS-2D/3D is being used for evaluating water flow in trickle irrigation systems. The number of such studies is extensive and has been growing steadily in recent years (Assouline, 2002; Lazarovitch et al., 2005; Zhou et al., 2007; Hanson et al., 2009; Samadianfard et al., 2012; Elnesr and Alazba, 2015; Autovino et al., 2018; Ghazouani et al., 2019; Rezayati et al., 2020; Rasheed, 2020). Some of these studies simulated subsurface drip irrigation (SDI) process as a line source (a lateral) (Ben-Gal et al., 2004; Skaggs et al., 2004); , while others simulated SDI by means of a point source, as individual emitter (Lazarovitch et al., 2005; Provenzano, 2007; Kandelous et al., 2011; Elnesr et al., 2013; Elnesr and Alazba, 2015) While some other authors assessed the ability of HYDRUS to simulate water movement from surface drip irrigation systems (Assouline, 2002; Gärdenäs et al., 2005). All these studies were done using either planar or axisymmetrical two-dimensional models, which is valid as long as the flow domain studied is not influenced by neighboring emitters.

Eltarabily et al. (2019) used HYDRUS-2D/3D to analyze field data, assuming the modeling approaches in which emitters were represented, either as a point source in an axisymmetrical two-dimensional domain, a line source in a planar two-dimensional domain or a point source in a fully three - dimensional domain. Results showed that SDI systems can be accurately described, using an axisymmetrical two-dimensional domain, only before wetting patterns start to overlap, and a planar two-dimensional domain, only after the full merging of the wetting fronts from neighboring emitters. The fully three-dimensional model appears to be required to entirely describe the subsurface trickle irrigation process.

Kandelous and Šimůnek, (2010) compared numerical, analytical and empirical models to estimate wetting patterns for surface and subsurface irrigation. They evaluated the accuracy of several approaches used to estimate wetting zone dimensions by comparing their predictions with field and laboratory data, including the numerical HYDRUS-2D model, the analytical WetUp software and selected empirical models (Schmitz et al., 2002; Amin and Ekhmaj, 2006; Kandelous et al., 2011). They used the mean absolute error to compare the model predictions and observations of wetting zone dimension. Mean absolute error for different experiments and directions varied from 0.9 to 10.4 cm for HYDRUS, from 1 to 58.1 cm for WetUp and from 1.3 to 12.2 cm for other empirical models.

Skaggs et al. (2010) used numerical simulations with HYDRUS-2D to investigate the effect of application rate, antecedent water content and pulsed water application on horizontal water spreading from drip irrigation emitters. Results showed that higher antecedent water content increases water spreading from trickle irrigation systems, but the increase is bigger in a vertical than a horizontal direction. Also, lower application rates and pulsing produced minor increases in the horizontal spreading of water. Some irrigation treatments were tested in field trials and they confirmed the simulation results. Overall they found out that soil texture (hydraulic properties), and antecedent water content largely determine the spreading and distribution of a given water application, with pulsing and flow rate has a very little effect.

Cote et al. (2003) also used numerical model HYDRUS -2D to investigate the effect of pulsed water applications on the size of the wetting pattern for subsurface drip irrigation for sand, silt and silty clay loam soils. They found that soil hydraulic properties greatly influence the geometry of wetting pattern. Irrigation frequency (pulsing) has slightly increased the dimensions of the wetting pattern in the highly permeable coarse-textured soil. Also, similarly to Skaggs et al. (2010), high discharge rates from a SDI tend to increase vertical spreading more than horizontal. The simulations also highlighted that, in order to achieve desired wetted volume, the drip irrigation system discharge rate has to be regulated according to particular soil type and consequently its hydraulic properties are of great importance.

Assouline, (2002) presented a study about the effect of different emitter discharge rates, including micro drip emitters (emitter discharge rate <0.5 L/h), on different water regimes in drip irrigated corn. In his study, three emitter discharge rates (0.25, 2.0 and 8 L/h) were compared in field experiments and for numerical simulations using HYDRUS-2D. Field experiments showed that, under microdrip irrigation, the highest relative water content occurred in the upper 30 cm of the soil profile and the lowest in the 60 to 90 cm layer. Numerical results showed that, under microdrip irrigation treatment, the wetted volume of soil was smallest in both, horizontal and vertical directions. The water content gradients for micro-irrigation treatment were also less extreme in both directions, compared to 2.0 and 8.0 L/h discharge rates. The saturated zone of soil was maintained only beneath the 8.0 L/h dripline. The depth of the wetting front below the dripline was shallowest under microdrip irrigation treatment.

Elnesr et al. (2013) presented a study about the effects of dual-drip subsurface irrigation and a physical barrier on water movement and solute transport in soils using HYDRUS simulations. In his study, three technologies were used to enhance a spatial distribution of water and solutes in the root zone and to limit downward leaching. The three technologies

include (a) a physical barrier, (b) a dual-drip system with concurrent irrigation, and (c) a dual-drip system with sequential irrigation. The results indicate that the physical barrier is more efficient than dual-drip systems in enhancing the water distribution in the root zone while preventing downward leaching. On the other hand, the dual-drip system improves water distribution in sandy soils.

3 Materials and Methods

This study aims to evaluate the effect of different discharge rates, frequency and spacing between drippers on the spatial and temporal changes that occur over the width and depth of the advancing of the wetting front under two simultaneously-working surface drippers. This chapter outlines the step-by-step procedures required to achieve these goals.

In this chapter, we study the modeling of different factors such as soil hydraulics, water quantity, crop properties which have a strong influence on the selection of the emitters, their spacing, and the discharge rate. Based on this it is clear that information about the dimensions of the wetted zone in the soil which forms beneath the emitter(s) is an important prerequisite at the beginning of the drip irrigation design process.

3.1 The study area

3.1.1 Geographical, and topographical properties

The field experiment was conducted at a private farm, located in Oum Drou province of Chlef Algeria. The field is geographically located at coordinate of 1° 27'20"E, 36 ° 13'60"N Figure3-1, the average elevation of 150 m above sea level. The climate site is classified as semi-arid with mild wet winter and hot dry summer.

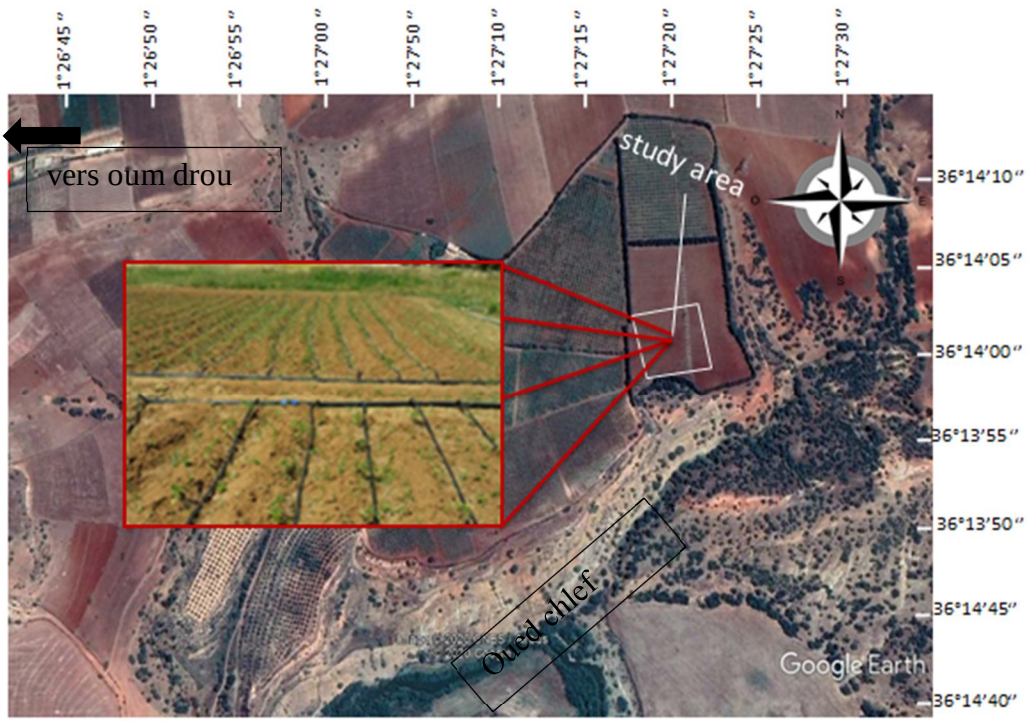

Fig.3. 1 : Location map of the studied area (Google Earth, 2020).

This area is characterized by a semi-arid climate with erratic rainfall distribution.

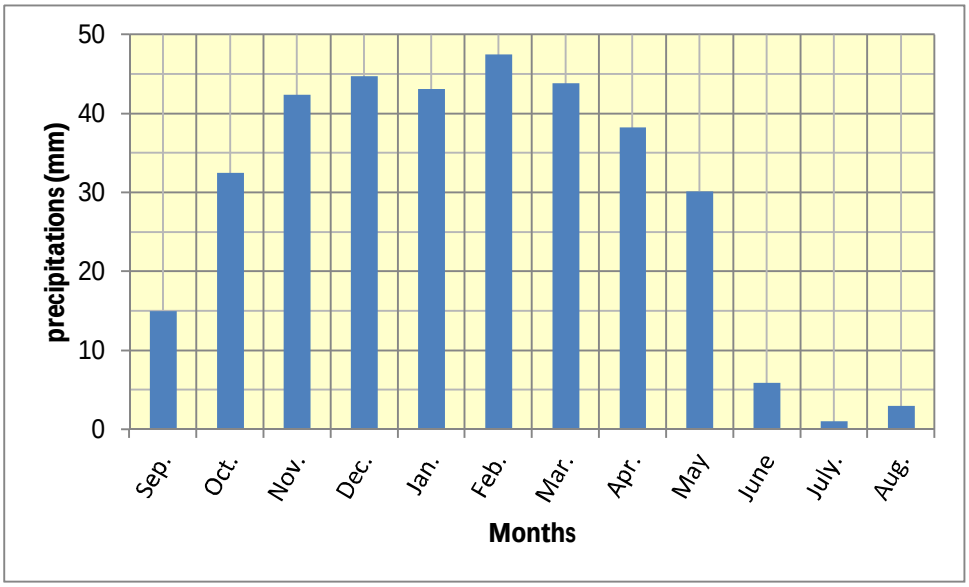

Fig.3. 2 : Monthly variation of precipitation (mm) 1998-2016 for study area (ONM Chlef , Algeria, 2016).

Figure3-2 show that the rainfall lasts for 6 months from November to April, with an average annual precipitation of 400 mm.

The mean annual temperature is about 28 ° C, the average reference evapotranspiration is 9 mm d^{-1}. The experimental site's area is 1.4 ha (140 m x 100 m) with average gradient of 1 $mm.m^{-1}$.

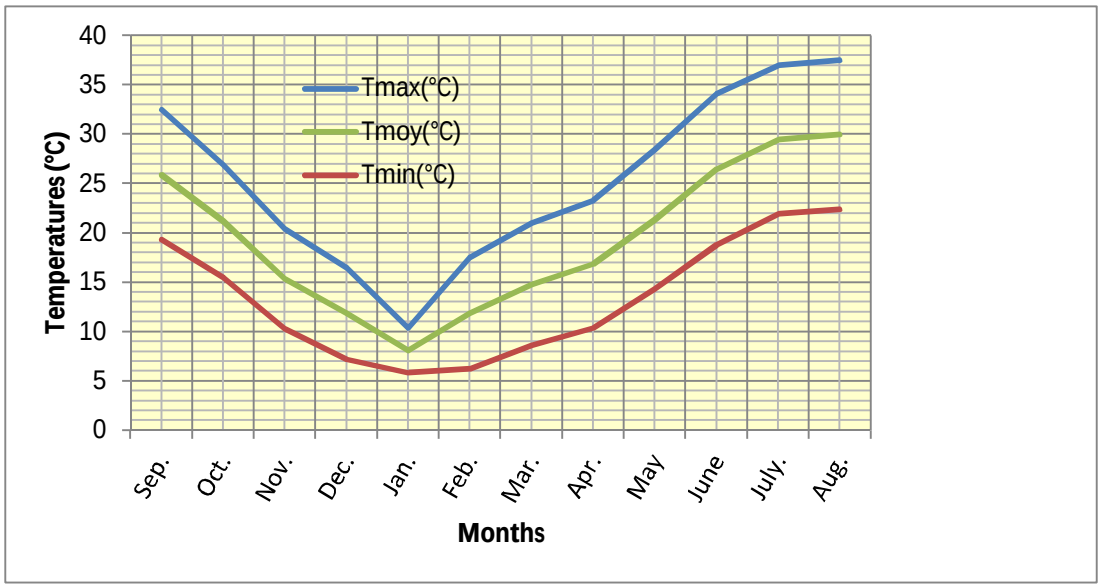

Fig.3. 3 : Monthly variation of temperature (°c) 1998-2016 for study area (ONM Chlef , Algeria, 2016)

The choice of this study site is motivated by the appropriate technical management of the tomato crop

3.1.2 Soil analysis

Determination of the Soil texture was necessary for characterization soil quality. The soil samples were obtained from the site using a hand auger at depths from 20 to 80 cm below land surface, and then they were analyzed in the laboratory to determine particle size distribution. The particle size analyzes were carried out by dry sieving for fractions greater than 2mm according to NF standard X 11-507 while the fine fraction were analyzed by sedimentation according to ASTM D422.

The analysis results show that the studied soil has a sandy-loam texture ("Soil Texture Calculator," Online Web Soil Survey, March 16, 2020), with an average permeability of 12 $mm.h^{-1}$.

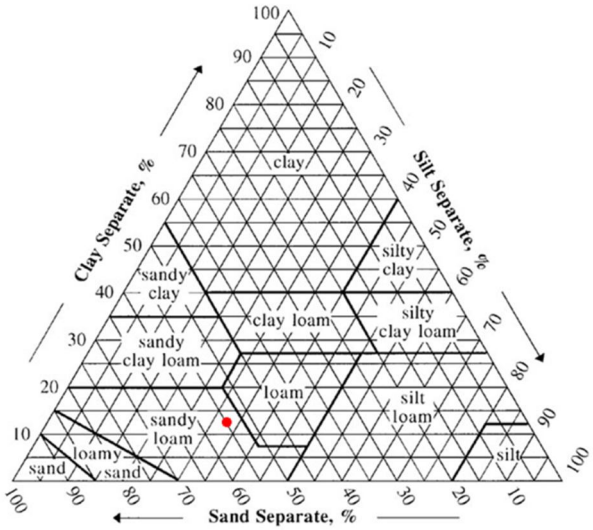

Fig.3. 4 : Soil texture of study area USDA soil textural triangle (USDA, 2020).

For measuring the soil bulk density five cylindrical metal samplers for which the volume was 60 cm^3,were used for collecting soil samples they were taken from 0-20,20-40,40-60 and 60-80 cm below surface at different locations in the study area and stored in a plastic bag for later drying and weighing, After sampling the cylindrical metal samplers was weighed to obtain the wet weight, After that they were placed in ovens at 105 degrees Celsius for a minimum of 24 hours for drying, and then they were weighed again to obtain the dry weight table 3-1and Figure 3-5 shows pictures of the soil analysis.

Fig.3. 5 : Preparing soil samples to analyses.

Table 3. 1 : Soil moisture content at different depth and times in the study area.

Depth (cm)	Tube number	moisture content %						
		t=0h	t=0,5h	t=1h	t=5h	t=12h	t=24h	t=48h
0-20	1-1	12.99	28.65	27.57	21.29	19.87	20.65	19.57
	1-2	12.70	29.48	27.30	21.40	20.24	20.51	18.97
20-40	2-1	12.04	30.98	27.47	20.40	20.64	20.28	21.00
	2-2	12.59	30.01	24.82	21.10	20.72	20.32	19.30
40-60	3-1	11.23	30.75	26.83	21.63	20.77	19.48	18.64
	3-2	11.33	29.11	26.33	21.94	20.99	19.64	19.39
60-80	4-1	12.22	31.69	27.19	21.93	20.15	19.63	18.73
	4-2	12.40	30.68	26.66	21.37	20.17	19.83	20.41

Dry Bulk density ρ_s is calculated by the following equation:

$$\rho_s = \frac{M_s}{V_s} \qquad (3.1)$$

Where M_s and V_s were the mass and volume of the soil sample respectively. The values represent the mean with number of samples which gives an average bulk density of 1,45 $t.m^{-3}$.

Table 3. 2 : Soil properties for study sites.

Depth, cm	Sand, %	Silt, %	Clay, %	Bulk density, g/cm3
0-20	56	32	12	1.45
20-40	52	32	16	1.45
40-60	52	40	8	1.45
60-80	60	28	12	1.45
80-100	48	32	20	1.45

3.1.3 Vegetative cover

The crop that was field plant is the tomato known as botany (Lycopersicon *esculentum* Mill..), which is one of the most prevalent crops in the Chlef area, however, this plant belongs to the Solanaceae family Figure 3.6. This family includes other species that are also well known, such as potato, pepper, and eggplant. The most cultivated varieties in Algeria are: Universal Mech, Riogrande, El Gon, Castlong, Heintz, Sabra, Zenith, Nema, Pico De Aneto, Roma (ITCMI, 2018)

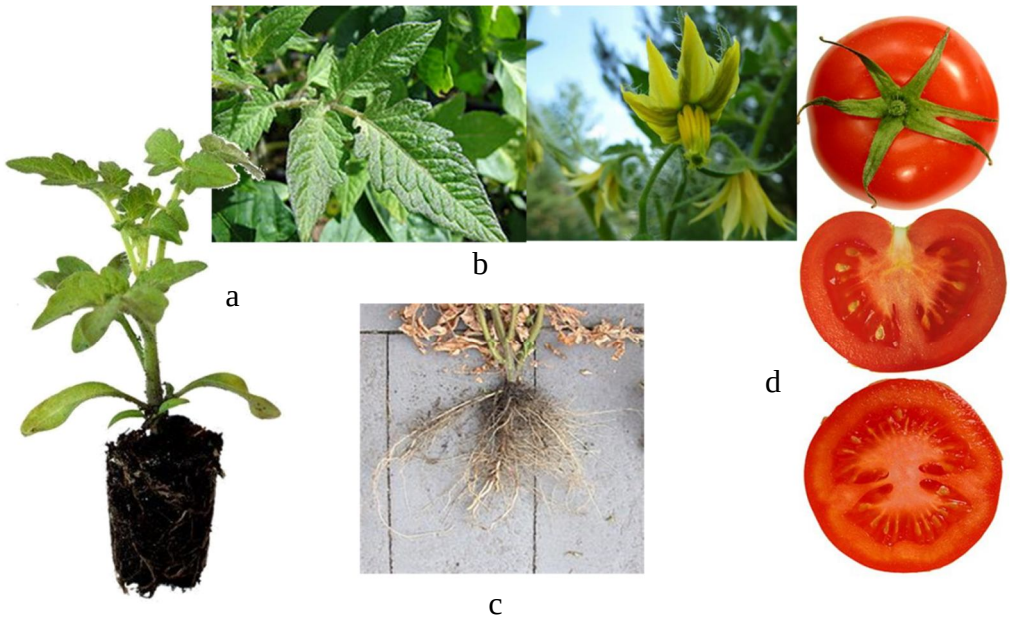

Fig.3. 6 : Tomato plant.
a: leafs, b: flowers c: roots d: fruits (ITCMI, 2018).

The root system of the tomato is of the pivoting type, being very dense and branched on the first 30 centimeters, to reach then one meter of depth.

3.2 HYDRUS-2D/3D Simulations

The numerical model HYDRUS -2D/3D Version 2 (Šimůnek et al., 2006), is a well-known windows based computer software package for simulating water, heat, and/or solute movement in two-dimensional, variably-saturated porous media.

HYDRUS enables, simulation of both simple and complex geometries for homogeneous or heterogeneous soils and for different combinations of initial and boundary conditions (BC) (Elnesr et al., 2013). The model was run for the main processes of water flow and root water uptake.

Basic input data required by the model include the values of soil parameters, spatial root distribution, Soil water evaporation (Ev), precipitation and irrigation. The model can deal with prescribed head and flux boundaries, controlled by atmospheric conditions, as well as free drainage boundary conditions. A detail description of model and related theory is presented in the documentation of version 2.0 of HYDRUS-2D (Šimůnek et al., 2006)

Conventionally, the equation that governs Darcian transient water flow in a rigid porous and variably saturated medium is Richards's equation (Richards, 1931). This equation combines the mass balance or continuity equation with a Darcy-Buckingham equation which is describing uniform flow in soils.

$$\frac{\partial \theta(h)}{\partial t} = \frac{\partial}{\partial x_i}\left[K(h)\left(K_{ij}^{A}\frac{\partial h}{\partial x_j} + K_{iz}^{A}\right)\right] - S \qquad (3.2)$$

where θ is the volumetric water content [L^3 L^{-3}], h is the pressure head [L], S is a sink term [T^{-1}] usually representing the root water uptake, x_i(i=1,2) are the spatial coordinates [L], t is time [T], K_{ij}^{A} are components of a dimensionless anisotropy tensor $\boldsymbol{K}_A$, and K is the unsaturated hydraulic conductivity function [LT^{-1}] given by :

$$K(h, x, y, z) = K_s(x, y, z)K_r(h, x, y, z) \qquad (3.3)$$

Where Kr is the relative hydraulic conductivity and *Ks* the saturated hydraulic conductivity [LT^{-1}]. The anisotropy tensor *KijA* in (3.2) is used to account for an anisotropic medium. The diagonal entries of *KijA* equal one and the off-diagonal entries zero for an isotropic medium. If (3.2) is applied to planar flow in a vertical cross-section, $x1=x$ is the horizontal coordinate and $x2=z$ is the vertical coordinate, the latter taken to be positive upward. Einstein's summation convention is used in (3.2) and throughout this report. Hence, when an index appears twice in an algebraic term, this particular term must be summed over all possible values of the index.

In our study the water movements are simulated using the HYDRUS 2D / 3D model. This software is able to simulate the transfer of solutes in saturated two or three dimensional porous media. HYDRUS therefore numerically solves the Richards equation.

The Richards equation governing water flow from a point source through variably saturated porous media can be written in spatial coordinates as follows:

$$\frac{\partial \theta}{\partial t} = \frac{\partial}{\partial x}\left[K(\theta)\frac{\partial h}{\partial x}\right] + \frac{\partial}{\partial y}\left[K(\theta)\frac{\partial h}{\partial y}\right] + \frac{\partial}{\partial z}\left[K(\theta)\frac{\partial h}{\partial z}\right] + \frac{\partial K(\theta)}{\partial z} - S(h) \qquad (3.4)$$

where θ is the volumetric water content [L^3L^{-3}], t is the time [T], h is the soil water pressure head [L], z is the vertical coordinate that is positive upward [L], $K(\theta)$ is the unsaturated hydraulic conductivity [LT^{-1}], and $S(h)$ is the sink term representing root water uptake expressed as a volume of water removed from a unit volume of soil per unit time [$L^3L^{-3}T^{-1}$] (Feddes et al., 1978) defined S as :

$$S(h) = \alpha(h)S_p \qquad (3.5)$$

where α(h) is the water stress response function of the soil water pressure head ($0 \leq \alpha \leq 1$) (Figure. 3.7), and Sp is the potential water uptake rate [T-1].

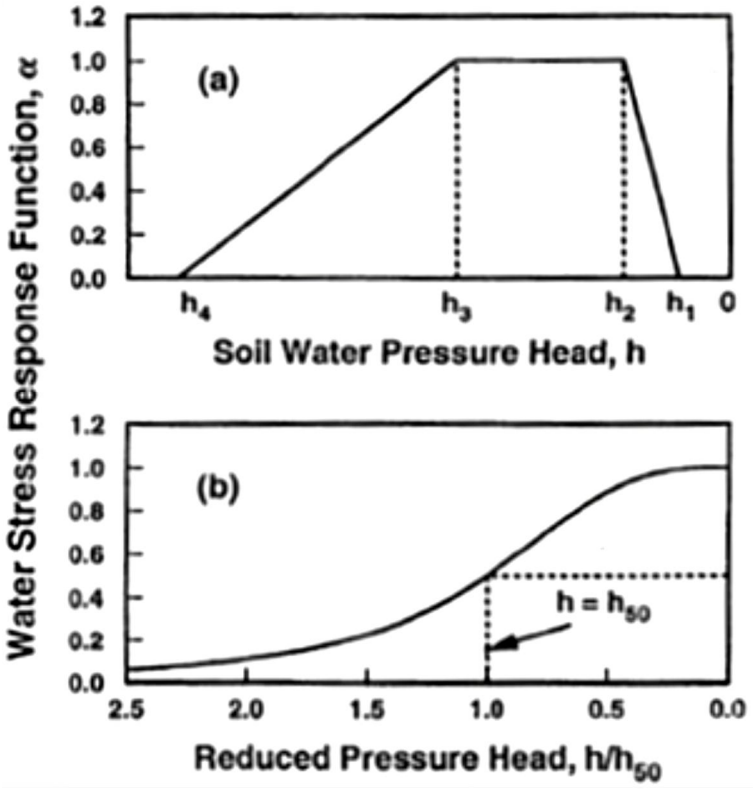

Fig.3. 7 : Schematic of the plant water stress response function, α(h),
as used by a) Feddes et al.(1978) and b) van Genuchten (1987).

The variable S_p in (3.5) is equal to the water uptake rate during periods of no water stress when α (h)=1. van Genuchten, (1980)expanded the formulation of Feddes by including osmotic stress as follows:

$$S(h, h_{\emptyset}) = \alpha(h, h_{\emptyset})S_p \qquad (3.6)$$

Where h_{φ} is the osmotic head [L],

van Genuchten, (1978) proposed an alternative S-shaped function to describe the water uptake stress response function (Figure. 3.7b), and suggested that the influence of the osmotic head reduction can be either additive or multiplicative as follows

$$\alpha(h, h_{\emptyset}) = \frac{1}{1 + \left(\frac{h + h_{\emptyset}}{h_{50}}\right)^{P}} \qquad (3.7)$$

Where p, is a experimental constant. The parameter h_{50} in (3.7) represent the pressure head at which the water extraction rate is reduced by 50%. Similarly, $h_{\phi 50}$ represents the osmotic head at which the water extraction rate is reduced by 50%.

When the potential water uptake rate is equally distributed over a two-dimensional rectangular root domain, S_p becomes

$$S_p = \frac{1}{L_x L_z} L_t T_p \qquad (3.8)$$

Where T_p is the potential transpiration rate [LT-1], L_z is the depth [L] of the root zone, L_x is the width [L] of the root zone, and L_t is the width [L] of the soil surface associated with the transpiration process.

Equation (3.8) may be generalized by introducing a non-uniform distribution of the potential water uptake rate over a root zone of arbitrary shape

$$S_p = b(x, z) L_t T_p \qquad (3.9)$$

Where *b(x,z)* is the normalized water uptake distribution [L^{-2}].

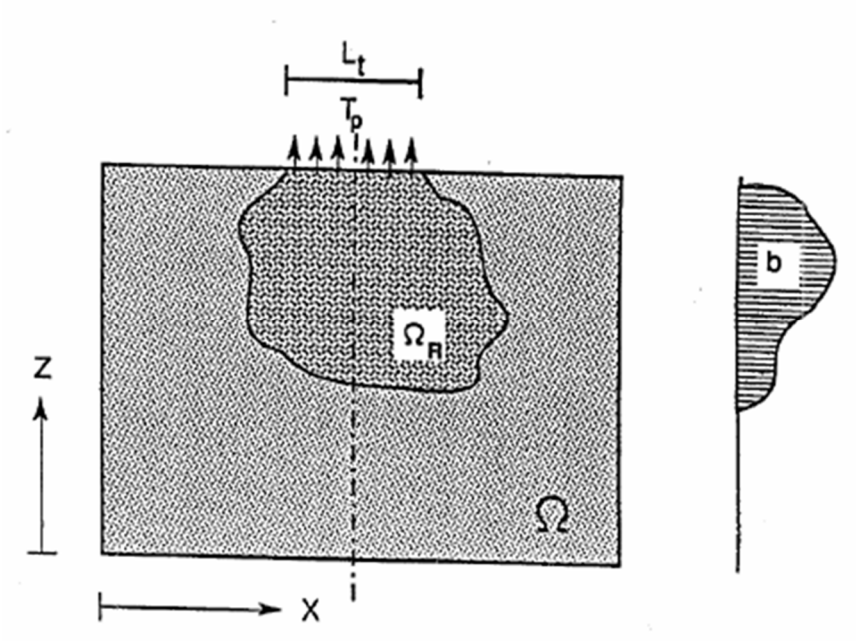

Fig.3. 8 : Schematic of the potential water uptake distribution function, b(x,z), in the soil root zone van Genuchten, (1978).

This function describes the spatial variation of the potential extraction term, S_p, over the root zone (Figure. 3.8).

3.2.1 The Unsaturated Soil Hydraulic Properties

The soil water retention, *θ(h),* and hydraulic conductivity, *K(h),* functions according to Brooks are given by:

$$S_e = \begin{cases} |\alpha h|^{-n} & h < -1/\alpha \\ 1 & h \geq -1/\alpha \end{cases} \qquad (3.10)$$

$$K = K_s S_e^{2/n+l+2} \qquad (3.11)$$

Where S_e is the effective water content

$$S_e = \frac{\theta - \theta_r}{\theta_s - \theta_r} \qquad (3.12)$$

HYDRUS2 implements the soil hydraulic functions of Van Genuchten (1980) who used the statistical pore-size distribution model of Mualem (1976) to obtain a predictive equation for the unsaturated hydraulic conductivity function in terms of soil water retention parameters. The expressions of Van Genuchten (1980) are given by:

$$\theta(h) = \begin{cases} \theta_r + \dfrac{\theta_s - \theta_r}{[1 + |\alpha h|^n]^m} & h < 0 \\ \theta_s & h \geq 0 \end{cases} \qquad (3.13)$$

$$K(h) = K_s S_e^l \left[1 - \left(1 - S_e^{\frac{1}{m}}\right)^m\right]^2 \qquad (3.14)$$

Where

$$m = 1 - \frac{1}{n}, \quad n > 1 \qquad (3.15)$$

With

θ_r and θ_s denote the residual and saturated water content, l the pore-connectivity parameter was estimated to be about 0.5 as an average for many soils (Mualem, 1976), n is a pore-size distribution index, α is the inverse of the air-entry value

3.2.2 Simulation criteria:

The current model takes into consideration several theoretical assumptions of soil-water relations to simulate the following circumstances:

1. Soil is assumed to have uniform physical properties, homogeneous and isotropic;
2. The initial water content is assumed to be uniform;
3. Darcy's law is applicable to saturated and unsaturated zones;
4. The hydraulic conductivity of the soil, and all its derived functions, are differentiable, continuous and single-valued functions of moisture content;
5. Root depth was assumed to be 30 cm.

3.2.3 Domain properties

The HYDRUS 2D/3D model was used to simulate soil moisture distribution patterns between two simultaneously working surface drippers.

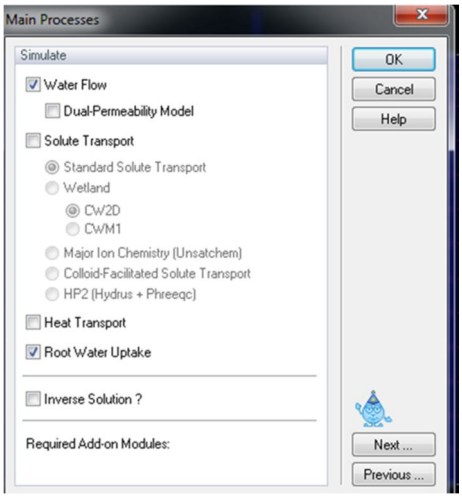

Fig.3. 9 : Main Processes Category (*Hydrus 2D/3D V 2.02.0680*, 2012).

The model starts by inputting parameters in the various categories in the Pre-processing menu on the left-hand side as shown in Figure 3.9.

Figure 3.9 shows simulation selections that can be made in the Main Process category, for our simulations we chose water flow and root water uptake. The Geometry category shown in Figure 3.10 below, allows the user to specify length units, type of flow to be modeled, geometry type, soil layers and soil materials. The general geometry type allows the user to draw the object to be modeled and the rectangular geometry type requires the user to input width and length. In our simulations, we chose 2D vertical flow for our landfill simulations.

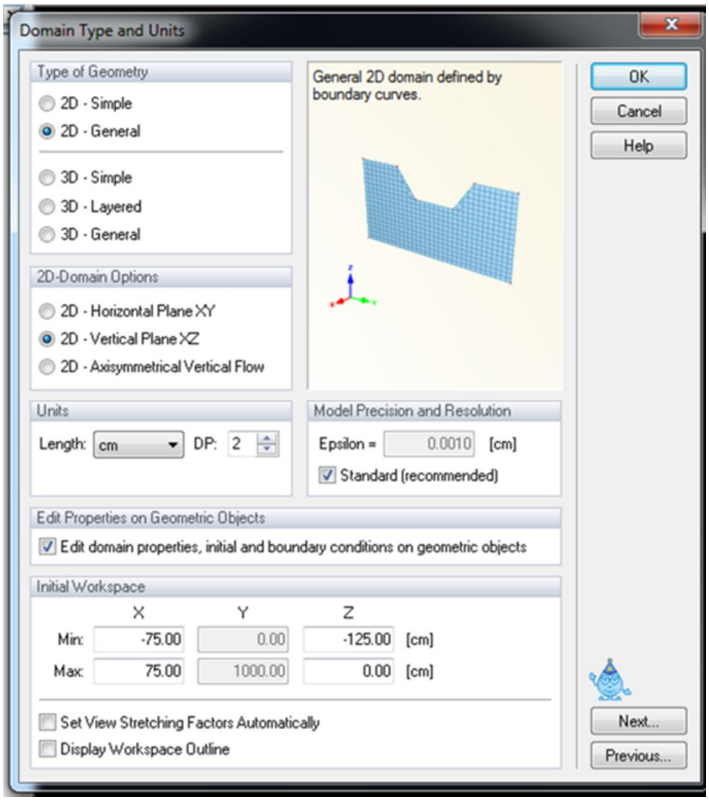

Fig.3. 10 : Geometry Information Category (*Hydrus 2D/3D V 2.02.0680,* 2012).

The flow domain (150 x 125 cm) was discretized into 20045 2D triangular finite elements with triangles significantly smaller around the source and then smoothly increasing with distance from the source. The half circle of the source was represented with 43 nodes.

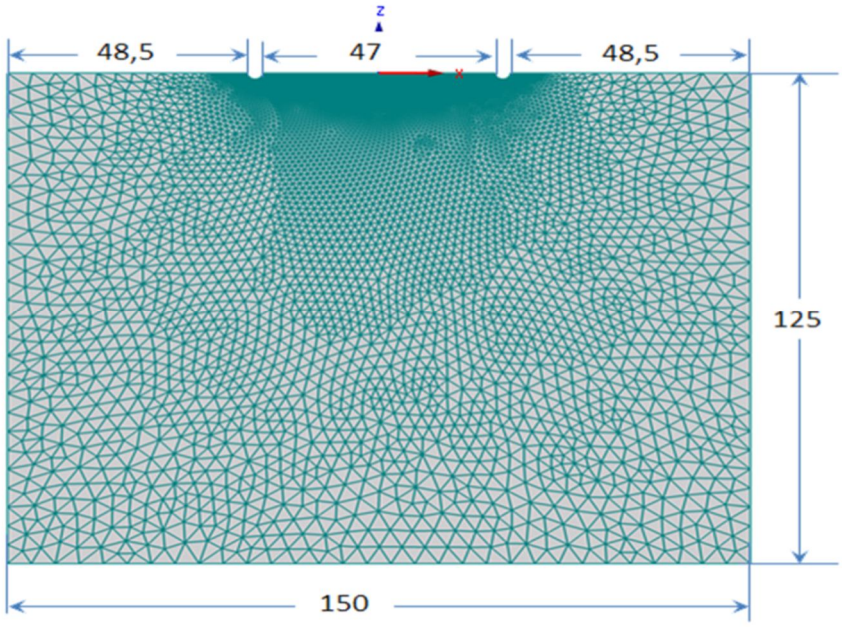

Fig.3. 11 : Discretized using unstructured finite element MESH considered in HYDRUS simulations of the flow domain.

Unstructured finite element MESH was generated using automatic triangulation that is implemented in HYDRUS-2D and that uses an algorithm based on the Delaunay's triangulation (Šimůnek et al., 1999) Fig 3.11.

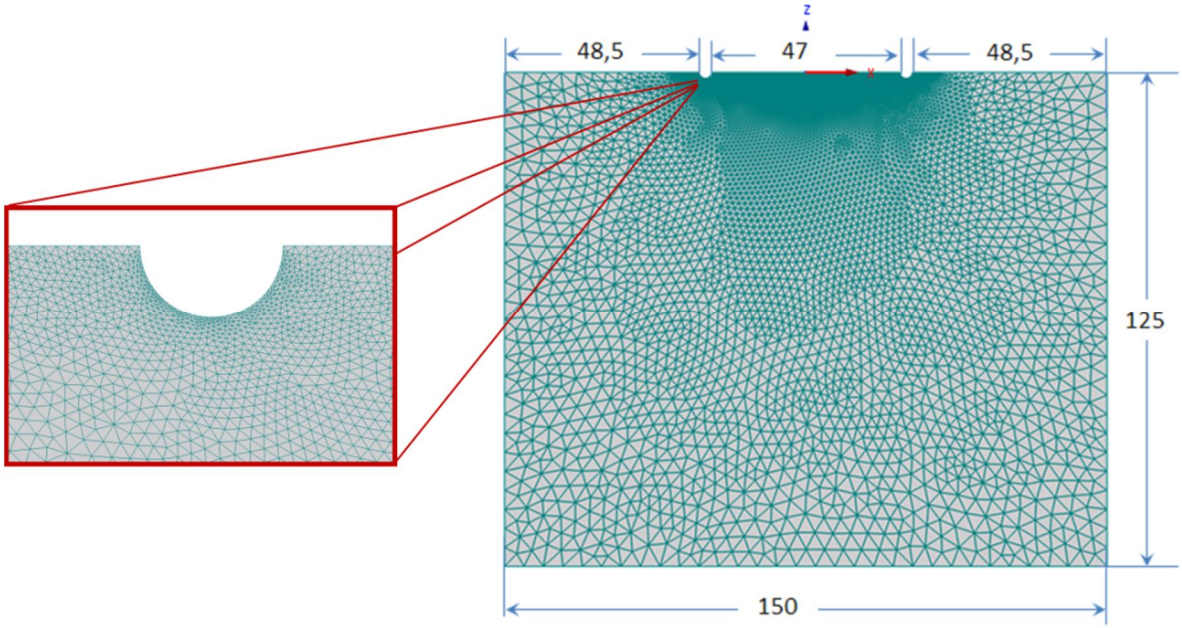

Fig.3. 12 : Location of the emitters in the transport domain (discretized using unstructured finite element MESH) considered in HYDRUS simulations, domain around a dripper is magnified in excerpts. Dimensions are given in cm.

Figure 3.12 shows the location of the emitters in the transport domain considered in HYDRUS simulations when the domain around a dripper is magnified in excerpts.

3.2.4 Time information

Under this section, time units, temporal discretization, and time-varying boundary conditions can be defined.

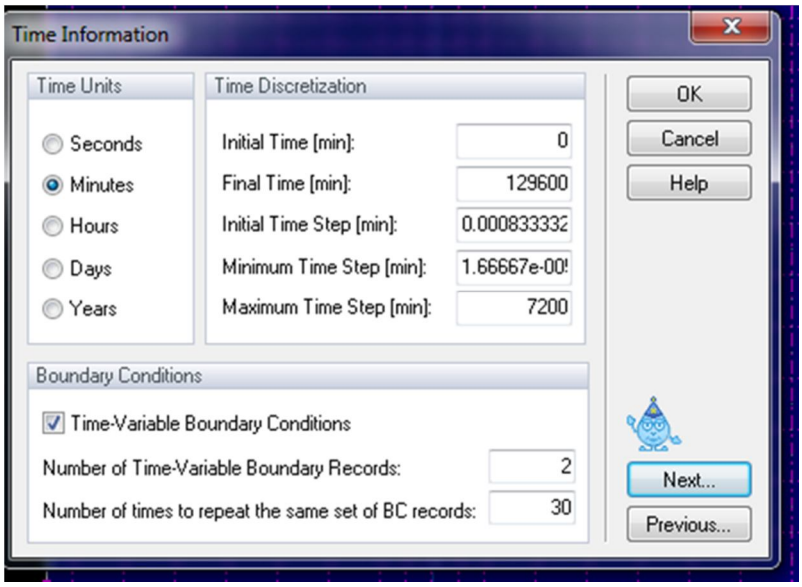

Fig.3. 13 : Time Information Category (*Hydrus 2D/3D V 2.02.0680*, 2012).

In figure 3.13, the unit of time was selected in minutes and the three month period was used for simulation purposes (129600 minutes) which is the typical period for tomatoes.

3.2.5 Boundary and Initial conditions

Boundary conditions were an important part of the simulation. They did not constitute numeric inputs but decided how the other inputs were being calculated by HYDRUS (2D/3D). Choosing realistic boundary conditions is one of the most important and challenging parts of setting up a simulation. The 2D soil profile in this model has four external boundaries which are the soil surface, left side, right side, and bottom of the profile; plus an internal boundary lining the hollow circular of the emitter. Each of the five boundaries needed to be specified a boundary setting for water flow and solute transport.

3.2.6 Soil hydraulic parameters

For water flow, in this study the following assumptions and assertions are considered:
In the soil hydraulic model control window, the hydraulic model and the hysteresis can be defined.

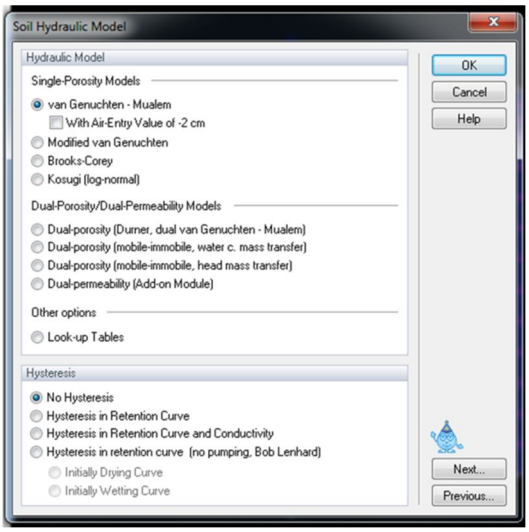

Fig.3. 14 : Soil hydraulic Category (*Hydrus 2D/3D V 2.02.0680*, 2012).

There are different hydraulic models that can be used as shown in Figure 3.14, in our case, In this research, van Genuchten-Mualem single porosity model was selected, and then without hysteresis.

The parameters needed for various soil hydraulic models, managed by Equation (3.13, 3.15) are residual and saturated water contents, saturated hydraulic conductivity, pore connectivity parameter, and empirical coefficients Alpha and n.

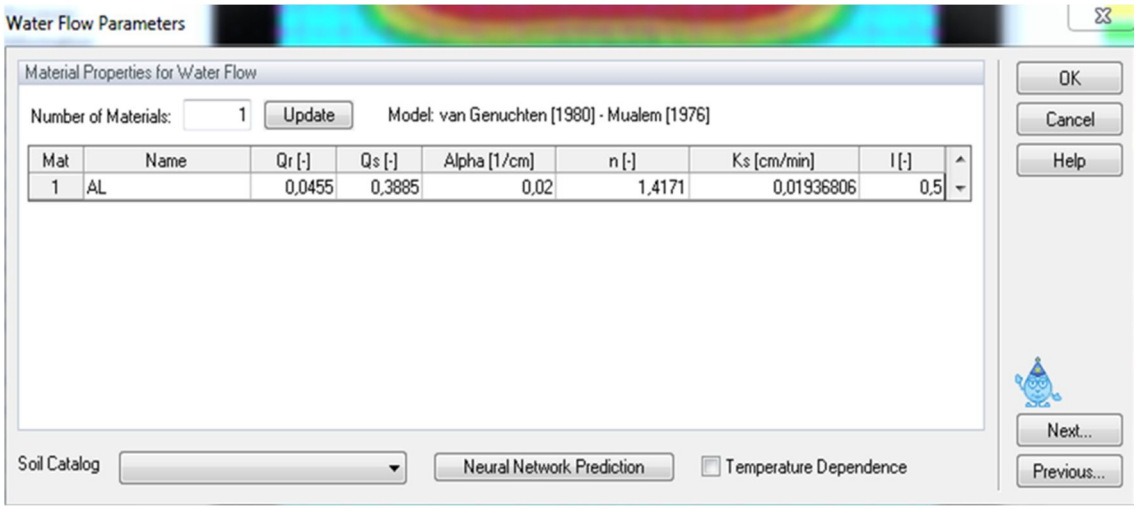

Fig.3. 15 : The transport domain with applied boundary conditions (*Hydrus 2D/3D V 2.02.0680*, 2012).

As well as the initial water content distribution. We estimated the hydraulic parameters using the ROSETTA pedotransfer model (Schaap et al., 2001) that is included in the HYDRUS software package. The Rosetta model is a neural network-based model that predicts hydraulic parameters from soil texture and related data, it's can be used to estimate water

retention parameters according to van Genuchten, saturated hydraulic conductivity, and unsaturated hydraulic conductivity parameters according to van Genuchten and Mualem.

To achieve this, the model uses a database of measured water retention and other properties for a wide variety of media. For a given a medium's particle-size distribution and other soil properties, the model estimates a retention curve with good statistical comparability to known retention curves of other media with similar physical properties. As the model uses basic more easily measured data, it is considered as a pedotransfer function model (PTFs) (Schaap et al., 2001).

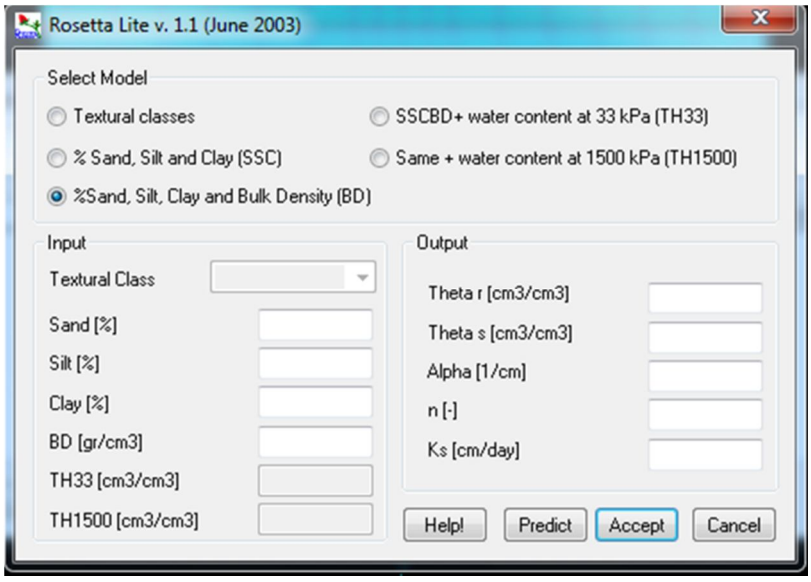

Fig.3. 16 :The dialog window of ROSETTA pedo-transfer model (*Hydrus 2D/3D V 2.02.0680*, 2012).

It's clearly show in figure 3.16., that the use of more input data (predictors) often leads to better predictions, but if only texture is available, Rosetta can still be very useful (Schaap et al., 2001). In this case only soil texture data, as presented in Table 3-2, was used as input. The hydraulic parameters obtained for soil texture class are listed in Table 3-3.

Percentage of sand, silt, and clay together with the bulk density for different soil layers were used to get values of all the parameters needed, that are given in Table 3-1.

Table 3. 3 : Physical properties of soil considered in HYDRUS Simulation (Parameters for the van Genuchten–Mualem model) .

Soil texture	**Bulk density (g cm^{-3})**	**θ_r (cm^3 cm^{-3})**	**θ_s (cm^3 cm^{-3})**	**α (cm^{-1})**	**n (-)**	**Ks (cm min^{-1})**	**l (-)**
Sandy loam	1.45	0.0455	0.3885	0.02	1.4171	0.01936806	0.5

3.2.7 The initial and boundary conditions:

Water flow boundary conditions are selected under this section. In all simulated scenarios, the soil surface of the transport domain was subjected to atmospheric conditions, in green color, while the lower boundary of the domain was free drainage, in blue color. Boundaries at the left and right sides of the soil profile were assigned a ‘‘no-flux’’ (impermeable) boundary, in purple color, so it was assumed that water did not flow horizontally across these boundaries. Finally, Emitters were represented in all cases as half circles with a radius of 1,5 cm, located on the right and left upper boundary of the transport domain at ±23,5 cm.

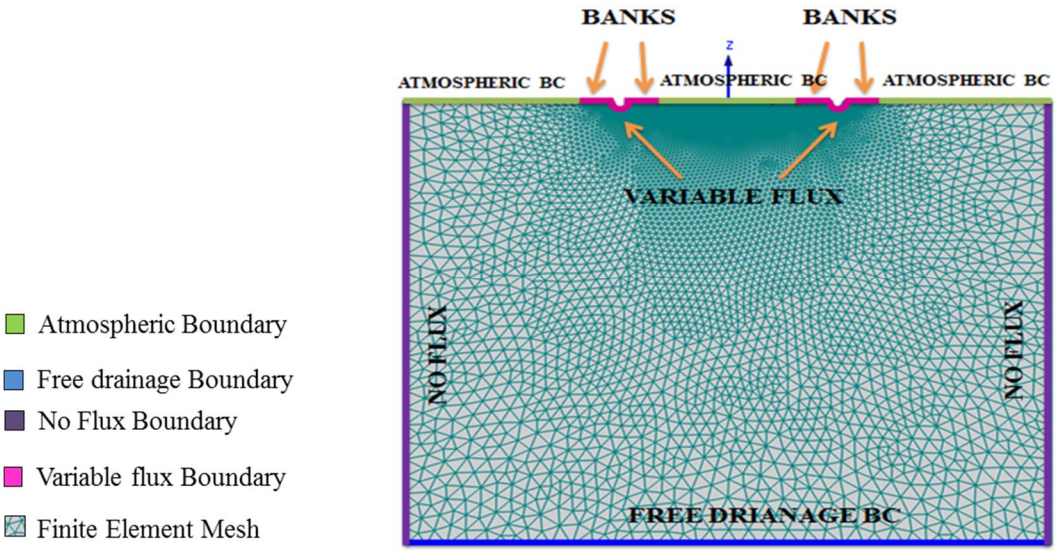

Fig.3. 17 : The transport domain with applied boundary conditions.

When the value of flux is greater than the soil's infiltration, we assumed that runoff will accurate a distance b to the right and left of the emitters, in magenta color, which will increase the influence of flow area and thus the amount of flux. The emitters were assigned a ‘‘Variable Flux 1’’ boundary conditions, Figure 3.17.

The initial water conditions were specified in terms of pressure heads. Was a key setting which could dictate the water balance for as much the total time of simulation, the pressure head was set as same value for all nodes and equal to -400 cm.

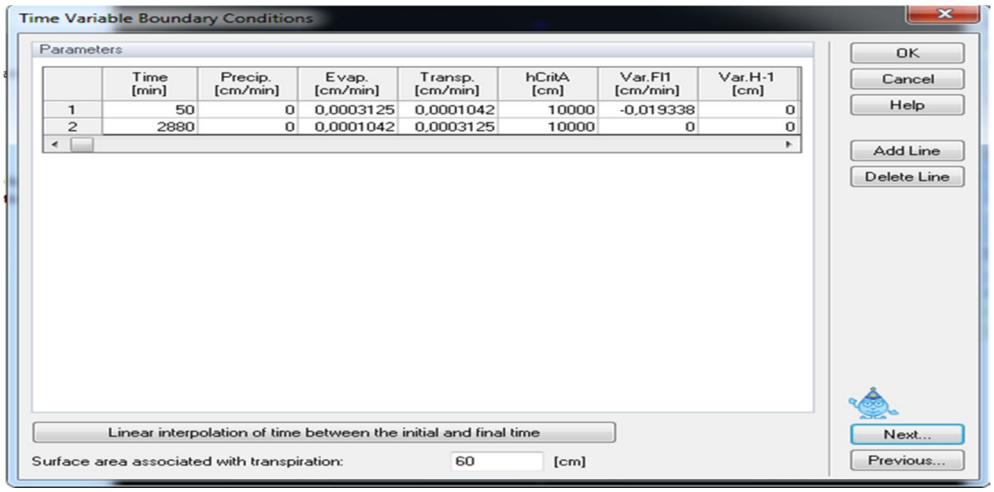

Fig.3. 18 : Variable Boundary Conditions window (*Hydrus 2D/3D V 2.02.0680,* 2012).

The transpiration rate was considered to be constant with time and equal to 0,45 mm/day Figure 3.18.

3.2.8 Root Water Uptake:

The HYDRUS 2D / 3D numerical model was used to modeling dynamics water and study the management of surface irrigation taking into account the root water uptake and spatial root distribution.

When root water uptake is modeled, the relevant box in “Main Processes”should be checked Figure 3.9, There are two models that define how transpiration is reduced below potential when the soil is no longer able to supply the amount of water demanded by the plant under the prevailing weather conditions: one by Feddes, commonly used, known as the Feddes model, and the other by van Genuchten,

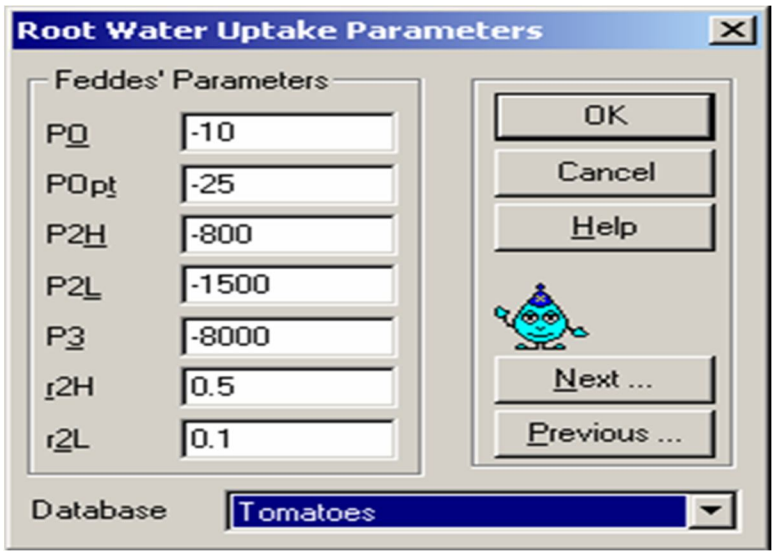

Fig.3. 19 : Feddes parameters (*Hydrus 2D/3D V 2.02.0680,* 2012)

The Feddes model assigns plant transpiration rates according to the soil's pressure head. Feddes' model parameters are shown in Figure 3.19.

With:

P0: Value of the pressure head below which roots start to extract water from the soil.

Popt: Value of the pressure head below which roots extract water at the maximum possible rate (potential transpiration).

P2H: Value of the limiting pressure head below which roots no longer extract water at the maximum rate (assuming a potential transpiration rate of r2H).

P2L: As above, but for a potential transpiration rate of r2L.

P3: Value of the pressure head below which root water uptake ceases (usually taken at the wilting point).

r2H: Potential transpiration rate (L/T) (currently set at 0.5 cm/day).

r2L: Potential transpiration rate (L/T) (currently set at 0.1 cm/day).

The parameters of the root absorption model, which represents the terms of the water stress response function for water uptake by plant roots (tomatoes) Feddés' are shown in Tables 3-4 and 3-5 respectively.

Table 3. 4 : Root water uptake parameters for analyzed crops.

crops	Values of the pressure head (cm) below which root water extraction					Limiting potential transpiration rates (cm/min)	
	Starts. (h_1)	Occur at the maximum possible rate (h_2)	Starts to decline from the maximum rate at the potential transpiration rate equals		Stops (h_4)		
			$(R_2^{High})(h_3^{High})$	$(R_2^{Low})(h_3^{Low})$		Highest (R_2^{High})	Lowest (R_2^{Low})
Tomatoes	-10	-40	-200	-1000	-8 000	0.003472	6.944e-5

Table 3. 5 : Parameters describing a spatial root distribution for analyzed crops.

Tomatoes Parametres	
Maximum rooting depth (cm)	40
Depth of maximum root uptake intensity (cm)	15
Maximum rooting radius (cm)	60
Radius of maximum root uptake intensity (cm)	15
Surface area associated with transpiration, AT(cm2)	10

3.2.9 Applied treatments for Hydrus simulation

The numerical model HYDRUS-2D/3D (v.2.02) was used with a purpose to simulate soil moisture distribution patterns between two simultaneously-working surface drippers for sandy-loam textural classes, different emitter discharge rates, different irrigation frequency and different spacing between emitter's were used.

The first treatment was the spacing between emitter's, thus 3 spacing were selected (30, 50, and 70cm).

During water application, The constant water flux per unit area (q) is equal to the emitter discharge rate (Q) at the modeled drip surface tape (2π R*L), where R is the radius of the drip tape, and L is the distance between two consecutive emitters.

When the value of flux is greater than the soil's infiltration on assumed that runoff will get at a distance b (emitter's runoff length) to the right and left of the emitters, which will increase the influence of flow area and thus the amount of flux, which we referred in this thesis by banks Figure 3.17 .

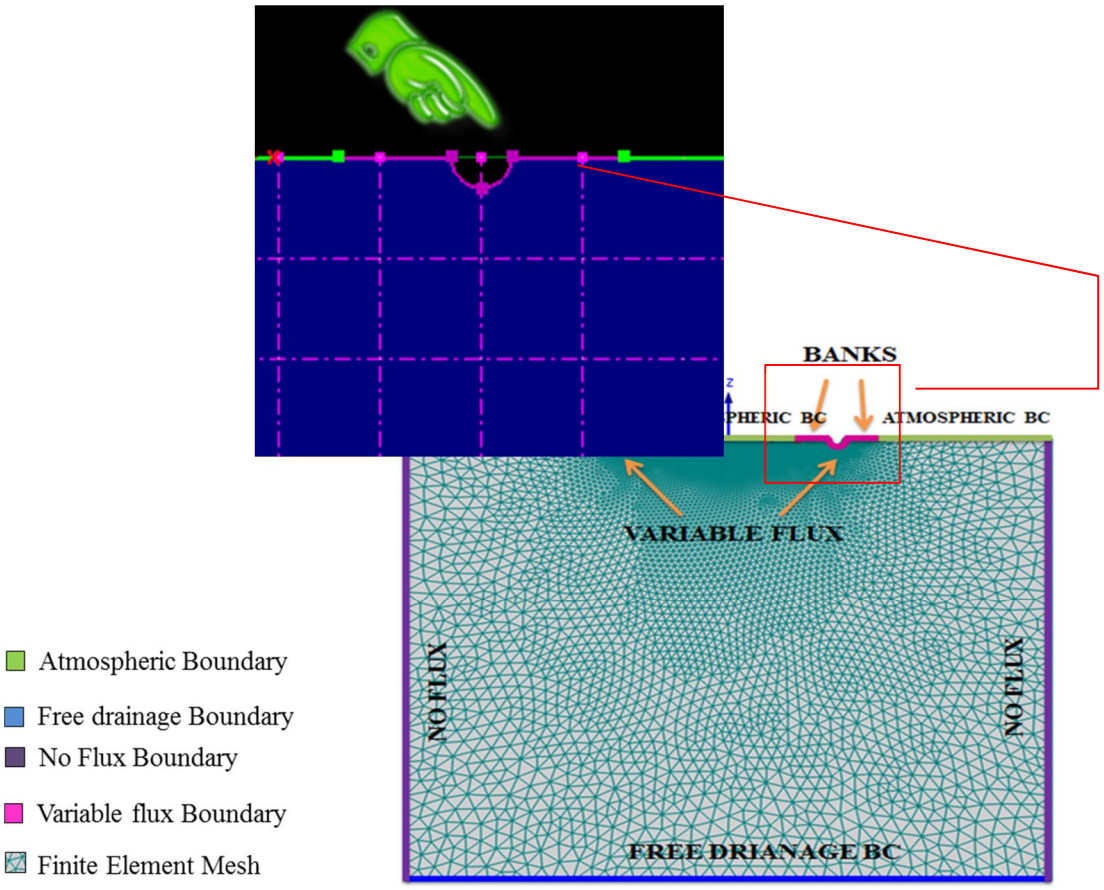

Fig.3. 20 : The transport domain with applied boundary conditions.

Each treatment is named by a code in it shows the spacing between the drippers the emitter's discharge and the frequency of irrigation

The table 3-6 given the parameters

The overall process of four irrigation flows applied in different treatments is presented in table 3.6 b and the detailed summary of simulated treatments were presented in Appendix 2

Table 3. 6 : Parameters and summary of simulated treatments.

Table 3.6.a: Parameters of simulated treatments

Simulated radius of emitter (cm)	1,5
Area of half cylinder A (cm^2)	471,24
runoff area	5600
Total area of the element	6071,2
Soil sat. hyd. Conductivity (cm min^{-1})	0,0737
Maximum allowable flux (cm min^{-1})	-0,0737
Minimum flux calculated with different discharge rate	-0,0505
Maximum flux calculated with different discharge rate	(0,0194)
Soil type	Sandy loam

table 3.6 b The overall process of four irrigation flows applied in different treatments

Nbre of treatment	distance between emitters (cm)	emitter's discharge (L h^{-1})	frequency (day)	duration (min)	Inverted calculations				Final corrected flux and area							
					Discharge (cm h^{-1})	Emitter's area (cm^2)	Total flux area (cm^2)	Flux (cm min^{-1})	Emitter's area (cm^2)	runoff area (cm^2)	Total area of flux (cm^2)	Max. Allow. Flux (cm min^{-1})	Rounded length bank(b) (cm)	runoff area (cm^2)	Total area of flux (cm^2)	Flux (cm min^{-1})
F50-1-3	**50**	**1**	**3**	**150**	**2000**	**471,24**	**471,24**	-0,071	**471,2**	**1247**	**1718**	**-0,0194**	**6.5**	**1300**	**1771**	**-0,0188**
F50-2-3	**50**	**2**	**3**	**75**	**4000**	**471,24**	**471,24**	**-0,141**	**471,2**	**2965**	**3436**	**-0,0194**	**15**	**3000**	**3471**	**-0,0192**
F50-3-3	**50**	**3**	**3**	**50**	**6000**	**471,24**	**471,24**	**-0,212**	**471,2**	**4683**	**5155**	**-0,0194**	**24**	**4700**	**5171**	**-0,0193**
F50-4-3	**50**	**4**	**3**	**40**	**8000**	**471,24**	**471,24**	**-0,283**	**471,2**	**6402**	**6873**	**-0,0194**	**33**	**6500**	**6971**	**-0,0191**

Figure 3-21 and table 3.6 b present an overview of the overall process of four irrigation flows applied in different treatments with each duration. In case (a) these drippers operate for 150 minutes at a flow rate of 1 $L.h^{-1}$, causing runoff (banks) of 65 mm on each side of the drippers. For cases b, c and d, the d discharge was considered to be 2, 3 and 4 $L.h^{-1}$ respectively, while the duration was 75, 50 and 40 minutes for cases b, c and d, respectively, banks are given by 150,235,325 mm respectively.

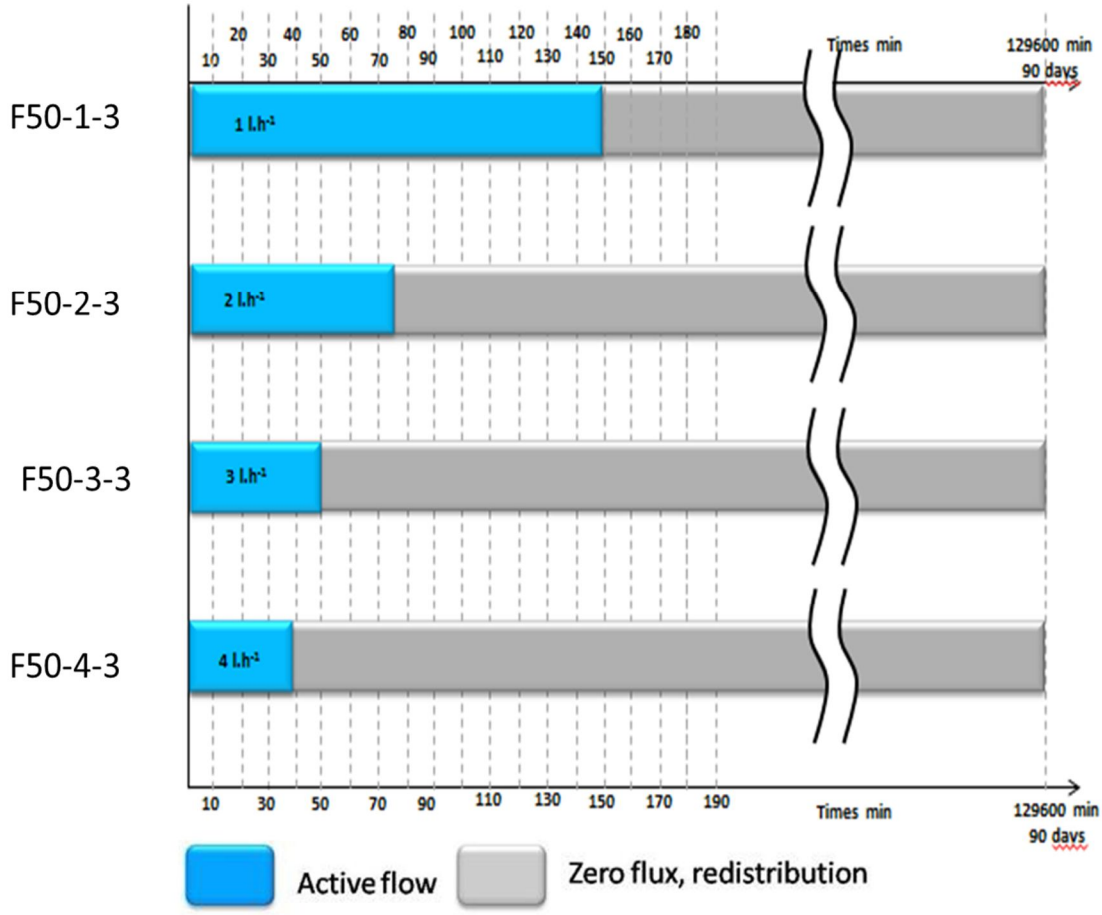

Fig.3. 21 : Irrigation fluxes applied in different scenarios.

Positions of soil wetting shape laterally outward and also vertically downward on the vertical and horizontal plane can be visually using a cross section (CS).

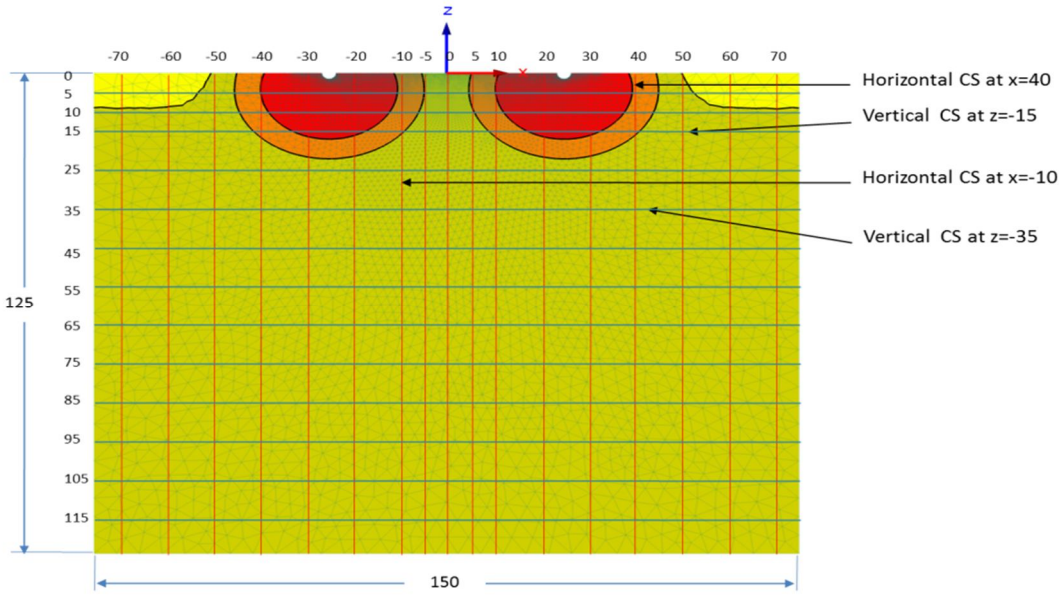

Fig.3. 22 : The analyzed cross section in the transport domain, dripper are presented as a half circle, vertical sections with the red color and the horizontal sections with the blue color.

Through the domain at any coordinates for more output with a growing time interval

The transport domain and the analyzed CS are illustrated in Figure 3-22.

3.3 Field experiment

3.3.1 Field layout

Four field experiment was planned to compare the treatments listed in Table 3-6 b out of 126 cases F50-1-3 and F50-2-3, F50-3-3 and F50-4-3,

Fig.3. 23 : View of the experimental plots with the four irrigation treatments.

Where were used with a discharge rate of 1,2,3 and 4 $L.h^{-1}$ with irrigation frequency of 3 day where it is most suitable for conditions Region, the experimental site, was part of a large field of 2.04 ha (240 m × 85 m).

These experiments were designs with 5 replicates in the tomato crop experiment. In April 2017 figure 3-22.

3.3.2 Field preparations

Before embarking on the preparation of the soil, one has to observe the state of the soil of the plot to be planted. Indeed, the soil is moderately heavy to a depth of (40 cm), hence mechanical work is required. The site was initially prepared using shallow discs to remove surface grasses and clean the surface of the soil, the establishment of the plants is carried out manually.

3.3.3 Field measurements:

Among the objectives of simulations the study of the influence of four different emitter discharge rates (1,2,3 and 4 L / h).During the growing season, some observations were recorded about the status of growing, and the amount of water taken, for each section in the field experiment. pressure heads measurements are carried out at different depths using tensiometers. The moisture pattern was measured and followed several times after and before irrigation.

Soil moisture was measured in the field using a portable digital a moisture meter soil (PMS 710, China) this device is composed of a measurement electronic unit connected via a coaxial cable and a connecting head to a length of transmission line L (the probe), the measurement of the moisture carried out by placing in the soil the probe, every 10 minutes and averaged hourly for a period of 90 days (growing season). Measurements were collected for the four irrigation treatments.

3.3.4 TDR Field Calibration

We have calibrated the probe by comparing its results to the gravimetric method (table 3-1), After taking gravimetric and device measurements a calibration equation was performed to calculate moisture content percent in soil from the count ratio of any reading.

Fig.3. 24 : Calibration curve of the moisture meter PMS 710.

Figure 3-24 shows the calibration chart and equation values for calibration moisture meter PMS 710.

3.3.5 Experimental design

The tomatoes were grown according to the recommendation of the Technical Institute of vegetable and industrial crops in Algeria ITCMI. The tomato plants were planted on April 5, 2017 in rows spaced 0.50 m apart. Simple lines were used for the sandy-loam soil

To control the irrigation level, volumetric flow meters were installed on the irrigation manifold pipes. A emitters spaced of 50 cm apart along the line , delivering a maximum discharge of 1,2,3 and 4 L h^{-1}at 1 bar operating pressure, were used.

3.4 Statistical approach

For statistical analysis root-mean-square-error (RMSE) was employed to evaluate the performance of the HYDRUS-2D/3D model and to test the goodness of fit between simulated and observed values. The RMSE equation [3.16] calculation, as given by Wallach, (2006) and used by Kandelous et al. (2011) and Phogat et al. (2011), for the measured and simulated wetting pattern dimensions represents the mean distance between measured and simulated values.

$$RMSE = \left[\frac{\sum_{i=1}^{n}(P_i - O_i)^2}{N}\right]^{\frac{1}{2}} \qquad [3.16]$$

Where P_i is the predicted value, O_i is the measured value, and N is the number of observation.

3.5 Measures of validation

The RMSE ranges between 0 and plus infinity; a value of 0 indicates no difference between simulated and measured results; the smaller the RMSE the better the performance of the model (Piegorsch and Bailer, 2005).

With the purpose of water content monitoring during irrigation simulations nine observation nodes for each treatment were placed at different soil depths which are oriented horizontally and vertically. Lateral observed nod (z=30cm) were placed at the half distance between two dripper and at a distances of 0.10and 35 cm of the emitter, vertically (x=0 and x=25.5cm), just below the emitters, 25 and 45 cm, to obtain water contents at different times (60 min 24 hours,20days and after 90 days of irrigation). For the statistical analysis comparing the numerical results obtained for the different proposed scenarios.

4 Results and Discussion

The main purpose of this part is to investigate numerically and experimentally the influence of different irrigation strategies on the size of the wetted area and therefore emitter spacing under surface drip irrigation systems. For the first part of this work, a comparison of measured and calculated values of soil volumetric water content was done to validate HYDRUS-2D / 3D. In the second part, the selected validate model, was carried out to investigate the influence of tomatoes crops in surface drip irrigation design parameters on soil water dynamics to select one that optimized the water distribution pattern.

4.1 Objective 1 - HYDRUS-2D/3D Validation

The first objective was to validate HYDRUS-2D / 3D for two simultaneously-working surface drippers with sandy-loam texture under tomatoes crops, for different water application rates of 1,2,3 and 4 $L.h^{-1}$. The validation consisted of comparing measured and calculated values of soil volumetric water content (VWC) θ.

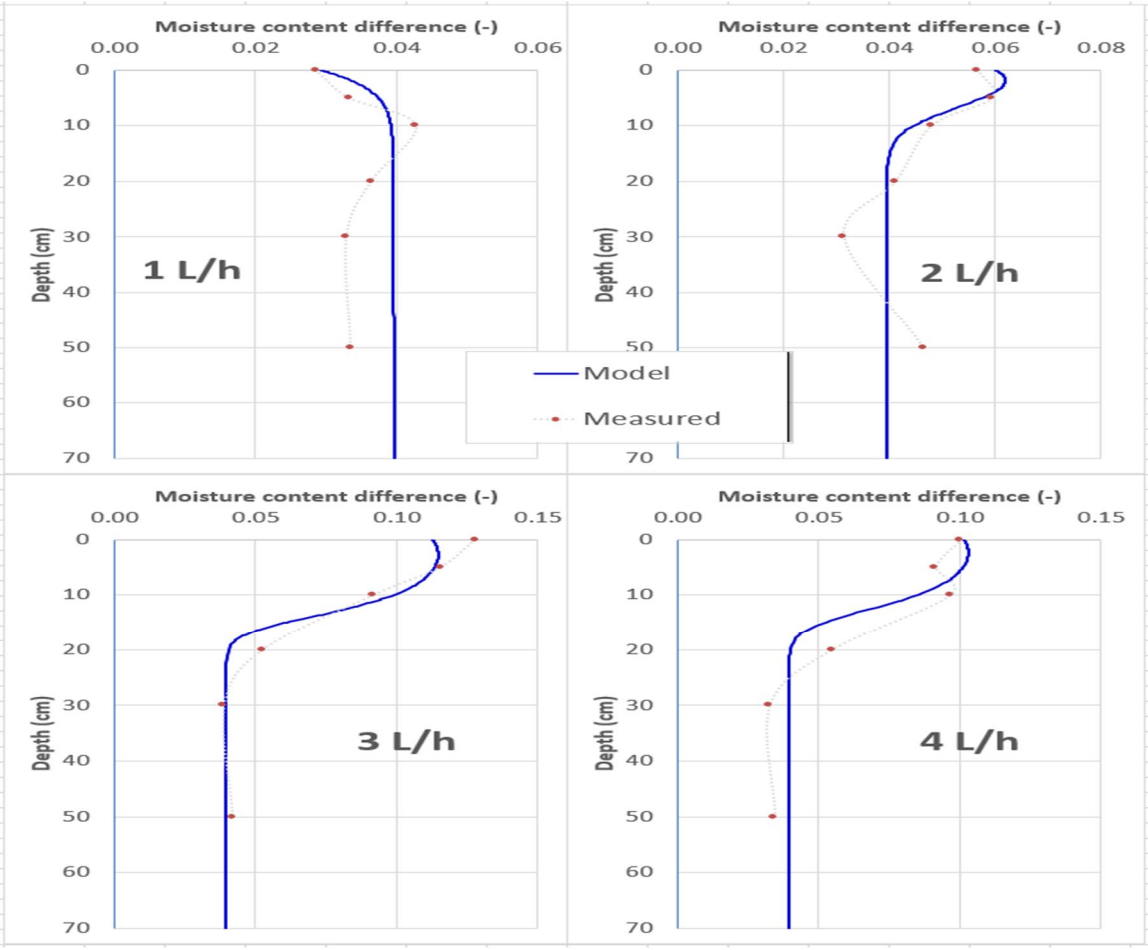

Fig. 4. 1 : Vertical Measured and calculated moisture content difference between values after 1h of infiltration and the initial values at a distance between the two drippers.

Measured and calculated soil VWC data were generated at different soil depths which are oriented horizontally and vertically. Lateral observed nod were placed at the half distance between two dripper and at a distances of 0.10 and 35 cm of the emitter, vertically, just below the emitters, at 5,10,20,30 and 50 cm, to obtain water contents at different times (60 min 24 hours, 20 days and after 90 days of irrigation) A comparison between calculated and measured soil VWC are shown in Figure 4.1.

The simulated values of the water content obtained at different depths and different times were compared with the values obtained with a portable digital a moisture meter soil. Root Mean Square Error Analysis (RMSE) is an indicator of model accuracy. The RMSE for comparing VWC soil-to-calculated soil values for each of the 32 snapshots along the simulated period (Figures in Appendix 3), and for each irrigation treatment, is shown in Table 4-1.

Table 4. 1 : Root mean square error (RMSE) between measured and simulated wetting pattern for Q(l/h) ranged from 1 to 4 L/h. For different time .

Table 4.1.a : Root mean square error (RMSE)for the vertical flow rate

	Vertical RMSE			
	Q			
Time (day)	1 $L.h^{-1}$	2 $L.h^{-1}$	3 $L.h^{-1}$	4 $L.h^{-1}$
1h	0,0057	0,0110	0,0238	0,0300
1	0,0110	0,0113	0,0284	0,0304
20	0,0132	0,0137	0,0294	0,0358
90	0,0141	0,0166	0,0343	0,0430

Table 4.1.b 1: Root mean square error (RMSE) for the horizontal flow rate

	Horizontal RMSE			
	Q			
Time (day)	1 $L.h^{-1}$	2 $L.h^{-1}$	3 $L.h^{-1}$	4 $L.h^{-1}$
1h	0,0069	0,090	0,0143	0,0253
1	0,070	0,0100	0,0168	0,0188
20	0,098	0,0102	0,0221	0,0244
90	0,0150	0,0173	0,0268	0,0305

The RMSE for the vertical flow rate of 1 L/h ranged from 0.57% of VWC soil at the beginning of the simulation period to 1.41% at the end. For the second treatment with a discharge rate of 2L/h, the RMSE values ranged from 1.1 to 1.66% from the beginning to the

end of the simulation period. For the other two treatments namely 3L / h and 4L/h, the RMSE values ranged from 2.38-3.0% at the start of the simulation period to 3.43-4.3% at the end respectively.

The RMSE values for 1 L/h and 2 L /h were different from the 3L and 4L / h treatments; however, the RMSE values for the 1 and 2 L/h treatments were not significantly different. as well as for large flow rates of 3 and 4 L/h, Despite the differences, the RMSE values were always between 0.57 and 4.3%. These results indicate that RMSE remained stable or slightly increased over time. The RMSE values confirm the strong relationship between VWC values calculated by HYDRUS-2D / 3D and those measured in the field. An increase in RMSE is to be expected since simulation errors accumulate over time. However, in this study, this variation was about 3.73%, which is an indication of the robustness of the calculated VWC soil values.

The comparison in Table 4.1 of the RMSE value after, 60 min, 24 h, 20 days, 60 or 90 days after irrigation, shows that the RMSE values were not different for the vertical water distribution, the error ranged from 0.69% to 3,05. Higher water applications were expected to lead to a decrease in the calculated VWC accuracy of the soil.

Horizontal RMSE error for different horizontal discharge rate and different time were showing in table 4.1 b. Specifically, it was anticipated that the higher water supply, the 4L/h treatment, would create higher VWC soil values and, therefore, decrease the accuracy of the model. However, the comparison in Table 4.1 shows that the model predicted correctly the vertical and horizontal distribution of water, vertical distribution of water with RMSE values < 4.3%. Good predictions of horizontal distribution were also obtained with RMSE values <3,05% over the four flow rates. These results indicate that RMSE increased slightly over time. Similar RMSE values (1-4 %) were found by (Skaggs et al., 2004b)when comparing HYDRUS-2D/3D calculated soil VWC to measurements taken on a Hanford sandy loam soil, with surface drip irrigation, homogeneous soil profile, and without Evapotronsperation, and root water uptake components.

Root mean squared error values (RMSE) ranging from 4,3 and 3,05. These results confirm the strong relationship between VWC values calculated by HYDRUS-2D / 3D and those measured in the field. The model predicts the distribution of water content at all distances from the ground at all times by therefore, it has been concluded that HYDRUS-2D can successfully simulate the dynamics of soil moisture change. This approach is consistent with the conclusions of Phogat et al. (2013), who used HYDRUS-2D to simulate field data recorded for an almond tree irrigated on the surface. HYDRUS was used to evaluate daily

changes in moisture content under a pulsed drip irrigation system, continuous impulse and continuous drip irrigation, same results were proved by Ghazouani et al. (2019) when he used

Hydrus-2D model to investigate the effects of different on-farm irrigation strategies on potato crop under subsurface drip irrigation.

HYDRUS-2D/3D model is suitable and can be used as an investigative and design tool for drip irrigation management practices under scenarios similar to those observed in this study. The main reasons for this conclusion are: i) the model calculated soil VWC with an absolute deviation similar to that obtained with field measurement equipment, ii) the model calculated the same level of accuracy despite the magnitude of soil VWC gradient in the soil profile, and iii) the small values of RMSE show that the HYDRUS-2D predictions of the moisture content distribution are in very good agreement with the field results.

The performance of the HYDRUS-2D/3D model was tested by comparing it to field experiments. In general, the depths and diameters of simulated and measured wetting patterns were in very good agreement. However, despite a relatively good agreement between measured and simulated wetted depth in the sandy loam soil, HYDRUS-2D/3D overestimated the wetted diameter and the discrepancy was large. The RMSE value wase about 3.73%. Overall the error was smaller. A good comparison of the model is suggesting that the model can be used by irrigation systems designers with the simple and sole knowledge of the soil's saturated hydraulic conductivity.

4.2 Objective 2 – Simulation of Irrigation Strategies

The second objective was to simulate different irrigation frequency, application rate and synchronization strategies using the validated HYDRUS-2D/3D model to optimize lateral and vertical leaching water movement, i.e., to create an optimum wetted soil area, larger horizontal and vertical wetted soil area (WSA) . Larger WSA would be conducive to a larger root distribution, more water and nutrient uptake by the roots, and thus, higher water use efficiency (WUE).

In this section the surface wetted radius and wetted depth are presented as a function of volume of applied water (L). Volume of applied water is a product of the application rate (L/h) and water application time (h). Figures show the relation between wetting pattern radius (X) and depth (Y) with volume of applied water for different emitter discharge Q and different frequency.

4.2.1 Influence of emitter spacing

The proposed strategies are presented in Table 4.2 with spacing of 30, 50 and 70 cm, the detailed values of different treatment test are presented in appendix 2 table 2.2, following these strategies were compared. In all strategies the soil type is sandy loam.

The maximum allowable flux [cm min^{-1}], which depends on the saturation conductivity of the soil, has been used as a basis for comparison in order to determine the tolerated space between the drippers.

Table 4. 2 : Proposed strategies with spacing of 30, 50 and 70 cm.

Proposed name	distance between emitters (cm)	emitter's discharge (L h^{-1})	Emitter's runoff length (b) (cm)	runoff area (cm^2)	Total area of flux (cm^2)	Flux (cm min^{-1})	test
F30-1-3	30	1	12	2400	2871	-0,019349	Ok
F30-2-3	30	2	27	5300	5771	-0,019253	No
F30-3-3	30	3	41	8200	8671	-0,019221	No
F30-4-3	30	4	55	11000	11471	-0,019372	No
F30-6-3	30	6	84	16800	17271	-0,019300	No
F30-8-3	30	8	113	22500	22971	-0,019348	No
F50-1-3	50	1	6.5	1300	1771	-0,018819	Ok
F50-2-3	50	2	15	3000	3471	-0,019205	Ok
F50-3-3	50	3	24	4700	5171	-0,019338	Ok
F50-4-3	50	4	33	6500	6971	-0,019126	Ok
F50-6-3	50	6	50	9900	10371	-0,019284	No
F50-8-3	50	8	67	13300	13771	-0,019364	No
F70-1-3	70	1	4	800	1271	-0,018729	Ok
F70-2-3	70	2	10	2000	2471	-0,019269	Ok
F70-3-3	70	3	17	3300	3771	-0,018940	Ok

F70-4-3	70	4	23	4500	4971	-0,019158	Ok
F70-6-3	70	6	35	6900	7371	-0,019380	Ok
F70-8-3	70	8	47	9400	9871	-0,019296	No

As it can be seen in this table (table 4.2) that all flux exceeds the value of the maximum allowable flux (-0,0194 (cm min^{-1}) table 3.6 a) which makes simulation impossible.

If the flow exceeds the Saturate Hydraulics conductivity, the models cannot be modeled because they will perform surface runoff, so these conditions are rejected

When the value of flux is greater than the soil's infiltration on assumed that runoff will get at a distance b (emitter's runoff length) to the right and left of the emitters, which will increase the influence of flow area and thus the amount of flux, which we referred in this thesis by banks.

To accept or reject a treatment a second test must be validated, when the value of 2b exceed the spacing between the drippers so this treatment is wrong. The new values of flux after adaptation with the soil's infiltration are given in Appendix 2.

From this, it can be conclude that the permeability feasibility tests, ie the value of the new flow compared with the value of the Maximum allowable flux Appendix 2, were all allowed for all treatments except for flow rates of 6 and 8L / h. with spacing of 30 cm between the drippers.

The second condition states that if the lengths are longer than the length of the domain, we will eliminate the whole situation which is the case with spacing between drippers equal to 70 cm.

4.2.2 Influence Irrigation Frequency:

Effect of the irrigation frequency on the distributions of wetting pattern along horizontal and vertical cross sections:

One of the objectives was to simulate different irrigation frequency strategies using the validated HYDRUS-2D / 3D model to optimize lateral and vertical water movement, ie to create a horizontal WSA and large upland areas that promote greater root distribution, greater water and nutrient uptake and, consequently, higher WUEs.

Figure 4.2 gives an overview of the overall process of four applied irrigation flows, the start and end of each irrigation strategy and the time required for each strategy are calculated according to the water requirements of the tomato plants as a function of climatic and soil

conditions of the study area, the figure shows the operational sequences of two transmitters operating simultaneously. In the case (a) these transmitters operate for 150 minutes at a rate of 1 $L.h^{-1}$. For cases b, c and d, the emitter discharge was 2, 3 and 4 Lh^{-1}, respectively, while the duration was 75, 50 and 40 minutes respectively.

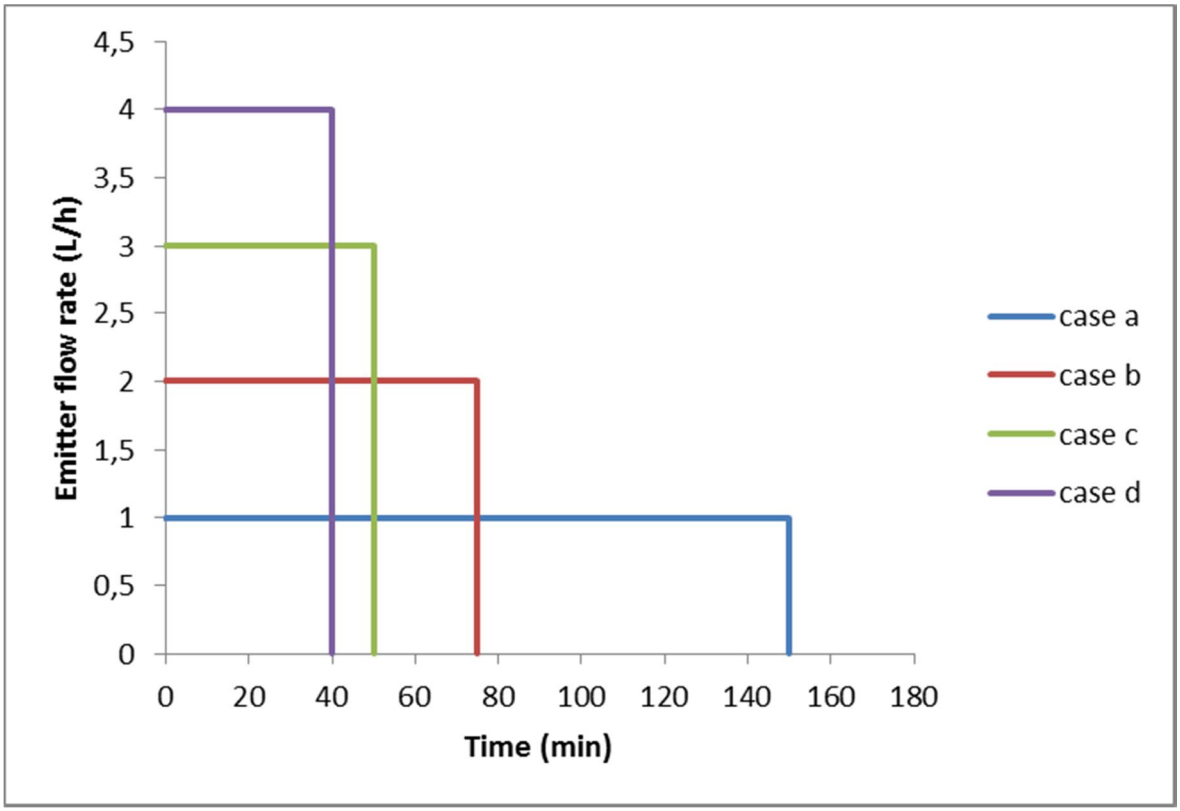

Fig. 4. 2 : Irrigation fluxes applied in different treatments.

we have chosen to evaluate the following application scheme for sandy-loam soil texture with two simultaneously-working drippers, variable irrigation frequency (once every 2 days, once every 3 days, once every 4 days and once every 5 days), and different water application rates1,2,3 and 4$L.h^{-1}$ figure 4.5.

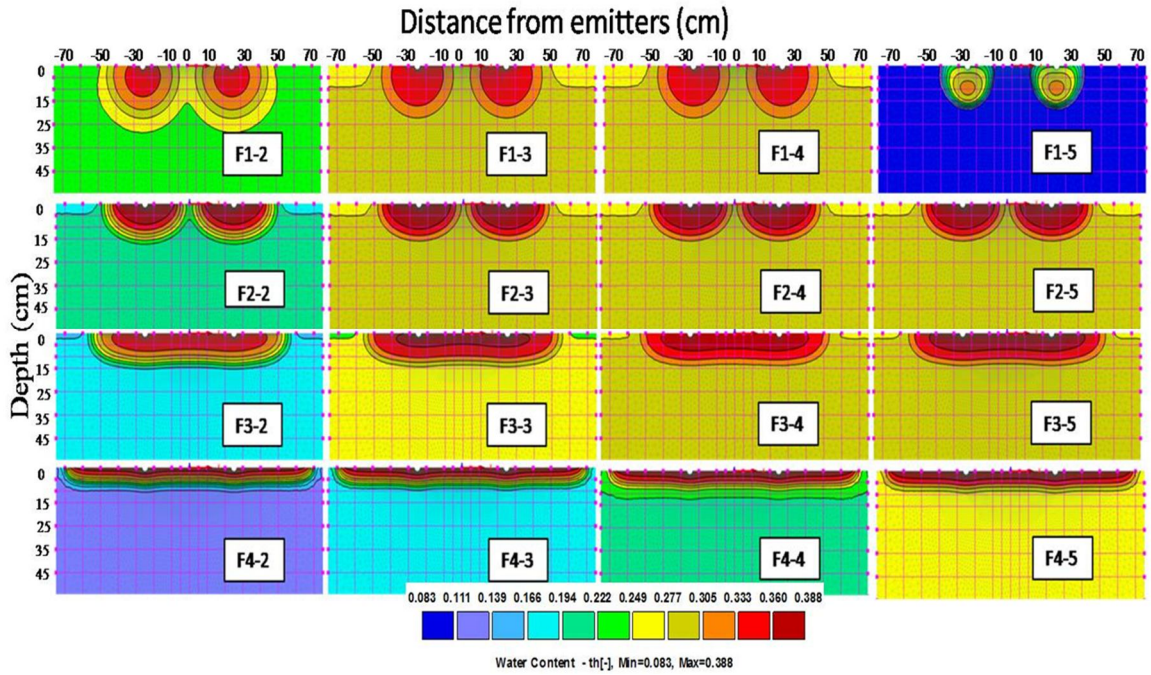

Fig. 4. 3 : Tow dimensional Simulated water distribution around the surface drip emitter for four emitter discharge rates of 1,2, 3 and 4 L/h and four frequency once every 2 days, 3, 4 and once every 5 days of water in the soil profile.

Figure 4.3 shows the maximum wet radius and wet depth achieved at the end of water application. A frequency of 1, 2, 3 and 4 days produced a wet diameter of 50, 40, 40 and 25 cm for a flow rate of 1 Lh^{-1} of 50 cm for a flow rate of 2 Lh^{-1}, 58, 56, 54 and 54 cm for a flow rate of 3 Lh^{-1} and 75 cm in soil at a flow rate of 4 Lh^{-1}, respectively. A wet depth was 25 cm for a flow rate of 1 Lh^{-1}, 15 cm for a flow rate of 2 and 3 Lh^{-1} and less than 10 cm for the soil of 4 Lh^{-1}, respectively. The increase of the wetting pattern is greater in a horizontal direction (X) than in a vertical direction (Y) under all flow rates of 3 and 4 Lh^{-1}.

The results indicate that soil water in the upper soil layer changed more dramatically than in the lower layer. It can be seen in figure 4.5 that the application of water at different frequencies slightly increases the isolines in the upper 5 cm of the soil profile. But with a treatment of a frequency of 4 days, we obtain a lower water content compared to other frequencies. From a physical point of view, these variations seem consistent since the moisture content is higher with shorter watering frequencies. This comparison can be compared by comparing treatment (F * -2) to (F * -3) (F* meaning the discharge rate application) and treatment (F * -5) to (F * -4) in figure 4.3. However, for treatment F * -3, parallel to the texture of the soil, one observes for this treatment a moisture of the higher horizons can exceed 36%, and which tends to decrease towards the horizons lower than 20 cm of depth to align with the other treatment and it stabilizes at 28%, we can see that when only

the wetting pattern near saturation is taken into account, the influence of the discharge rate of the dripper has a greater effect on the radius and depth of the wetting. An increase in the discharge rate of the dripper resulted in an increase in the depth (Y) and radius (X) of the saturated wetting profile. In order to establish the appropriate flow and frequency for the emitters, to give a complete lateral wetting of the soil, the form of the wetting has an important role. For example, for the emission rate of 1 Lh-1 the frequency of watering must be at least every 3 days (Figure 4.3 F1-3 treatment). At this frequency, the soil in the middle, between two successive emitters will be too dry and the plants will undergo a certain degree of stress. Therefore, it is important to know the desired soil moisture content at which plants extract water easily from the soil. If the watering frequency is very short and the flow of the emitters is too great, the neighboring emitters overlap and the water content adds up and may, in this case, exceed the soil capacity of the soil, resulting in drainage and therefore a loss of water. Overall, an increase in watering frequency resulted in an increase in wetting size in both directions and produced a less pronounced moisture content gradient at the wetting front. The results confirm that a frequency of three days gives a more adequate wetting; this approach is consistent with the conclusions of Elnesr and Alazba, (2015); García Morillo et al. (2017).

4.2.3 Influence of emitter discharge rates

Measurements of wetting patterns dimensions for sandy-loam soil texture classes, as a function of volume of applied water (irrigation duration), for the four different surface drip emitter Q.

Effect of the discharge rate on the shape of wetting pattern:

The wetting pattern are characterized by the depth of the front wetting feed along the vertical axis (Z) under the point source (emitters) and the lateral wetting front advances in the soil profile along the axis (x) . The variables are mainly influenced by the applied water amount and the rate of application figure 4.4.

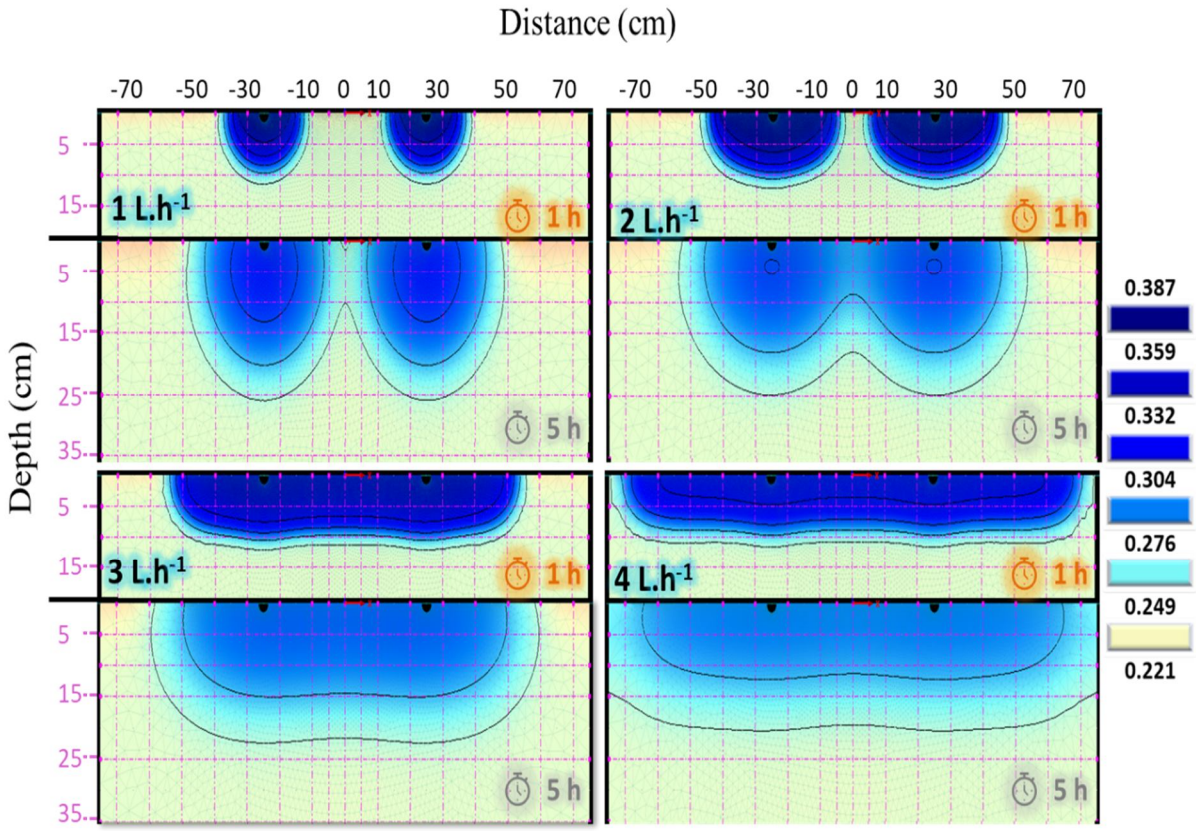

Fig. 4. 4 : Simulated wetting patterns for different emitter discharge rates after 1 hour and 5 hours of infiltration start time.

Figures 4.4 shows the wet bulbs in two dimensions for treatments with different flow rate of 1,2,3 and 4 Lh^{-1} (more results of wet bulbs in two dimensions for different flow rate are presented in appendix). It is noted in these treatments that the bulbs had rounded and elliptical shapes.

The figure shows the wetting patens after 1 and 5 hours of infiltration. The 1 h illustrations are placed at the top of each discharge chart. It is worth to say that the 1 h is just after the end of the infiltration stage, while the 5 h illustrations represent the redistribution stage. The figure shows the differences between the discharge rates of the emitters, as the higher flow rate emitters overlap faster, and the water patterns go deeper. The patterns tend to move in the horizontal direction way more than the vertical direction, this is because the soil texture effect. On contrary, the 1 and 2 Lh^{-1} discharges show less overlap.

As observed, the increase of the dripper discharge at 4 L h^{-1} increases the horizontal radius which gives a truncated ellipsoid shape, figure 4.4. However, decreasing the flow rate to 1 Lh^{-1} increases the vertical radius of the wet bulb so the shape of the wet zone is round figure 4.4. This occurs due to the change of the infiltration zone depending on the treatments

under the effect of the bank, but it is important to note that, the discharge rate is directly proportional to the water content of the soil around the dripper

It can also be seen in this figure that water flow applications of 1 Lh^{-1} can produce a wet bulb with a maximum radius of 17cm, on the one hand and the other of the two emitters and 24cm, 40cm, 50cm respectively for other flow rates of 2, 3 and 4 Lh-1with formation of overlapping wetting patterns between drippers, and a maximum depth of 15 cm, 26.5 cm, 25.5 cm and 32 cm, respectively for 1,2,3 and 4 Lh^{-1}.On the other hand, a saturated zone below the dripper's was obtained only for the highest discharge rate of 3 Lh-1 and 4 Lh-1at a radius of 10 cm and 15 cm respectively, from the water source. For the two least discharge rates, there was no saturated zone below the dripper, and the water content at that point decreased with the dripper discharge rate. This is consistent with the Modeling soil water redistribution under surface drip irrigation results obtained by Arraes et al. (2019).

In this study, the vertical movement of water up to 32 cm was recorded. The maximum density of the roots of the simulated culture (tomato) does not exceed 30 cm deep, so that the losses of deep percolation would be practically undeniable for these cultures. However, deep percolation could also be controlled through appropriate rates of management and enforcement of issuers.

4.2.4 Distributions of wetting pattern along horizontal and vertical cross sections:

Below we will discuss water content profiles along horizontal and vertical cross sections and the distributions of wetting at different time for sixteen output times with an increasing time interval

Water Distribution along Vertical Cross-Sections

The different irrigation programs applied are shown in Figure 4.5, which allows the evolution of the water stock to be monitored along with irrigation conditions and crop development.

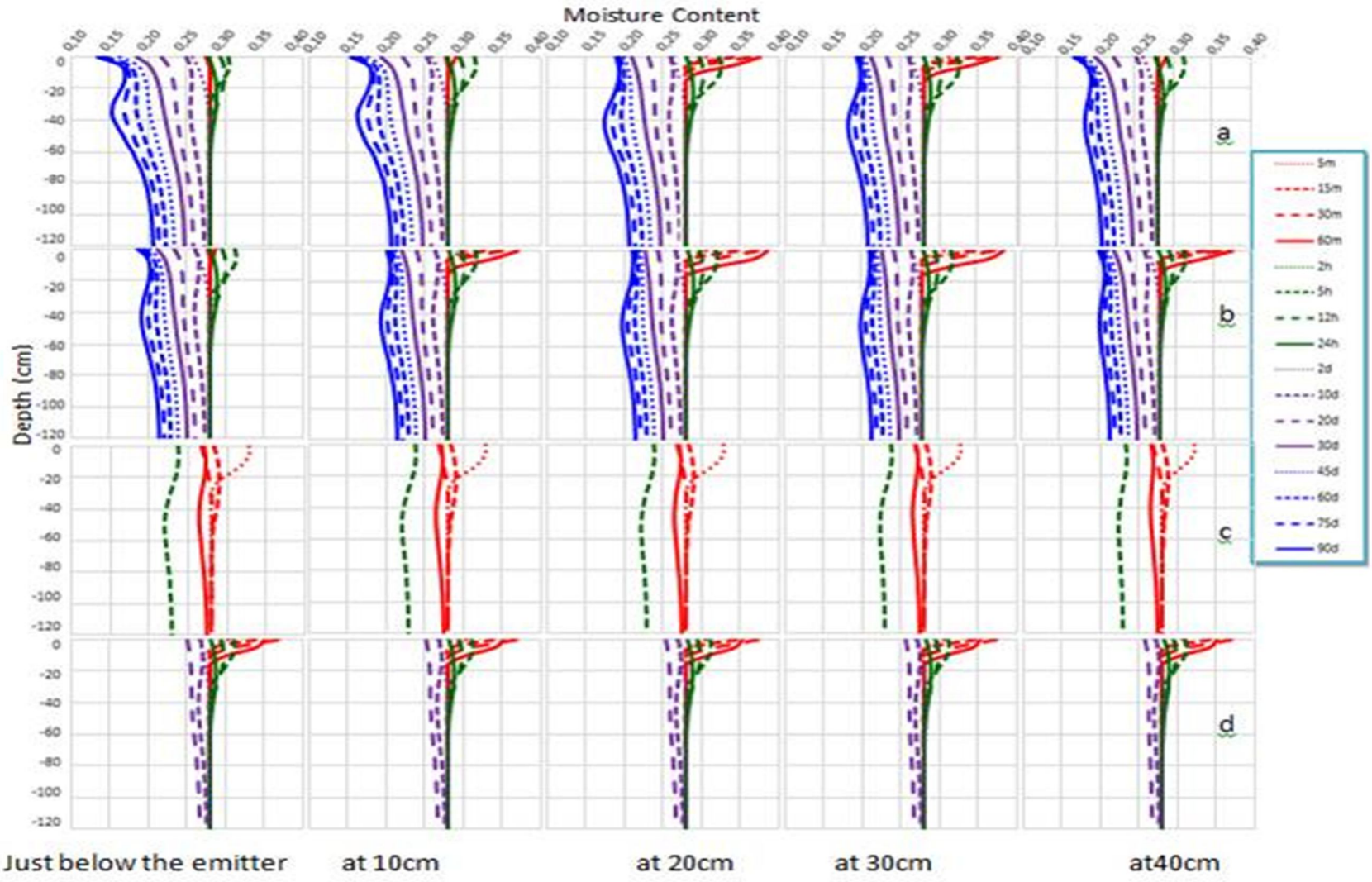

Fig. 4. 5 : Vertical water content distributions at 0, 10, 20, 30, and 40 cm from the dripper for different irrigation scenarios.

The water content profiles are established under the following conditions: red after 6, 15, 30 and 60 min in green 2, 5,.12.and 12 hours, purple 2,.10,.20.and 20 days of irrigation, blue 45,.60 , 75, and after 90 days of irrigation ,. In all cases, the water content profiles are simulated at 0, 10, 20, 30, and 40 cm from the emitter. Note that the depth of the transport domain is on average 125 cm in the studied scenarios.

During the first two days following irrigation water inflows (Figure 4.5, just below the emitter), soil drying is very low and essentially superficial because the depth of rooting didn't exceed 20 cm. The water content profile is fairly similar and is approximately vertical (29-32% of water) in the top 60 cm of the soil except for the case d with a flow rate of drippers equal to 4 L. h^{-1} which shows a slight deference of the wetting front, which reaches 40% in the surface layer (depth of 0-10 cm), the humectation begins to decrease, which explains the infiltration due to the Banks, which equals to 32.5 cm case a, while a some dryness begins to manifest from the 10th day to reaching a value of 18% after 30 days, this difference in water form tends to increase over time, which reflects the effect of cultivation on soil drying. In case b, the wetting front at a distance of 10 cm from the emitter reaches a water content of 40%, this evolution differs markedly from that presented in the case a at the same emitter distance, the effect is essentially manifested with the increase of the flow rate case c and d and thus the presence of the banks while the depths are variations negligible.

The maximum water content reach after 25min of irrigation 35% in case c for the upper 20cm irrespective of the distance from the emitter, while the other three cases are quite similar.

Water content distributions at different time

The water content distributions for the four strategies proposed are shown in figure 4.6 at distances of 0.10, 20, 30 and 40 cm of the emitter the same output times such as in figure 4.8 are displayed.

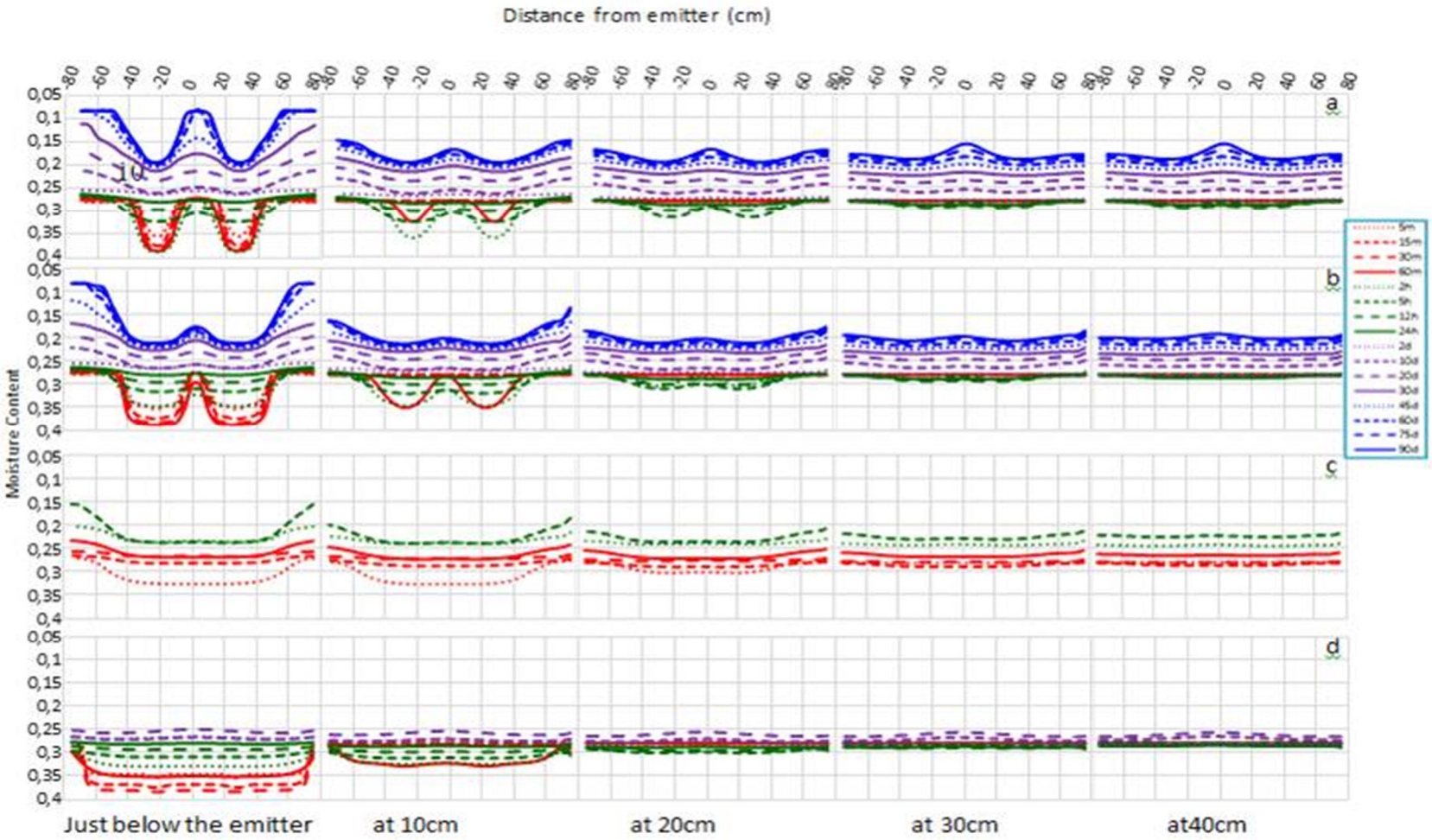

Fig. 4. 6 : The horizontal water content distributions at different times at 0, 10, 20, 30, and 40 cm from the dripper for different irrigation scenarios.

The effect of the watering frequency and the application of the flow rate and the duration are well envisaged in this figure, figure 8a and 8b show that in the adjacent layers of emitters at radius of 10 cm, the maximum water content recorded are just below the emitters, it is about 35% during the first hours of irrigation, then this value is reduced by 30% after 24 hours. This is due to the low flow redistribution process in case a and b. The soil remains saturated at a horizontal distance of about 20 cm during these 24 hours for both first scenarios and 30 minutes for the two others. Differences in the maximum distance of lateral movement in irrigation frequency strategies were low. This is consistent with the numerical and experimental results obtained by Cote and Bristow,(2003).

By comparing of figure 4.6c, 4.6d with figure 4.6a, 4.6b, we can see that for different rates and durations of irrigation, the horizontal movement of wetting front is higher in the last case than in the low-flow scenarios, higher water contents are occur during the first 60 minutes. No significant differences are showed in each case for 20 cm away from the transmitter, in case c at the time of 60 min the water content remains constant at 25% for a distance of 40 cm away from the emitter. This is consistent with the results by Abou-Lila et al. (2013) in which analyzed the numerical assessment of subsurface trickle irrigation with brackish water. On the other hand, the scenario c show improved horizontal distribution of water, up to a period of 24 hours at a distance of 40 cm on both sides of the transmitters. This obviously reflects the fact that the bank is equal to 235 mm. At a half of the emitter distance, the higher water contents were obtained in the case of 30 minutes with a rate of 38%, while the lower water contents were obtained in cases a and b due to the existence of low volume irrigation time in the presence of evapotranspiration, This is consistent with the results obtained by Wang et al. (2017)

4.2.5 Root water uptake

Figure 4.7 shows the root water uptake for the entire irrigation cycle, 90 days of irrigation simulations. Root water uptake is compared to see how much root water absorption has been reduced for all four irrigation strategies.

The choice of the simulation period corresponds to the period of average growth during which the plants are fully developed and the root system is constant. To reduce the potential water uptake by the roots to the actual uptake of water by the roots.

Overall, the calculated soil VWC values obtained with Hydus-2D/3D are in good agreement with the measured values, despite some discrepancies. The agreement is good, particularly considering the complexity of the simulation scenario that the model was

subjected to, i.e., heterogeneous soil properties, a relatively long simulation period, several consecutive irrigation events, high evaporative and transpiration demand and most notably, a time static root distribution for such a long simulation period (90 days).

Currently, the HYDRUS-2D/3D model does not allow the input of a dynamic root system, i.e., a growing root system. To avoid larger differences in root development, a crop growth period with almost constant LAI was chosen for the simulations. However, some changes in LAI did occur, supporting the assumption that a dynamic root distribution input could positively affect the accuracy of HYDRUS-2D/3D simulations.

This figure (Fig.4.7) shows that root water uptake was significantly decreased as irrigation amount was reduced.

Figure below clearly shows that beneath the wetting patterns dry zone occurred in all strategies, which was due to the root water uptake. Between irrigation events this dry zone spread to the top of the soil according to the plant root distribution

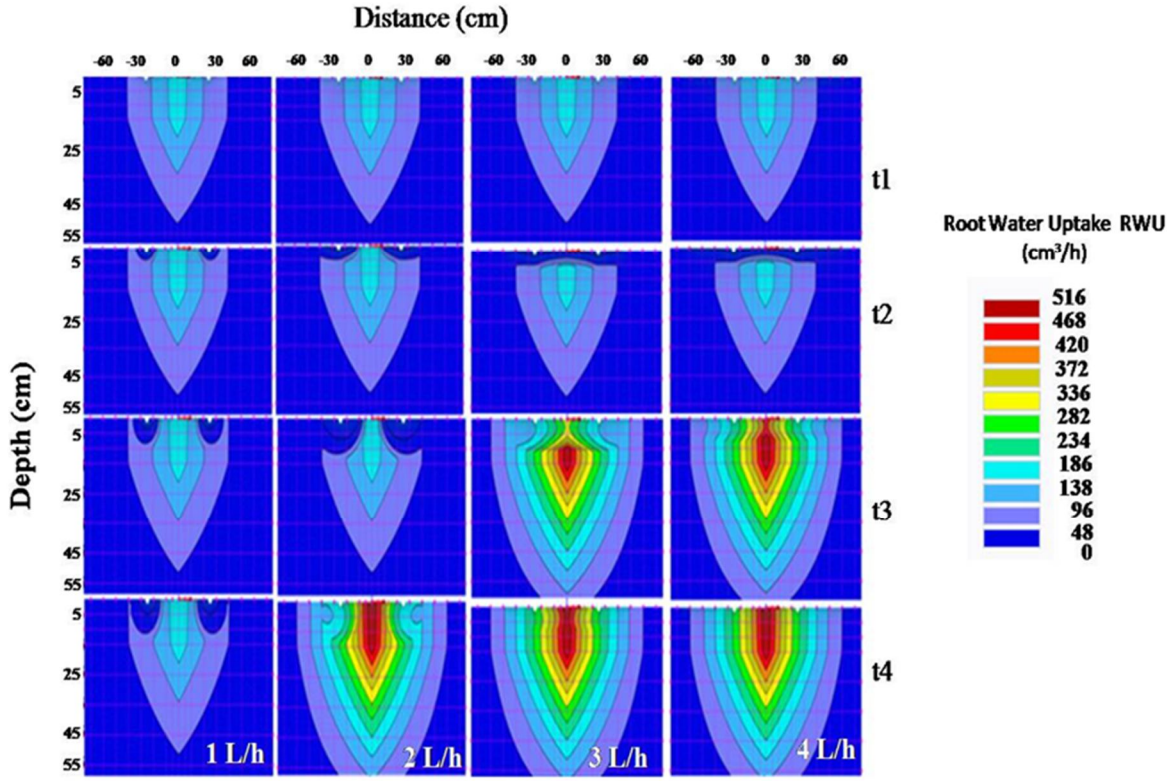

Fig. 4. 7 : 2D Simulated root water uptake (RWU) at different times and different discharge during the experimental period. (t1=5min, t2=30min, t3=60min, t4=5h).

Overall, the highest root water uptake started after 60 min of irrigation and was observed for T3 and T4 Fig. 4.9 (515 cm^3/h), followed by T2 and T1 with (171 cm^3/h), 60min ago we note that the root water uptake process is very small, as it does not exceed 172 cm^3/h in all the proposed strategies, because irrigation water does not reach the activated area of the

roots. We can also observe that after 5 h root water uptake of strategy 2 and 1 reaches the same values as RWU of the third and fourth strategies, there is a perturbation of RWU in the root zone, the RWU ranged from 350 cm^3/h to 100 cm^3/h which explains why there is the highest root absorption is associated with the presence of moisture content in the active roots area witch confirmed in the following figure for the same flow rate and at the same time, clearly observed in Fig. 4.8 that the water content in this zone is more than 23%.

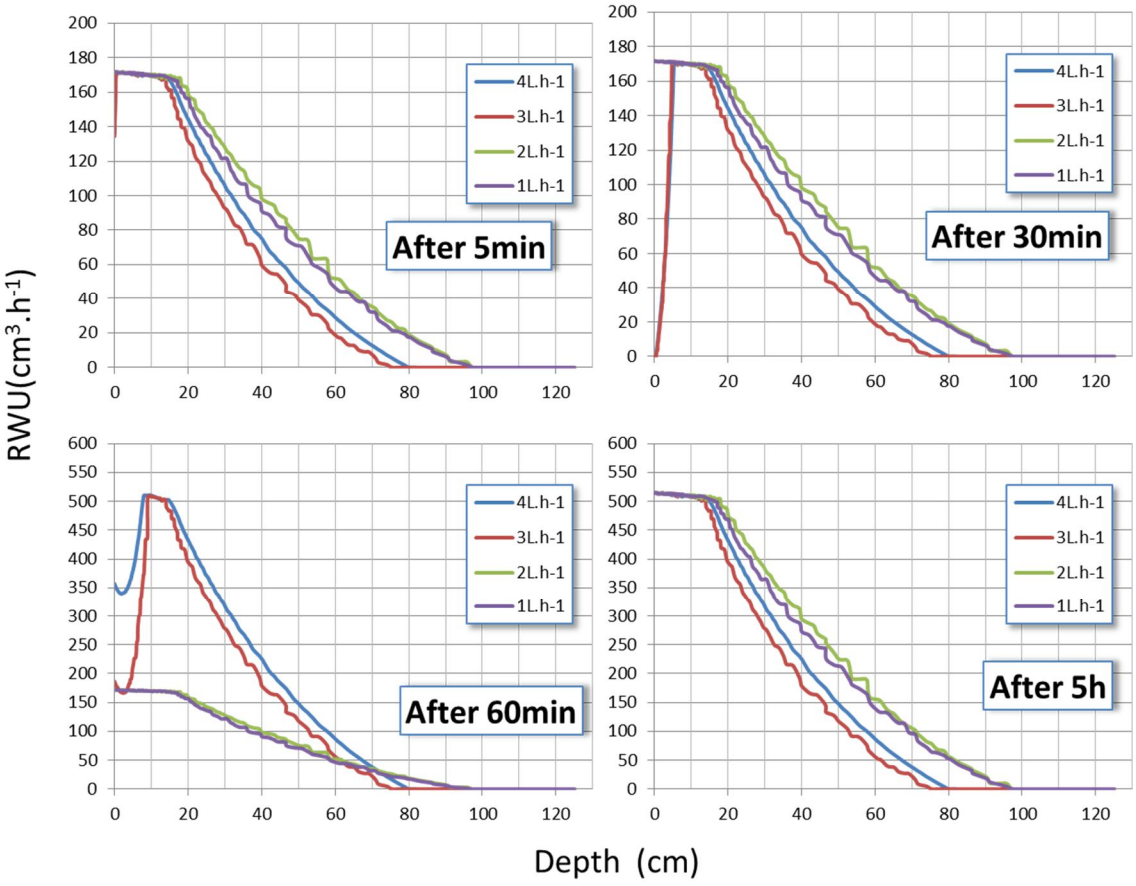

Fig. 4. 8 : Simulated root water uptake in the half distance from emitter at different times (t1=5min, t2=30min, t3=60min, t4=5h) and different discharge during the experimental period.

The recommended strategy 3 was the best irrigation strategy, as shown in Figures 4.9, as the water had sufficient time to redistribute into the soil. So the results of the drip irrigation simulation for the tomato crop studied showed that the irrigation strategy strongly affected water uptake by plant roots. Root water uptake was most important in strategies where water content was maintained in the Root Zone

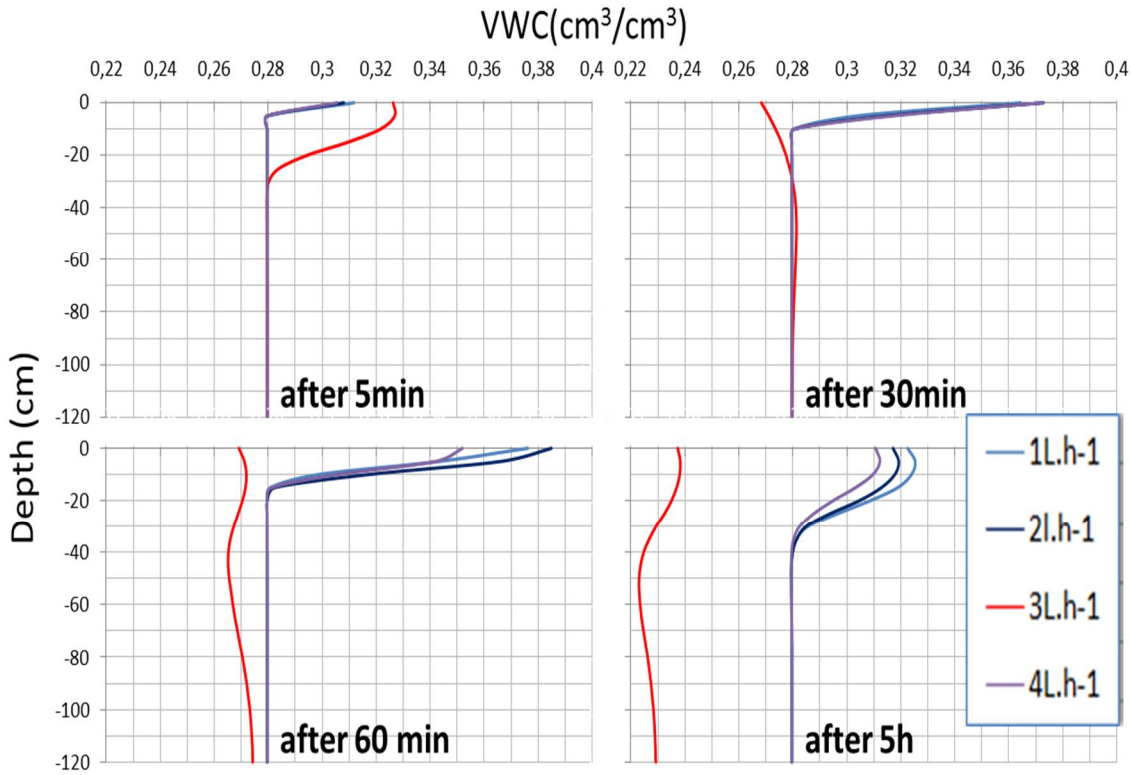

Fig. 4. 9 : Simulated water content in the half distance from emitter at different times (t1=5min, t2=30min, t3=60min, t4=5h) and different discharge during the experimental period.

For low WC the low amount of roots in deeper layers is not sufficient to supply high water uptake rates. When the upper layers become drier, WC reduction is immediate. Under medium and high WC, the RWU front moves gradually downward as water from the upper layers is depleted. For high WC the RWU front goes even deeper compared to medium WC and it show that it is sustained at potential rate for more time. Accordingly, the plant exploits the whole root zone and little water is left when WC reduction onsets, causing a sudden drop in RWU patterns. Regarding the evaluation of WC during the time as a function of the rate of discharge applied, the simulated RWU patterns are very similar for four rates evaluated discharge rate, differing only on timescale: for high WC the shift in RWU front occurs earlier. The highest actual root water uptake was observed for strategies where the soil water content at the depth of maximum root intensity was maintained between 22%. Because the root density was highest at soil depth of 30 cm, the root water uptake at the depth of 20 and 40 cm, when compared to the depth of 10 cm, did not have such a large influence on the actual root water uptake. However, at the soil depth of 20 and 40 cm in the 3rd strategy the water content was more of 24%, and it was maintained at the level of maximum root water uptake throughout all simulation period. The recommended strategy 3 was the best irrigation

strategy, as shown in Fig. 4.4, as the water had sufficient time to redistribute into the soil. So the results of the drip irrigation simulation for the tomato crop studied showed that the irrigation strategy strongly affected water uptake by plant roots. Root water uptake was most important in strategies where water content was maintained in the root zone. Roots can redirect their areas of maximum activity towards zones where water availability is favorable. For example, according to Panigrahi and Sharma, (2016) and Eltarabily et al. (2019), usually, after water applications, root water uptake occurs initially near the plant's principal root, and then progresses towards the root's periphery, thus changing locations of maximum root water.

Results confirm the conclusions of Assouline, (2002) where a higher initial water content in the soil has resulted in an increase in the root water uptake from a drip irrigation system in their studies concerning the effect of different emitter discharge rates on water distribution under surface drip irrigated corn, the effects of microdrip and conventional drip irrigation on water distribution and uptake.

4.2.6 Tomato yield

The effects of discharge rate on tomato yield are presented in table 4.2.

Table 4. 3 : The total yields (Kg ha^{-1}) of tomato.

Treatment	Discharge rate ($L.h^{-1}$)	yield ($Kg.ha^{-1}$)
T1	1	1473^{a}
T2	2	1776^{a}
T3	3	2790^{b}
T4	4	2376^{b}

The same letters are not significantly different (p<0.05) according to a Duncan's Multiple Range test. Les mêmes lettres ne sont pas significativement différents aux seuil (p<0.05) selen le test de comparaisons multiples (test de Duncan).

In general, increasing the amount of irrigation water applied tended to increase tomato yield, it is evident that the yield increased in the third treatment with a discharge rate of $3L.h^{-1}$ (increase of 30%). No significant difference at the threshold of (P <5%) neither between the pair T1 and T2, nor between the pair T3 and T4, while there was significant difference between these discharges groups, this may be attributed to the fact that the root system could not properly explore the volume of the moistened soil for the T1 and T2 treatments as opposed to the T3 and T4 treatments.

As shown in Fig. 4.10, the final yield of the mean fruit weight is significantly higher for T4 and T3 with 2376 Kg/ha and 2790 Kg/ha respectively compared to T2 with 1776 and 1473 Kg/ha for T1. Based on these results the maximum values of 2790 Kg/ha was obtained

from T3 when the water patterns go deeper and the flow rate emitters overlap faster (Fig. 4.4). It appears that for the T1 and T2 treatments where the water supply is relatively limited less than 22% a phenomenon of water stress has affected the crop and has affected the plant's root vegetative development (Fig. 4.4). Indeed, the highest RWU is recorded at the level of T3 and T4 (Fig. 4.7), Taking into account the nature of the root system with significant lateral development of this crop, it seems that at T1 and T2 the root system could not properly explore the volume of the moistened soil from the drippers, this did not satisfy the water requirements of the plants. However, in the case of T3 and T4, the dripper promotes the lateral movement of the moisture content fig. 4.4 and allowed humidifying a bulb easily operated by the root system, while for the strategy with 4 L.h^{-1} it has a high humidity in a very short time in the area of the root system. This is confirmed by Phene et al. (1987) who showed that the shape of the bulb moistened by a dripper is more elongated in depth, especially in sandy soils compared to clay.

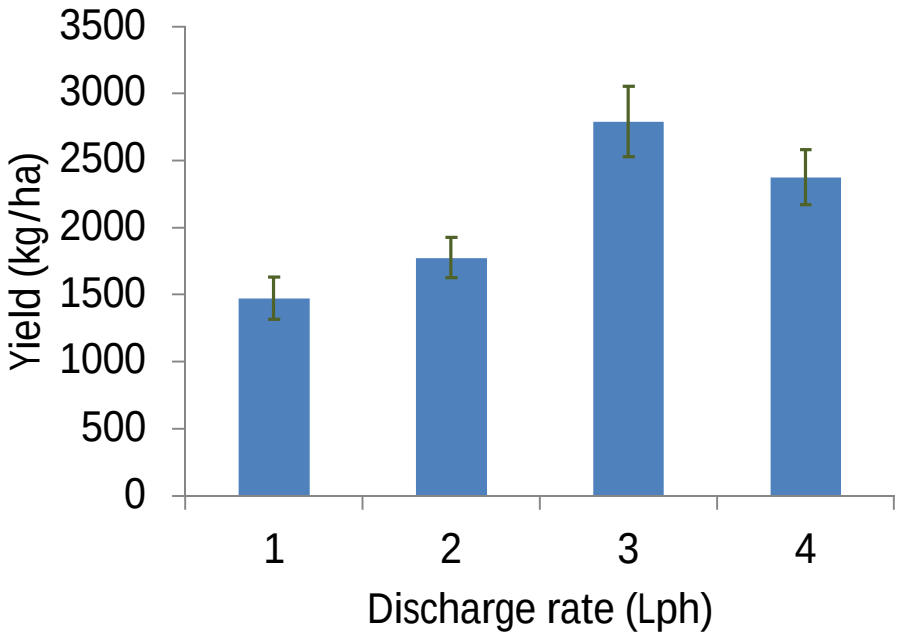

Fig. 4. 10 : Tomato yield as affected by discharge rate.

The tomato yield was lower with 1.2 and 4 L h^{-1}. This could be attributed to the shallow root of the tomato, for low flow the root zone does not have a good moisture content and for the strategy with 4 L h^{-1} it has a high humidity in a very short time in the area of the root system, which confirms that the superficial drip at 3 L h^{-1} is better than the others in the growth of greens during the growing season both in quantity and quality.

The symptoms of water deficiency appeared on the drip plants with low flow rates small yellow leaves wilting, drying plants And especially in the period of growth which expresses the low yield.

Fig. 4. 11 : Photos of weight fruit with the 3rd strategy.

For the other two strategies 3 and 4 observed plants with green foliage, for the strategy to 3 L h^{-1} was even obtained a fruit that weighs a weight of 500g as shown in Figure 4.11. This is consistent with the results obtained by Phene et al. (1987; Ya-dan et al. (2017)

The recommended strategy 3 was the best irrigation strategy, as the water had sufficient time to redistribute into the soil. So the results of the drip irrigation simulation for the tomato crop studied showed that the irrigation strategy strongly affected water uptake by plant roots. Root water uptake was most important in strategies where water content was maintained in the Root Zone.

The results of the crops indicated that the return on the application of 3L.h^{-1} has a significant increase compared to other applications (up to 30%).

These results indicate the following recommended practices: Use surface drip discharge of 3L.h^{-1} h due to its beneficial results and potential for increased yields.

5 Conclusions

The influence of irrigation system design parameters (soil texture, soil hydraulic properties, discharge rate frequency and timing) on the soil moisture distribution patterns between two simultaneously working surface drippers was studied numerically with the HYDRUS-2D / 3D model and experimentally in field.

The literature generally suggests that higher flow rates of emitters (drippers) extend the wetting pattern in the horizontal direction, particularly in fine textured soils. For the texture of study area sandy loam soil the water flow rates for all discharge rate 1,2,3 and 4Lh^{-1}, causes water to accumulate on the soil surface and then seep into the soil.

The study of variable irrigation frequency of different emitter discharge rates was conducted to investigate the influence on dimensions of wetting patterns. At the end of water application, for each flow, the different frequencies had a small effect on the final wetting size but large differences in the position of the saturated wet front.

The results indicate that soil water in the upper soil layer changed more dramatically than in the lower layer, the application of water at different frequencies slightly increases water content's isolines (contours) in the upper 5 cm of soil profile. But with a treatment of a frequency of 4 days gives a higher water content compared to other frequencies, From a physical point of view, these variations appear consistent since the water content is higher with shorter watering frequencies, the influence of the discharge rate of the emitter has a greater effect on the radius and depth of the wetting. An increase in the discharge rate of the transmitter resulted in an increase in the depth (Y) and radius (X) of the saturated wetting profile.

The increase of the dripper discharge at 4 L h^{-1} increases the horizontal radius which gives a truncated ellipsoid shape, However, decreasing the flow rate to 1 Lh^{-1} increases the vertical radius of the wet bulb so the shape of the wet zone is round, This occurs due to the change of the infiltration zone depending on the treatments under the effect of the bank, but it is important to note that, the discharge rate is directly proportional to the water content of the soil around the dripper.

In this study, the vertical movement of water up to 32 cm was recorded. The maximum density of the roots of the simulated culture (tomato) does not exceed 30 cm deep, so that the losses of deep percolation would be practically undeniable for these cultures. However, deep percolation could also be controlled through appropriate rates of management and enforcement of issuers.

The results indicate that the soil moisture was more uniform under a discharge of 3 Lh^{-1} with 3 days frequency, the same treatment responds well to the distribution of water directly in the root zone and allows a maximum humidification of this zone, a decrease of the losses by evapotranspiration and deep percolation, and an increase of the efficiency of use of irrigation water.

The performance of the HYDRUS-2D/3D model was tested by comparing it to field experiments. In general, the depths and diameters of simulated and measured wetting patterns were in very good agreement. However, despite a relatively good agreement between measured and simulated wetted depth in the sandy loam soil, HYDRUS-2D/3D overestimated the wetted diameter and the discrepancy was large. The RMSE value wase about 3.73%. Overall the error was smaller. A good comparison of the model is suggesting that the model can be used by irrigation systems designers with the simple and sole knowledge of the soil's saturated hydraulic conductivity.

Results showed that drip irrigation strategy strongly affected plants root water uptake. The root water uptake was largest for irrigation strategies where high water content was maintained in the zone of maximum root intensity which directly affects the wetting pattern shape and soil water distribution in the soil profile.

The recommended strategy 3 was the best irrigation strategy, as the water had sufficient time to redistribute into the soil. So the results of the drip irrigation simulation for the tomato crop studied showed that the irrigation strategy strongly affected water uptake by plant roots. Root water uptake was most important in strategies where water content was maintained in the Root Zone.

The results of the crops indicated that the return on the application of 3$L.h^{-1}$ has a significant increase compared to other applications (up to 30%).

These results indicate the following recommended practices: Use surface drip discharge of 3$L.h^{-1}$ h due to its beneficial results and potential for increased yields.

In general, for the irrigation of tomatoes, under the given conditions of soil and root absorption, when, simultaneously, the initial soil water conditions and the volume of water applied per irrigation cycle are taken account is taken that the irrigation water applied is at a rate of 3$L.h^{-1}$ with a frequency of 3 days so that the soil moisture content at a depth of 30 cm is maintained at a level of constant. The results also suggest that a 50cm dripper spacing is appropriate for tummy irrigation in sandy loam soil. However, more simulations with different spacing of drippers and volumes of water applied per irrigation cycle must be

performed to determine even more optimal design and management parameters of the irrigation system for each crop and soil and given climatic conditions.

Recommendation

The drip irrigation system in our region needs future studies to benefit from this system, but due to the high cost of such studies, simulation is one of the most important steps to choose irrigation strategy.

- Future computer studies of sub-surface irrigation (SDI) and SDI with treated waste-water are needed especially as the region is known as high evaporation coefficients and limited water resources.
- The possibility of placing a physical barrier under the root zone to avoid deep percolation of irrigation water can also be studied.
- Future computer studies are needed to set the optimum application time with relation to soil type, emitter discharge, and plant growth.

Bibliography

Abou-Lila, T.S., Berndtsson, R., Persson, M., Somaida, M., El-Kiki, M., Hamed, Y., Mirdan, A., 2013. Numerical evaluation of subsurface trickle irrigation with brackish water. Irrigation Science, 31, 1125–1137.

Amin, M.S.M., Ekhmaj, A.I.M., 2006. DIPAC-drip irrigation water distribution pattern calculator In: 7th International micro irrigation congress, 10–16 Sept, PWTC, Kuala Lumpur, Malaysia.

Arraes, F.D.D., de Miranda, J.H., Duarte, S.N., 2019. Modeling soil water redistribution under surface drip irrigation. Engenharia agrícola. Jaboticabal 39, 55–64.

Soil and Water Terminology. American Society of Agricultural and Biological Engineers, 2007. S526..

Assouline, S., 2002. The effects of microdrip and conventional drip irrigation on water distribution and uptake. Soil Science Society of America J. 66, 1630–1636.

Aujla, M.S., Thind, H.S., Buttar, G.S., 2005. Cotton yield and water use efficiency at various levels of water and N through drip irrigation under two methods of planting. agricultural water management J. 71, 167–179.

Autovino, D., Rallo, G., Provenzano, G., 2018. Predicting soil and plant water status dynamic in olive orchards under different irrigation systems with Hydrus-2D: Model performance and scenario analysis. agricultural water management J.,203, 225–235.

Badni, N., 2012. Eaux d'irrigation et salinité des sols en zone semi aride : exemple dans le moyen Chellif « parcelle à ouled ben AEK » conception et modélisation des systèmes « irrigation-drainage ». hassiba ben bouali de chlef, thèse de magister.

Barragan, J., Cots, L., Monserrat, J., Lopez, R., Wu, I.P., 2010. Water distribution uniformity and scheduling in micro-irrigation systems for water saving and environmental protection. Biosyst. Eng. 107, 202–211.

Bar-Yosef, B., Sheikholslami, M.R., 1976. Distribution of water and ions in soils irrigated and fertilized from a trickle source. Soil Science Society of America J. , 40, 575–582.

Ben-Gal, A., Lazarovitch, N., Shani, U., 2004. Subsurface drip irrigation in gravel-filled cavities. Vadose Zone J. 3, 1407–1413.

Brandt, A., Bresler, E., Diner, N., Ben-Asher, I.K., Heller, J., Goldberg, D., 1971. Infiltration from a trickle source: I. Mathematical models. Soil Science Society of America J., 35, 683–689.

Bresler, E., 1975. Two-dimensional transport of solutes during non-steady infiltration from a trickle source 39:604-613.

Bresler, E., Heller, J., Diner, N., Ben-Asher, J., Brandt, A., Goldberg, D., 1971. Infiltration from a trickle source. II: Experimental data and theoretical predictions, Soil Science Society of America J., 37, 658–671.

Brooks, R.H., Corey, A.T., 1964. Hydraulic properties of porous media, Hydrol. Paper No. 3, Colorado State Univ., Fort Collins, CO.pp27

Bruand, A., Coquet, Y., 2005. Les sols et le cycle de l'eau. Science du Sol et Environnement. Dunod 345–363.

Bruinsma, J., 2003. World agriculture: towards 2015/2030 .An FAO perspective, Earthscan, London and FAO, Rome.

Burdine, N.T., 1953. Relative permeability calculations from pore-size distribution data. American Institute of Mining, Metallurgical, and Petroleum Engineers, 198, 71–78.

Campbell, G.S., 1974. A simple method for determining unisatured conductivity moisture retention data. Soil Science. 311–314.

Cassel, D.K., Nielsen, D.R., 1986. Field capacity and available water capacity. In: Methods of soil analysis. Part 1, Physical and mineralogical methods. American Society of Agronomy: Madison, WI. 901-926.

Chamsa, 2020. Main advantages of underground drip irrigation [WWW Document]. URL https://grupochamartin.com/en/news/advantages-underground-drip-irrigation/# (accessed 9.6.17).

Childs, E.C., Collis-George, N., 1950. The permeability of porous materials. Proceedings of the Royal Society of London 201, 392–404.

Cook, F.J., Thorburn, P.J., Fitch, P., Bristow, K.L., 2003. WetUp: a software tool to display approximate wetting patterns from drippers. Irrigation Science J., 22, 129–134.

Cote, C.M., Bristow, K.L., Charlesworth, P.B., Cook, F.J., Thorburn, P.J., 2003. Analysis of soil wetting and solute transport in subsurface trickle irrigation. Irrigation Science J. 22, 143–156.

Dasberg, S., Or, D., 1999. Drip irrigation, Berlin, Springer Verlag.pp162.

Derek, C., Martin, S., Khaled, E.-A., 1998. CropWat for Windows: User Guide. FAO. pp43.

Drip Depot, 2014. Drip Irrigation Blog [WWW Document]. URL http://dripdepot.blogspot.com/ (accessed 9.6.17).

Elnesr, M.N., Alazba, A.A., Šimůnek, J., 2013. HYDRUS simulations of the effects of dualdrip subsurface irrigation and a physical barrier on water movement and solute transport in soils. Irrigation Science J. 1–15.

Elnesr, M.N., Alazba, A.A., 2015. The effects of three techniques that change the wetting patterns over subsurface drip-irrigated potatoes. Spanish Journal of Agricultural Research. Spanish Journal of Agricultural Research. Res. 13, 12.

Eltarabily, M.G., Bali, K.M., Negm, A.M., Yoshimura, C., 2019. Evaluation of root water uptake and urea fertigation distribution under subsurface drip irrigation. Water 1487, pp15.

FAO, 2016. AQUASTAT Main Database, Food and Agriculture Organization of the United Nations (FAO).

FAO, 1990. Méthodes d'irrigation rapport N°05.

FAO, 2002. Irrigation manual. Planning, development monitoring and evaluation of irrigated agriculture with farmer participation, Module 9: Localized irrigation systems planning, design, operation and maintenance. Harare, FAO, Subregional Office for Southern and East Africa.

Feddes, R.A., Kowalik, P.J., H., Z., 1978. Simulation of field water use and crop yield. New York, NY, John Wiley & Sons. pp 188

Fischer, G., Tubiello, F.N., van Velthuizen, H., Wiberg, D., 2007. Climate change impacts on irrigation water requirements: Effects of mitigation, 1990–2080 1083–1107.

Fredlund, D.G., Xing, A., 1994. Equations for the soil-water characteristic curve. Can. Geotech. J. 31, 521–532.

Freeze, R.A., Cherry, J.A., 1979. Groundwater, Englewood Cliffs, NJ, Prentice-Hall. pp 604.

García Morillo, J.G., Rodríguez Díaz, J.A., Camacho, E., Montesinos, P., 2017. Drip irrigation scheduling using Hydrus 2-D numerical model application for strawberry production in south-west Spain, , 66, 797-807. Irrigation. Drainage J. 66, 797–807.

Gärdenäs, A.I., Hopmans, J.W., Hanson, B.R., Šimůnek, J., 2005. Two-dimensional modeling of nitrate leaching for various fertigation scenarios under micro-irrigation. Agricultural Water Management J. 74, 219–242.

Gardner, W.R., 1958. Some steady state solutions of the unsaturated moisture flow equation with application to evaporation from a water table. Soil Science. 85, 228–232.

Ghazouani, H., Rallo, G., Mguidiche, A., Latrech, B., Douh, B., Boujelben, A., Provenzano, G., 2019. Assessing Hydrus-2D Model to Investigate the Effects of Different On-Farm Irrigation Strategies on Potato Crop under Subsurface Drip Irrigation. water 540,18p.

Hanson, B.R., May, D.E., Šimůnek, J., Hopmans, J.W., Hutmacher, R.B., 2009. Drip irrigation provides the salinity control needed for profitable irrigation of tomatoes in the San Joaquin Valley. California Agriculture J. 63, 131–136.

Hardie, M., Ridges, J., Swarts, N., Close, D., 2018. Drip irrigation wetting patterns and nitrate distribution: comparison between electrical resistivity (ERI), dye tracer, and 2D soil water modelling approaches. Irrigation Science 32, 97–110.

Hebei Jinshi Industrial Metal Co., 2020. Agriculture Vegetable Garden Drip Irrigation Belt Watering System Garden Drip Irrigation Tape [WWW Document]. URL https://ejinshi.en.made-in-china.com/product/fdmxUErHoGhY/China-Agriculture-Vegetable-Garden-Drip-Irrigation-Belt-Watering-System-Garden-Drip-Irrigation-Tape.html (accessed 9.6.17).

Hillel, D., 2004. Introduction to environmental soil physics, Academic Press.pp511.

Hydrus 2D/3D V 2.02.0680, 2012a. . PC-Progress, Prague Czech Republic.

ITCMI, I.T. des C.M. et I., 2018. Fiches techniques valorisées des cultures maraîchères et Industrielles

Kandelous, M.M., Šimůnek, J., 2010. Comparison of numerical, analytical, and empirical models to estimate wetting patterns for surface and subsurface drip irrigation. Irrigation Science J. 28, 435–444.

Kandelous, M.M., Šimůnek, J., van Genuchten, M.Th., Malek, K., 2011. Soil water content distributions between two emitters of a subsurface drip irrigation system. Soil Science Society of America Journal. 75, 488–497.

Keller, J., Karmeli, D., 1975. Trickle irrigation design, Rain Bird Sprink. Manif. Corp.pp133.

Keller, J., Bliesner, R., 1990. Sprinkle and trickle irrigation, Chapman and Hall. New York. pp739.

Khan, A.A., Yitayew, M., Warrick, A.W., 1996. Field evaluation of water and solute distribution from a point source. Irrigation and Drainage Engineering J. 22, 221–227.

Kosugi, K., 1999. General Model for Unsaturated Hydraulic Conductivityfor Soils with Lognormal Pore-Size Distribution. Soil Science Society of America Journal J 63, 270–277.

Lamm, F.R., Ayars, J.E., Nakayama, F.S., 2007. Microirrigation for Crop Production,Design, Operation, and Management, Elsevier publication. pp608

Lazarovitch, N., Šimůnek, J., Shani, U., 2005. System dependent boundary condition for water flow from subsurface source. Soil Science Society of America Journal 69, 46–50.

Lazarovitch, N., Warrick, A.W., Furman, A., Šimůnek, J., 2007. Subsurface water distribution from drip irrigation described by moment analyses. Vadose Zone J. 6, 116–123.

Li, J., Zhang, J., Ren, L., 2003. Water and nitrogen distribution as affected by fertigation of ammonium nitrate from a point source. Irrigation. Science J. 22, 12–30.

MADR, M. de l'Agriculture et du D.R., 2019. Evolution des superficies irriguées 2000 à 2018. Rapport interne.

Mmolawa, K., Or, D., 2000. Water and Solute Dynamics under a Drip-Irrigated Crop: Experiments and Analytical Model, Transactions of the ASAE 43(6) 1597–1608.

Monteith, J.L., 1965. Evaporation and the Environment. 19th Symp. Soc. Exp. Biol. 19, 205–234.

Mostaghimi, S., Mitchel, J.K., Lembke, W.D., 1981. Effect of discharge rate on distribution of moisture in heavy soils irrigated from a trickle source. Soil Science Society of America Journal. 81, 975–980.

Mualem, Y., 1976. A new model for predicting the hydraulic conductivity of unsaturated porous media. Water Resour J.12, 513–522.

Office International de l'Eau, (OIE), 2009. Les modes de tarification et de distribution de l'eau pour l'agriculture dans le bassin mediterraneen.

Omuto, C.T., 2007. HydroMe: Estimation of Soil Hydraulic Parameters from Experimental Data. Netw. USA.618-623

Omuto, C.T., 2009. Biexponential Model for Water Retention Characteristics. Geoderma 149, 235–242.

Panigrahi, P., Sharma, R.K., 2016. Using HYDRUS-2D model for simulating soil water dynamics in drip-irrigated citrus. Agricultural Engineering, 59–68.

Phene, C.J., Davis, K.R., Hutmacher, R.B., McCormick, R.L., 1987. Advantage of subsurface drip irrigation for processing tomatoes. Acta Horticulturae J. 200, 101–113.

Philip, J.R., 1968. Steady infiltration from buried point sources and spherical cavities. Water Resour. Res. 4, 1039–1047.

Philip, J.R., 1984. Travel-times from buried and surface infiltration point sources. Water Resources Research J. 20, 990–994.

Phogat, V., Mahadevan, M., Skewes, M., Cox, J.W., 2011. Modelling soil water and salt dynamics under pulsed and continuous surface drip irrigation of almond and implications of system design. Irrigation Science. 30, 315–333.

Phogat, V., Skewes, M.A., Mahadevan, M., Cox, J.W., 2013. Evaluation of soil plant system response to pulsed drip irrigation of an almond tree under sustained stress conditions. Agric. Water Management. 118, 200–2011.

Piegorsch, W.W., Bailer, A.J., 2005. Analyzing Environmental Data, John Wiley and Sons. pp496

Provenzano, G., 2007. Using HYDRUS-2D simulation model to evaluate wetted soil volume in subsurface drip irrigation systems. J Irrigation and Drain Engineering 342–349.

Rao, V.P., Suneetha, K.B., Hemalatha, S., 2010. Irrigation water management, Department of Agronomy, College of Agriculture. Rajendranagar, Hyderabad.pp148

Rasheed, Z.K., 2020. Analysis the wetted area for subsurface drip irrigation in different soils texture. Iraqi Journal of Agricultural Science, 51, 712–722.

Reinders, F.B., 2007. Micro-irrigation: world overview on technology, 7th international micro-irrigation congress in Kuala Lumpur Malaysia.

Rezayati, S., Khaledian, M., Razavipour, T., Rezaei, M., 2020. Water flow and nitrate transfer simulations in rice cultivation under different irrigation and nitrogen fertilizer application managements by HYDRUS-2D model. Irrigation Science J. 38, 353–363.

Richards, L.A., 1931. Capillary conduction of liquids in porous mediums. Physics 1, 318–333.

Rieul, L., Ruelle, P., 2003. Irrigation - guide pratique, 3eme édition. Cemagref.pp344

Russo, D., Zaideland, J., Laufer, A., 1998. Numerical analysis of flow and transport in a three dimensional partially saturated heterogeneous soil. Water Resources Research J .34, 1451–1468.

Samadianfard, S., Sadraddini, A.A., Nazemi, A.H., Provenzano, G., Kisi, Ö., 2012. Estimating soil wetting patterns for drip irrigation using genetic programming. Spanish Journal of Agricultural Research. 1155–1166.

Saskia, van der K., Zwarteveen, M., Boesveld, H., Kuper, M., 2013. The efficiency of drip irrigation unpacked. agricultural water management J. 123, 103–110.

Schaap, M.G., Leij, F.J., van Genuchten, M.T., 2001. ROSETTA: a computer program for estimating soil hydraulic parameters with hierarchical pedotransfer functions. Journal of Hydrology. 251, 163–176.

Schmitz, G.H., Schutze, N., Petersohn, U., 2002. New strategy for optimizing water application under trickle irrigation. J. Irrigation and Drainage Engineering. ASCE 128, 287–297.

Šimůnek, J., Šejna, M., van Genuchten, M.Th., 1996. The HYDRUS-2D software package for simulating water flow and solute transport in two dimensional variably saturated media, Int. Ground Water Modeling Ctr. ed, Version 1.0. IGWMC-TPS-53. Colorado School of Mines, Golden.pp167

Šimůnek, J., Sejna, M., van Genuchten, MT., 1999. The HYDRUS-2D software package for simulating two-dimensional movement of water, in variably saturated media, version 2.0. Rep. IGCWMC-TPS-53, Int. Ground Water Model. Cent., Colo. Sch. of Mines, Golden, CO, pp. 251.

Šimůnek, J., van Genuchten, M.Th., Šejna, M., 2006. The HYDRUS software package for simulating two- and three-dimensional movement of water, heat, and multiple solutes in variably-saturated media: Technical manual. Version 1.0., PC-Progress. ed. Prague, Czech Republic.pp161

Šimůnek, J., Van Genuchten, M.T., Sejna, M., 2011. The HYDRUS software package for simulating two- and three-dimensional movement of water, heat, and multiple solutes in variably saturated media, technical manual, version 2.0, PC progress, Prague, Czech Republic, pp 258.

Skaggs, T.H., Trout, T.J., Rothfuss, Y., 2010. Drip Irrigation Water Distribution Patterns: Effects of emitter rate, pulsing, and antecedent water. Soil Science Society of America Journal. 74, 1886–1896.

Skaggs, T.H., Trout, T.J., Šimůnek, J., Shouse, P.J., 2004. Comparison of HYDRUS-2D simulations of drip irrigation with experimental observations. J of Irrigation and Drainage Engineering .130, 304–310.

Tani, M., 1982. The Properties of Water-Table Rise Produced by a One-Dimensional, Vertical, Unsaturated Flow. J.of the Japanese Forestry Society. 64, 409–418.

USDA, U.S.D. of A., 2020. Guide to Texture by Feel [WWW Document]. URL https://grupochamartin.com/en/news/advantages-underground-drip-irrigation/# (accessed 9.6.17).

van Genuchten M. Th. 1987. A numerical model for water and solute movement in and below the root zone. Research Report No 121, U.S. Salinity Laboratory, USDA, ARS, Riverside, CA. In: The HYDRUS software package for simulating two- and three-dimensional movement of water, heat, and multiple solutes in variably-saturated media. 2006. Šimůnek J., van Genuchten, M. Th, Šejna M. (eds). Technical manual. Version 1.0. PC-Progress, Prague, Czech Republic: 7-13

van Genuchten, M.T., 1980. A closed-form equation for predicting the hydraulic conductivity of unsaturated soils. Soil Science Society of America Journal . 44 892–898.

van Genuchten, M.Th., Leij, F.J., Yates, S.R., 1991. The RETC code for quantifying the hydraulic functions of unsaturated soils. (No. EPA/600/2-91/065. R. S.). Kerr Environmental Research Laboratory, U. S. Environmental Protection Agency, Ada, OK.85p

Vermeiren, L., Jobling, G.A., 1984. Localized irrigation (No. 36). FAO Irrigation and Drainage, FAO-UN, Rome, Italy.

Wallach, D., 2006. Working with dynamic crop models - evaluation, analysis, parameterization and applications. Elsevier B.V.pp462

Wang, J., Li, J., Guan, H., 2017. Evaluation of drip irrigation system uniformity on cotton yield in an arid region using a two-dimensional soil water transport and crop growth coupling model. Irrigation and Drainage J. 66, 351–364.

Warrick, A.W., 1974. Time-dependent linearized infiltration: I. Point sources. Soil Science Society of America Journal. 38, 383–386.

Wooding, R.A., 1968. Steady infiltration from a shallow circular pond. Water Resource. Res. 4, 1259–1273.

Ya-dan, D., Hong-xia, C., Shi-quan, L., Xiao-bo, G., Yu-xin, C., 2017. Response of yield, quality, water and nitrogen use efficiency of tomato to different levels of water and nitrogen under drip irrigation in Northwestern China. Journal of Integrative Agriculture. 16, 1153–1161.

Zhou, Q., Kang, S., Zhang, L., Li, F., 2007. Comparison of APRI and Hydrus-2D models to simulate soil water dynamics in a vineyard under alternate partial root zone drip irrigation. Plant Soil 291, 211–223.

THE APPENDIX

APPENDIX 1

Food and Agriculture Organization of the United Nations

AQUASTAT

Algeria

	2013-2017
Irrigation potential *(1000 ha)*	1 300 *(2015)*
Area equipped for full control irrigation: surface irrigation *(1000 ha)*	596 *(2017)*
Area equipped for full control irrigation: sprinkler irrigation *(1000 ha)*	409 *(2017)*
Area equipped for full control irrigation: localized irrigation *(1000 ha)*	307 *(2017)*
Area equipped for full control irrigation: total *(1000 ha)*	1 312 *(2017)*
Area equipped for irrigation: total *(1000 ha)*	1 312 *(2017)*
% of the cultivated area equipped for irrigation *(%)*	15.59K *(2017)*
% of irrigation potential equipped for irrigation *(%)*	100.9 *(2017)*
Total agricultural water managed area *(1000 ha)*	1 312 *(2017)*
% of agricultural water managed area equipped for irrigation *(%)*	100 *(2017)*

REPUBLIQUE ALGERIENNE DEMOCRATIQUE ET POPULAIRE

MINISTERE DE L'AGRICULTURE, DU DEVELOPPEMENT RURAL ET DE LA PECHE

Direction du Développement Agricole dans les Zones Arides et Semi-Arides

EVOLUTION DES SUPERFICIES IRRIGUEES de 2000 à 2018

Campagne agricoles	Superficie irriguée totale (ha)	Système d'irrigation (ha)				Estimation des consommations en eau (m^3)
		Gravitaire	Aspersion	Goutte à Goutte	Total équipé	
2000/2001	**350 000**	275 000	70 000	5 000	**75 000**	2 100 000 000
2001/2002	**617 427**	449 421	111 978	56 028	**168 006**	3 704 562 000
2002/2003	**644 978**	453 531	127 570	63 877	**191 447**	3 869 868 000
2003/2004	**722 320**	485 019	138 301	99 000	**237 301**	4 333 920 000
2004/2005	**793 334**	518 108	150 739	124 487	**275 226**	4 760 004 000
2005/2006	**825 206**	520 503	153 006	151 697	**304 703**	4 951 236 000
2006/2007	**835 590**	515 046	162 056	158 488	**320 544**	5 013 540 000
2007/2008	**905 293**	512 496	204 859	187 938	**392 797**	5 431 758 000
2008/2009	**906 174**	513 012	205 026	188 136	**393 162**	5 437 044 000
2009/2010	**972 862**	540 604	230 924	201 334	**432 258**	5 837 172 000
2010/2011	**981 736**	545 698	233 854	202 184	**436 038**	5 890 416 000
2011/2012	**1 004 530**	556 149	241 980	206 401	**448 381**	6 027 180 000
2012/2013	**1 053 523**	578 846	263 148	211 529	**474 677**	6 321 138 000
2013/2014	**1 136 259**	617 754	284 321	234 184	**518 505**	6 817 554 000
2014/2015	**1 215 261**	620 950	344 726	249 585	**594 311**	7 291 566 000
2015/2016	**1 260 508**	621 457	388 081	250 970	**639 051**	7 563 048 000
2016/2017	**1 301 231**	622 057	418 473	260 701	**679 174**	7 807 386 000
2017/2018	**1 330 670**	573 175	444 706	312 788	**757 494**	7 984 020 000

REPUBLIQUE ALGERIENNE DEMOCRATIQUE ET POPULAIRE
MINISTERE DE L'AGRICULTURE, DU DEVELOPPEMENT RURAL ET DE LA PECHE

BILAN FINAL - EXTENSION DES SUPERFICIES IRRIGUEES 2018

L'examen des bilans transmis par les wilayas au 30 septembre 2018, fait ressortir la situation ci-après :

Wilaya	Gravitaire	Aspersion	Goutte à goutte	Total équipé	Sup irriguée totale àsept 2018
1 Adrar	15 626	8 687	12 257	20 944	36 570
2 Chlef	9 347	9 532	4 500	14 032	23 379
3 Laghouat	21 106	9 656	6 267	15 923	37 029
4 O.E.Bouaghi	6 255	16 057	438	16 495	22 750
5 Batna	39 311	16 684	3 870	20 554	59 865
6 Bejaia	7 650	895	1 715	2 610	10 260
7 Biskra	58 017	1 154	52 249	53 403	111 420
8 Béchar	11 290	712	10 310	11 022	22 312
9 Blida	24 700	3 563	4 017	7 580	32 280
10 Bouira	4 801	9 861	1 586	11 447	16 248
11 Tamanrasset	11 161	744	3 743	4 487	15 648
12 Tébessa	11 401	12 806	3 922	16 728	28 129
13 Tlemcen	11 313	11 912	6 380	18 292	29 605
14 Tiaret	7 091	24 172	4 237	28 409	35 500
15 Tizi-Ouzou	4 335	6 177	551	6 728	11 063
16 Alger	11 961	2 713	6 086	8 799	20 760
17 Djelfa	5 959	23 323	14 483	37 806	43 765
18 Jijel	5 351	232	1 995	2 227	7 578
19 Sétif	17 607	26 844	2 508	29 352	46 959
20 Saida	7 774	16 532	6 045	22 577	30 351
21 Skikda	15 487	5 549	1 505	7 054	22 541
22 S.B.Abbes	3 013	3 983	2 270	6 253	9 266
23 Annaba	3 677	3 141	880	4 021	7 698
24 Guelma	2 837	6 461	2 411	8 872	11 709
25 Constantine	786	2 412	627	3 039	3 825
26 Médéa	5 352	5 734	2 091	7 825	13 177
27 Mostaganem	11 600	11 742	23 050	34 792	46 392
28 M'Sila	27 052	7 834	6 201	14 035	41 087
29 Mascara	16 950	27 100	6 700	33 800	50 750
30 Ouargla	31 841	4 194	3 956	8 150	39 991
31 Oran	5 263	558	3 917	4 475	9 738
32 El-Bayadh	6 843	6 075	4 622	10 697	17 540
33 Illizi	1 448	19	611	630	2 078
34 B.B.Arreridj	6 660	918	560	1 478	8 138
35 Boumerdès	12 688	5 871	4 287	10 158	22 846
36 El-Tarf	4 622	6 107	3 084	9 191	13 813
37 Tindouf	91	20	686	706	797
38 Tissemsilt	4 672	2 469	431	2 900	7 572
39 El-Oued	27 187	40 350	35 463	75 813	103 000
40 Khenchela	42 412	8 604	7 925	16 529	58 941
41 Souk-Ahras	3 063	3 010	1 274	4 284	7 347
42 Tipaza	5 001	5 432	14 942	20 374	25 375
43 Mila	1 459	11 161	69	11 230	12 689
44 Ain-Defla	5 964	44 264	8 772	53 036	59 000
45 Naâma	5 334	7 633	5 849	13 482	18 816
46 A.Temouchent	2 123	3 771	3 599	7 370	9 493
47 Ghardaïa	11 991	10 602	12 972	23 574	35 565
48 Relizane	15 703	7 436	6 875	14 311	30 014
Total National	**573 175**	**444 706**	**312 788**	**757 494**	**1 330 669**

Crop water requirements under drip irrigation

Daily needs

$$B_{jl} = B_j(0.10 + CS) \qquad [1.1]$$

B_{jl}: Daily needs of localized irrigation (mm/day)

B_j: the daily needs of culture (mm)

CS: Soil cover (%).

Net dose

$$D_{net} = (H_{fc} - H_{pf}) \times Y' \times Z \times P\% \qquad [1.2]$$

D_{net}: net dose (mm)

H_{fc}: Humidity at the field capacity (%).

H_{pw}: Moisture at the point of wilting (%).

Y': Degree of allowable drying (%).

Z: Root depth (mm)

P: Percentage of humidified soil (%).

Raw dose:

$$D_{Raw} = \frac{D_{net}}{\eta \times Cu} \qquad [1.3]$$

With :

D_{Raw}: Raw dose (mm)

η:Irrigation yield (%)

Cu: Coefficient of uniformity of irrigation (%)

The frequency of irrigation :

$$F = \frac{D_{Raw}}{B_{jl}} \qquad [1.4]$$

With :

F: frequency of irrigation (day).

D_{Raw}: Raw dose (mm)

B_{jl}: Daily needs of localized irrigation (mm/day)

Required irrigation duration

$$T = \frac{D_{Raw} \times P \times E_g \times E_r}{Q_d} \qquad [1.5]$$

With :

T': required irrigation duration (min)

D_{Raw}: Raw dose (mm)

P: Percentage of humidified soil (%).

Eg: distance between drip lines (m)

E_r : emitter spacing (m)

Q_d : Emitter discharge rate (L/h)

APPENDIX 2

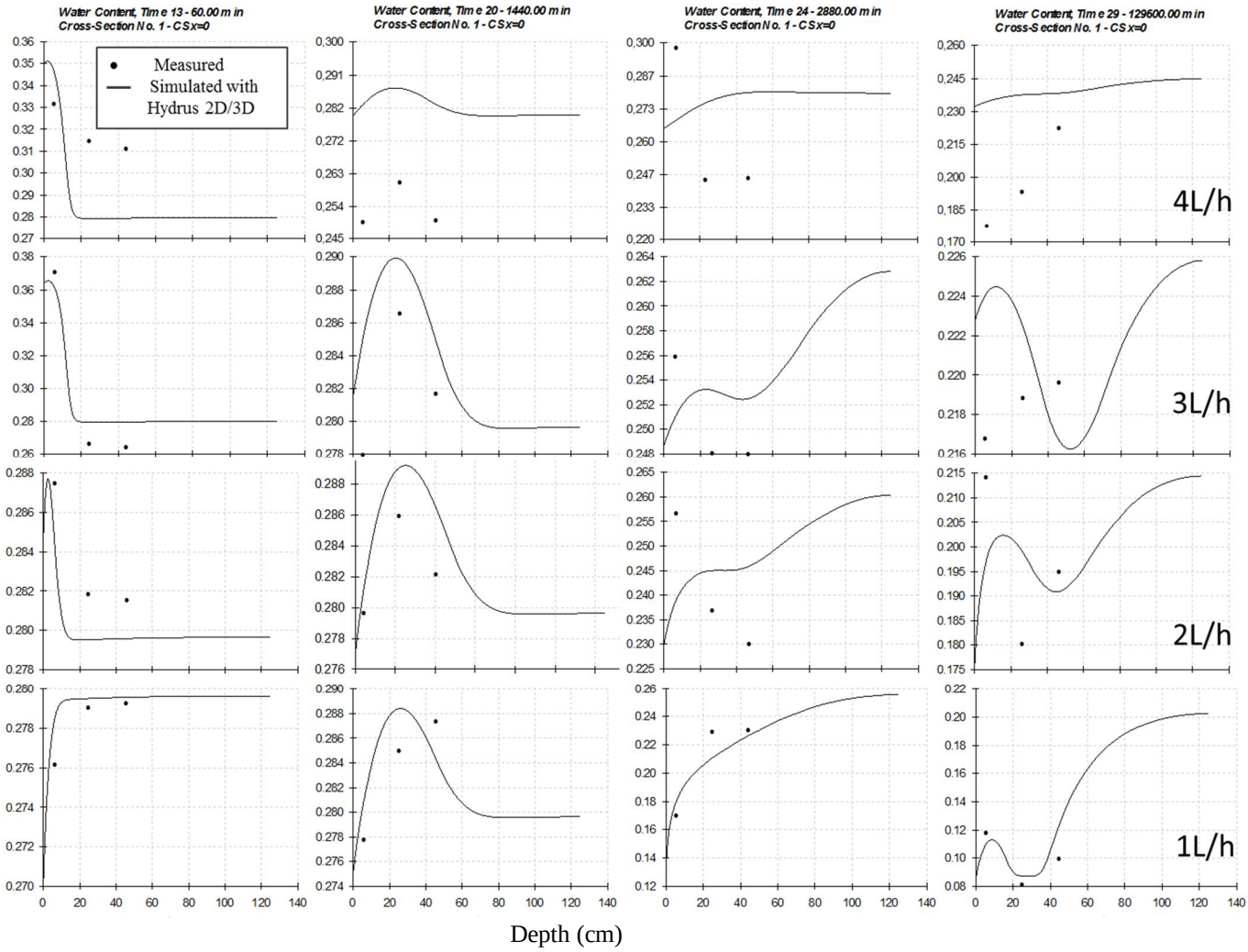

Fig. 01 vertical Measured and calculated soil volumetric water content (VWC) values at the half distance between two dripper: at:60 min ,24 hours, 20 days and 90 days of irrigation for different discharge rate .

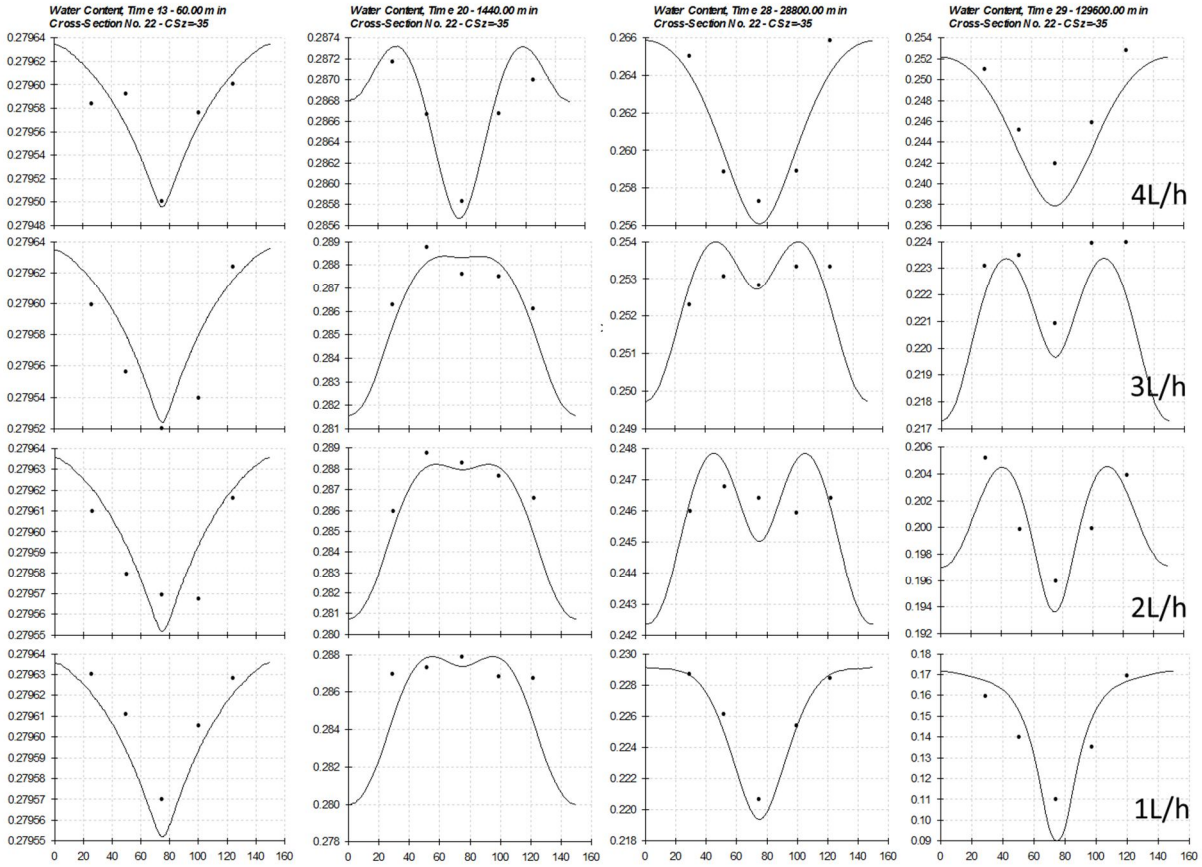

Fig.2 : Lateral Measured and calculated soil volumetric water content (VWC) values at 35 cm depth : 60 min ,24 hours, 20 days and9 0 days of irrigation for different discharge rate.

APPENDIX 3

Table 3.1: Summary of simulated treatments

Nbre of treatment	distance between emitters (cm)	emitter's discharge (L h^{-1})	frequency (day)	duration (min)	Inverted calculations					Final corrected flux and area								
					Discharge (cm h^{-1})	Emitter's area	runoff area	Total flux area	Flux (cm min^{-1})	Emitter's area	runoff area	Total area of flux	Max. Allow. Flux (cm min^{-1})	Emitter's runoff length (b)	Rounded length bank(b)	runoff area	Total area of flux	Flux (cm min^{-1})
F30-1-1	30	1	1	150	3333,3	471,24	0	471,24	-0,1179	471,2	2392	2864	-0,01940	11,96	12	2400	2871	-0,0193
F30-1-2	30	1	2	150	3333,3	471,24	0	471,24	-0,1179	471,2	2392	2864	-0,01940	11,96	12	2400	2871	-0,0193
F30-1-3	30	1	3	150	3333,3	471,24	0	471,24	-0,1179	471,2	2392	2864	-0,01940	11,96	12	2400	2871	-0,0193
F30-1-4	30	1	4	150	3333,3	471,24	0	471,24	-0,1179	471,2	2392	2864	-0,01940	11,96	12	2400	2871	-0,0193
F30-1-5	30	1	5	150	3333,3	471,24	0	471,24	-0,1179	471,2	2392	2864	-0,01940	11,96	12	2400	2871	-0,0193
F30-1-6	30	1	6	150	3333,3	471,24	0	471,24	-0,1179	471,2	2392	2864	-0,01940	11,96	12	2400	2871	-0,0193
F30-1-7	30	1	7	150	3333,3	471,24	0	471,24	-0,1179	471,2	2392	2864	-0,01940	11,96	12	2400	2871	-0,0193
F30-2-1	30	2	1	75	6666,7	471,24	0	471,24	-0,2358	471,2	5256	5727	-0,01940	26,28	27	5300	5771	-0,0193
F30-2-2	30	2	2	75	6666,7	471,24	0	471,24	-0,2358	471,2	5256	5727	-0,01940	26,28	27	5300	5771	-0,0193
F30-2-3	30	2	3	75	6666,7	471,24	0	471,24	-0,2358	471,2	5256	5727	-0,01940	26,28	27	5300	5771	-0,0193
F30-2-4	30	2	4	75	6666,7	471,24	0	471,24	-0,2358	471,2	5256	5727	-0,01940	26,28	27	5300	5771	-0,0193
F30-2-5	30	2	5	75	6666,7	471,24	0	471,24	-0,2358	471,2	5256	5727	-0,01940	26,28	27	5300	5771	-0,0193

Nbre of treatment	distance between emitters (cm)	emitter's discharge (L h^{-1})	frequency (day)	duration (min)	Inverted calculations					Final corrected flux and area								
					Discharge (cm h^{-1})	Emitter's area	runoff area	Total flux area	Flux (cm min^{-1})	Emitter's area	runoff area	Total area of flux	Max. Allow. Flux (cm min^{-1})	Emitter's runoff length (b)	**Rounded length bank(b)**	runoff area	Total area of flux	**Flux (cm min^{-1})**
F30-2-6	30	2	6	75	6666,7	471,24	0	471,24	-0,2358	471	5256	5727	-0,0194	26,28	27	5300	5771	-0,0193
F30-2-7	30	2	7	75	6666,7	471,24	0	471,24	-0,2358	471	5256	5727	-0,0194	26,28	27	5300	5771	-0,0193
F30-3-1	30	3	1	50	10000,0	471,24	0	471,24	-0,3537	471	8120	8591	-0,0194	40,60	41	8200	8671	-0,0192
F30-3-2	30	3	2	50	10000,0	471,24	0	471,24	-0,3537	471	8120	8591	-0,0194	40,60	41	8200	8671	-0,0192
F30-3-3	30	3	3	50	10000,0	471,24	0	471,24	-0,3537	471	8120	8591	-0,0194	40,60	41	8200	8671	-0,0192
F30-3-4	30	3	4	50	10000,0	471,24	0	471,24	-0,3537	471	8120	8591	-0,0194	40,60	41	8200	8671	-0,0192
F30-3-5	30	3	5	50	10000,0	471,24	0	471,24	-0,3537	471	8120	8591	-0,0194	40,60	41	8200	8671	-0,0192
F30-3-6	30	3	6	50	10000,0	471,24	0	471,24	-0,3537	471	8120	8591	-0,0194	40,60	41	8200	8671	-0,0192
F30-3-7	30	3	7	50	10000,0	471,24	0	471,24	-0,3537	471	8120	8591	-0,0194	40,60	41	8200	8671	-0,0192
F30-4-1	30	4	1	40	13333,3	471,24	0	471,24	-0,4716	471	10984	11455	-0,0194	54,92	55	11000	11471	-0,0194
F30-4-2	30	4	2	40	13333,3	471,24	0	471,24	-0,4716	471	10984	11455	-0,0194	54,92	55	11000	11471	-0,0194
F30-4-3	30	4	3	40	13333,3	471,24	0	471,24	-0,4716	471	10984	11455	-0,0194	54,92	55	11000	11471	-0,0194
F30-4-4	30	4	4	40	13333,3	471,24	0	471,24	-0,4716	471	10984	11455	-0,0194	54,92	55	11000	11471	-0,0194
F30-4-5	30	4	5	40	13333,3	471,24	0	471,24	-0,4716	471	10984	11455	-0,0194	54,92	55	11000	11471	-0,0194

Nbre of treatment	distance between emitters (cm)	emitter's discharge (L h^{-1})	frequency (day)	duration (min)	Inverted calculations					Final corrected flux and area								
					Discharge (cm h^{-1})	Emitter's area	runoff area	Total flux area	Flux (cm min^{-1})	Emitter's area	runoff area	Total area of flux	Max. Allow. Flux (cm min^{-1})	Emitter's runoff length (b)	**Rounded length bank(b)**	runoff area	Total area of flux	**Flux (cm min^{-1})**
F30-4-6	30	4	6	40	13333,3	471,24	0	471,24	-0,4716	471,2	10984	11455	-0,01940	54,92	55	11000	11471	-0,0194
F30-4-7	30	4	7	40	13333,3	471,24	0	471,24	-0,4716	471,2	10984	11455	-0,01940	54,92	55	11000	11471	-0,0194
F30-6-1	30	6	1	25	20000,0	471,24	0	471,24	-0,7074	471,2	16711	17182	-0,01940	83,55	84	16800	17271	-0,0193
F30-6-2	30	6	2	25	20000,0	471,24	0	471,24	-0,7074	471,2	16711	17182	-0,01940	83,55	84	16800	17271	-0,0193
F30-6-3	30	6	3	25	20000,0	471,24	0	471,24	-0,7074	471,2	16711	17182	-0,01940	83,55	84	16800	17271	-0,0193
F30-6-4	30	6	4	25	20000,0	471,24	0	471,24	-0,7074	471,2	16711	17182	-0,01940	83,55	84	16800	17271	-0,0193
F30-6-5	30	6	5	25	20000,0	471,24	0	471,24	-0,7074	471,2	16711	17182	-0,01940	83,55	84	16800	17271	-0,0193
F30-6-6	30	6	6	25	20000,0	471,24	0	471,24	-0,7074	471,2	16711	17182	-0,01940	83,55	84	16800	17271	-0,0193
F30-6-7	30	6	7	25	20000	471,24	0	471,24	-0,7074	471,2	16711	17182	-0,01940	83,55	84	16800	17271	-0,0193
F30-8-1	30	8	1	20	26667	471,24	0	471,24	-0,9431	471,2	22438	22910	-0,01940	112,19	113	22500	22971	-0,0193
F30-8-2	30	8	2	20	26667	471,24	0	471,24	-0,9431	471,2	22438	22910	-0,01940	112,19	113	22500	22971	-0,0193
F30-8-3	30	8	3	20	26667	471,24	0	471,24	-0,9431	471,2	22438	22910	-0,01940	112,19	113	22500	22971	-0,0193
F30-8-4	30	8	4	20	26667	471,24	0	471,24	-0,9431	471,2	22438	22910	-0,01940	112,19	113	22500	22971	-0,0193
F30-8-5	30	8	5	20	26667	471,24	0	471,24	-0,9431	471,2	22438	22910	-0,01940	112,19	113	22500	22971	-0,0193

Nbre of treatment	distance between emitters (cm)	emitter's discharge (L h^{-1})	frequency (day)	duration (min)	Inverted calculations					Final corrected flux and area								
					Discharge (cm h^{-1})	Emitter's area	runoff area	Total flux area	Flux (cm min^{-1})	Emitter's area	runoff area	Total area of flux	Max. Allow. Flux (cm min^{-1})	Emitter's runoff length (b)	Rounded length bank(b)	runoff area	Total area of flux	Flux (cm min^{-1})
F30-8-6	30	8	6	20	26667	471,24	0	471,24	-0,9431	471,2	22438	22910	-0,01940	112,19	113	22500	22971	-0,0193
F30-8-7	30	8	7	20	26667	471,24	0	471,24	-0,9431	471,2	22438	22910	-0,01940	112,19	113	22500	22971	-0,0193
F50-1-1	50	1	1	150	2000	471,24	0	471,24	-0,0707	471,2	1247	1718	-0,01940	6,23	6,5	1300	1771	-0,0188
F50-1-2	50	1	2	150	2000	471,24	0	471,24	-0,0707	471,2	1247	1718	-0,01940	6,23	6,5	1300	1771	-0,0188
F50-1-3	**50**	**1**	**3**	**150**	2000	471,24	0	471,24	-0,0707	471,2	1247	1718	-0,01940	6,23	6,5	1300	1771	-0,0188
F50-1-4	50	1	4	150	2000	471,24	0	471,24	-0,0707	471,2	1247	1718	-0,01940	6,23	6,5	1300	1771	-0,0188
F50-1-5	50	1	5	150	2000	471,24	0	471,24	-0,0707	471,2	1247	1718	-0,01940	6,23	6,5	1300	1771	-0,0188
F50-1-6	50	1	6	150	2000	471,24	0	471,24	-0,0707	471,2	1247	1718	-0,01940	6,23	6,5	1300	1771	-0,0188
F50-1-7	50	1	7	150	2000	471,24	0	471,24	-0,0707	471,2	1247	1718	-0,01940	6,23	6,5	1300	1771	-0,0188
F50-2-1	50	2	1	75	4000	471,24	0	471,24	-0,1415	471,2	2965	3436	-0,01940	14,83	15	3000	3471	-0,0192
F50-2-2	50	2	2	75	4000	471,24	0	471,24	-0,1415	471,2	2965	3436	-0,01940	14,83	15	3000	3471	-0,0192
F50-2-3	**50**	**2**	**3**	**75**	4000	471,24	0	471,24	-0,1415	471,2	2965	3436	-0,01940	14,83	15	3000	3471	-0,0192
F50-2-4	50	2	4	75	4000	471,24	0	471,24	-0,1415	471,2	2965	3436	-0,01940	14,83	15	3000	3471	-0,0192
F50-2-5	50	2	5	75	4000	471,24	0	471,24	-0,1415	471,2	2965	3436	-0,01940	14,83	15	3000	3471	-0,0192

Nbre of treatment	distance between emitters (cm)	emitter's discharge (L h^{-1})	frequency (day)	duration (min)	Inverted calculations					Final corrected flux and area								
					Discharge (cm h^{-1})	Emitter's area	runoff area	Total flux area	Flux (cm min^{-1})	Emitter's area	runoff area	Total area of flux	Max. Allow. Flux (cm min^{-1})	Emitter's runoff length (b)	**Rounded length bank(b)**	runoff area	Total area of flux	**Flux (cm min^{-1})**
F50-2-6	50	2	6	75	4000	471,24	0	471,24	-0,1415	471,2	2965	3436	-0,01940	14,83	15	3000	3471	-0,0192
F50-2-7	50	2	7	75	4000	471,24	0	471,24	-0,1415	471,2	2965	3436	-0,01940	14,83	15	3000	3471	-0,0192
F50-3-1	50	3	1	50	6000	471,24	0	471,24	-0,2122	471,2	4683	5155	-0,01940	23,42	24	4700	5171	-0,0193
F50-3-2	50	3	2	50	6000	471,24	0	471,24	-0,2122	471,2	4683	5155	-0,01940	23,42	24	4700	5171	-0,0193
F50-3-3	**50**	**3**	**3**	50	6000	471,24	0	471,24	-0,2122	471,2	4683	5155	-0,01940	23,42	24	4700	5171	-0,0193
F50-3-4	50	3	4	50	6000	471,24	0	471,24	-0,2122	471,2	4683	5155	-0,01940	23,42	24	4700	5171	-0,0193
F50-3-5	50	3	5	50	6000	471,24	0	471,24	-0,2122	471,2	4683	5155	-0,01940	23,42	24	4700	5171	-0,0193
F50-3-6	50	3	6	50	6000	471,24	0	471,24	-0,2122	471,2	4683	5155	-0,01940	23,42	24	4700	5171	-0,0193
F50-3-7	50	3	7	50	6000	471,24	0	471,24	-0,2122	471,2	4683	5155	-0,01940	23,42	24	4700	5171	-0,0193
F50-4-1	50	4	1	40	8000	471,24	0	471,24	-0,2829	471,2	6402	6873	-0,01940	32,01	33	6500	6971	-0,0191
F50-4-2	50	4	2	40	8000	471,24	0	471,24	-0,2829	471,2	6402	6873	-0,01940	32,01	33	6500	6971	-0,0191
F50-4-3	**50**	**4**	**3**	40	8000	471,24	0	471,24	-0,2829	471,2	6402	6873	-0,01940	32,01	33	6500	6971	-0,0191
F50-4-4	50	4	4	40	8000	471,24	0	471,24	-0,2829	471,2	6402	6873	-0,01940	32,01	33	6500	6971	-0,0191
F50-4-5	50	4	5	40	8000	471,24	0	471,24	-0,2829	471,2	6402	6873	-0,01940	32,01	33	6500	6971	-0,0191

Nbre of treatment	distance between emitters (cm)	emitter's discharge (L h^{-1})	frequency (day)	duration (min)	Inverted calculations					Final corrected flux and area								
					Discharge (cm h^{-1})	Emitter's area	runoff area	Total flux area	Flux (cm min^{-1})	Emitter's area	runoff area	Total area of flux	Max. Allow. Flux (cm min^{-1})	Emitter's runoff length (b)	**Rounded length bank(b)**	runoff area	Total area of flux	**Flux (cm min^{-1})**
F50-4-6	50	4	6	40	8000	471,24	0	471,24	-0,2829	471,2	6402	6873	-0,01940	32,01	33	6500	6971	-0,0191
F50-4-7	50	4	7	40	8000	471,24	0	471,24	-0,2829	471,2	6402	6873	-0,01940	32,01	33	6500	6971	-0,0191
F50-6-1	50	6	1	25	12000	471,24	0	471,24	-0,4244	471,2	9838	10309	-0,01940	49,19	50	9900	10371	-0,0193
F50-6-2	50	6	2	25	12000	471,24	0	471,24	-0,4244	471,2	9838	10309	-0,01940	49,19	50	9900	10371	-0,0193
F50-6-3	50	6	3	25	12000	471,24	0	471,24	-0,4244	471,2	9838	10309	-0,01940	49,19	50	9900	10371	-0,0193
F50-6-4	50	6	4	25	12000	471,24	0	471,24	-0,4244	471,2	9838	10309	-0,01940	49,19	50	9900	10371	-0,0193
F50-6-5	50	6	5	25	12000	471,24	0	471,24	-0,4244	471,2	9838	10309	-0,01940	49,19	50	9900	10371	-0,0193
F50-6-6	50	6	6	25	12000	471,24	0	471,24	-0,4244	471,2	9838	10309	-0,01940	49,19	50	9900	10371	-0,0193
F50-6-7	50	6	7	25	12000	471,24	0	471,24	-0,4244	471,2	9838	10309	-0,01940	49,19	50	9900	10371	-0,0193
F50-8-1	50	8	1	20	16000	471,24	0	471,24	-0,5659	471,2	13274	13746	-0,01940	66,37	67	13300	13771	-0,0194
F50-8-2	50	8	2	20	16000	471,24	0	471,24	-0,5659	471,2	13274	13746	-0,01940	66,37	67	13300	13771	-0,0194
F50-8-3	50	8	3	20	16000	471,24	0	471,24	-0,5659	471,2	13274	13746	-0,01940	66,37	67	13300	13771	-0,0194
F50-8-4	50	8	4	20	16000	471,24	0	471,24	-0,5659	471,2	13274	13746	-0,01940	66,37	67	13300	13771	-0,0194
F50-8-5	50	8	5	20	16000	471,24	0	471,24	-0,5659	471,2	13274	13746	-0,01940	66,37	67	13300	13771	-0,0194

Nbre of treatment	distance between emitters (cm)	emitter's discharge (L h^{-1})	frequency (day)	duration (min)	Inverted calculations					Final corrected flux and area								
					Discharge (cm h^{-1})	Emitter's area	runoff area	Total flux area	Flux (cm min^{-1})	Emitter's area	runoff area	Total area of flux	Max. Allow. Flux (cm min^{-1})	Emitter's runoff length (b)	**Rounded length bank(b)**	runoff area	Total area of flux	**Flux (cm min^{-1})**
F50-8-6	50	8	6	20	16000	471,24	0	471,24	-0,5659	471,2	13274	13746	-0,01940	66,37	67	13300	13771	-0,0194
F50-8-7	50	8	7	20	16000	471,24	0	471,24	-0,5659	471,2	13274	13746	-0,01940	66,37	67	13300	13771	-0,0194
F70-1-1	70	1	1	150	1428,6	471,24	0	471,24	-0,0505	471,2	756	1227	-0,01940	3,78	4	800	1271	-0,0187
F70-1-2	70	1	2	150	1428,6	471,24	0	471,24	-0,0505	471,2	756	1227	-0,01940	3,78	4	800	1271	-0,0187
F70-1-3	70	1	3	150	1428,6	471,24	0	471,24	-0,0505	471,2	756	1227	-0,01940	3,78	4	800	1271	-0,0187
F70-1-4	70	1	4	150	1428,6	471,24	0	471,24	-0,0505	471,2	756	1227	-0,01940	3,78	4	800	1271	-0,0187
F70-1-5	70	1	5	150	1428,6	471,24	0	471,24	-0,0505	471,2	756	1227	-0,01940	3,78	4	800	1271	-0,0187
F70-1-6	70	1	6	150	1428,6	471,24	0	471,24	-0,0505	471,2	756	1227	-0,01940	3,78	4	800	1271	-0,0187
F70-1-7	70	1	7	150	1428,6	471,24	0	471,24	-0,0505	471,2	756	1227	-0,01940	3,78	4	800	1271	-0,0187
F70-2-1	70	2	1	75	2857,1	471,24	0	471,24	-0,1011	471,2	1983	2455	-0,01940	9,92	10	2000	2471	-0,0193
F70-2-2	70	2	2	75	2857,1	471,24	0	471,24	-0,1011	471,2	1983	2455	-0,01940	9,92	10	2000	2471	-0,0193
F70-2-3	70	2	3	75	2857,1	471,24	0	471,24	-0,1011	471,2	1983	2455	-0,01940	9,92	10	2000	2471	-0,0193
F70-2-4	70	2	4	75	2857,1	471,24	0	471,24	-0,1011	471,2	1983	2455	-0,01940	9,92	10	2000	2471	-0,0193
F70-2-5	70	2	5	75	2857,1	471,24	0	471,24	-0,1011	471,2	1983	2455	-0,01940	9,92	10	2000	2471	-0,0193

Nbre of treatment	distance between emitters (cm)	emitter's discharge (L h^{-1})	frequency (day)	duration (min)	Inverted calculations					**Final corrected flux and area**								
					Discharge (cm h^{-1})	Emitter's area	runoff area	Total flux area	Flux (cm min^{-1})	Emitter's area	runoff area	Total area of flux	Max. Allow. Flux (cm min^{-1})	Emitter's runoff length (b)	**Rounded length bank(b)**	runoff area	Total area of flux	**Flux (cm min^{-1})**
F70-2-6	70	2	6	75	2857,1	471,24	0	471,24	-0,1011	471,2	1983	2455	-0,01940	9,92	10	2000	2471	-0,0193
F70-2-7	70	2	7	75	2857,1	471,24	0	471,24	-0,1011	471,2	1983	2455	-0,01940	9,92	10	2000	2471	-0,0193
F70-3-1	70	3	1	50	4285,7	471,24	0	471,24	-0,1516	471,2	3211	3682	-0,01940	16,05	17	3300	3771	-0,0189
F70-3-2	70	3	2	50	4285,7	471,24	0	471,24	-0,1516	471,2	3211	3682	-0,01940	16,05	17	3300	3771	-0,0189
F70-3-3	70	3	3	50	4285,7	471,24	0	471,24	-0,1516	471,2	3211	3682	-0,01940	16,05	17	3300	3771	-0,0189
F70-3-4	70	3	4	50	4285,7	471,24	0	471,24	-0,1516	471,2	3211	3682	-0,01940	16,05	17	3300	3771	-0,0189
F70-3-5	70	3	5	50	4285,7	471,24	0	471,24	-0,1516	471,2	3211	3682	-0,01940	16,05	17	3300	3771	-0,0189
F70-3-6	70	3	6	50	4285,7	471,24	0	471,24	-0,1516	471,2	3211	3682	-0,01940	16,05	17	3300	3771	-0,0189
F70-3-7	70	3	7	50	4285,7	471,24	0	471,24	-0,1516	471,2	3211	3682	-0,01940	16,05	17	3300	3771	-0,0189
F70-4-1	70	4	1	40	5714,3	471,24	0	471,24	-0,2021	471,2	4438	4909	-0,01940	22,19	23	4500	4971	-0,0192
F70-4-2	70	4	2	40	5714,3	471,24	0	471,24	-0,2021	471,2	4438	4909	-0,01940	22,19	23	4500	4971	-0,0192
F70-4-3	70	4	3	40	5714,3	471,24	0	471,24	-0,2021	471,2	4438	4909	-0,01940	22,19	23	4500	4971	-0,0192
F70-4-4	70	4	4	40	5714,3	471,24	0	471,24	-0,2021	471,2	4438	4909	-0,01940	22,19	23	4500	4971	-0,0192
F70-4-5	70	4	5	40	5714,3	471,24	0	471,24	-0,2021	471,2	4438	4909	-0,01940	22,19	23	4500	4971	-0,0192

Nbre of treatment	distance between emitters (cm)	emitter's discharge (L h^{-1})	frequency (day)	duration (min)	Inverted calculations					**Final corrected flux and area**								
					Discharge (cm h^{-1})	Emitter's area	runoff area	Total flux area	Flux (cm min^{-1})	Emitter's area	runoff area	Total area of flux	Max. Allow. Flux (cm min^{-1})	Emitter's runoff length (b)	**Rounded length bank(b)**	runoff area	Total area of flux	**Flux (cm min^{-1})**
F70-4-6	70	4	6	40	5714,3	471,24	0	471,24	-0,2021	471,2	4438	4909	-0,01940	22,19	23	4500	4971	-0,0192
F70-4-7	70	4	7	40	5714,3	471,24	0	471,24	-0,2021	471,2	4438	4909	-0,01940	22,19	23	4500	4971	-0,0192
F70-6-1	70	6	1	25	8571,4	471,24	0	471,24	-0,3032	471,2	6893	7364	-0,01940	34,46	35	6900	7371	-0,0194
F70-6-2	70	6	2	25	8571,4	471,24	0	471,24	-0,3032	471,2	6893	7364	-0,01940	34,46	35	6900	7371	-0,0194
F70-6-3	70	6	3	25	8571,4	471,24	0	471,24	-0,3032	471,2	6893	7364	-0,01940	34,46	35	6900	7371	-0,0194
F70-6-4	70	6	4	25	8571,4	471,24	0	471,24	-0,3032	471,2	6893	7364	-0,01940	34,46	35	6900	7371	-0,0194
F70-6-5	70	6	5	25	8571,4	471,24	0	471,24	-0,3032	471,2	6893	7364	-0,01940	34,46	35	6900	7371	-0,0194
F70-6-6	70	6	6	25	8571,4	471,24	0	471,24	-0,3032	471,2	6893	7364	-0,01940	34,46	35	6900	7371	-0,0194
F70-6-7	70	6	7	25	8571,4	471,24	0	471,24	-0,3032	471,2	6893	7364	-0,01940	34,46	35	6900	7371	-0,0194
F70-8-1	70	8	1	20	11429	471,24	0	471,24	-0,4042	471,2	9347	9818	-0,01940	46,74	47	9400	9871	-0,0193
F70-8-2	70	8	2	20	11429	471,24	0	471,24	-0,4042	471,2	9347	9818	-0,01940	46,74	47	9400	9871	-0,0193
F70-8-3	70	8	3	20	11429	471,24	0	471,24	-0,4042	471,2	9347	9818	-0,01940	46,74	47	9400	9871	-0,0193
F70-8-4	70	8	4	20	11429	471,24	0	471,24	-0,4042	471,2	9347	9818	-0,01940	46,74	47	9400	9871	-0,0193
F70-8-5	70	8	5	20	11429	471,24	0	471,24	-0,4042	471,2	9347	9818	-0,01940	46,74	47	9400	9871	-0,0193

Nbre of treatment	distance between emitters (cm)	emitter's discharge (L h^{-1})	frequency (day)	duration (min)	Inverted calculations					Final corrected flux and area								
					Discharge (cm h^{-1})	Emitter's area	runoff area	Total flux area	Flux (cm min^{-1})	Emitter's area	runoff area	Total area of flux	Max. Allow. Flux (cm min^{-1})	Emitter's runoff length (b)	**Rounded length bank(b)**	runoff area	Total area of flux	**Flux (cm min^{-1})**
F70-8-6	70	8	6	20	11429	471,24	0	471,24	-0,4042	471,2	9347	9818	-0,01940	46,74	47	9400	9871	-0,0193
F70-8-7	70	8	7	20	11429	471,24	0	471,24	-0,4042	471,2	9347	9818	-0,01940	46,74	47	9400	9871	-0,0193

Table 3.2: The new value of flux after adaptation with the soil's infiltration

Proposed name	distance between emitters (cm)	emitter's discharge ($L\ h^{-1}$)	Emitter's runoff length (b) (cm)	runoff area	Total area of flux	Flux ($cm\ min^{-1}$)	test
F30-1-1	30	1	12	2400	2871	-0,0193	Ok
F30-1-2	30	1	12	2400	2871	-0,0193	Ok
F30-1-3	30	1	12	2400	2871	-0,0193	Ok
F30-1-4	30	1	12	2400	2871	-0,0193	Ok
F30-1-5	30	1	12	2400	2871	-0,0193	Ok
F30-1-6	30	1	12	2400	2871	-0,0193	Ok
F30-1-7	30	1	12	2400	2871	-0,0193	Ok
F30-2-1	30	2	27	5300	5771	-0,0193	No
F30-2-2	30	2	27	5300	5771	-0,0193	No
F30-2-3	30	2	27	5300	5771	-0,0193	No
F30-2-4	30	2	27	5300	5771	-0,0193	No
F30-2-5	30	2	27	5300	5771	-0,0193	No
F30-2-6	30	2	27	5300	5771	-0,0193	No
F30-2-7	30	2	27	5300	5771	-0,0193	No
F30-3-1	30	3	41	8200	8671	-0,0192	No
F30-3-2	30	3	41	8200	8671	-0,0192	No
F30-3-3	30	3	41	8200	8671	-0,0192	No
F30-3-4	30	3	41	8200	8671	-0,0192	No
F30-3-5	30	3	41	8200	8671	-0,0192	No
F30-3-6	30	3	41	8200	8671	-0,0192	No
F30-3-7	30	3	41	8200	8671	-0,0192	No

Proposed name	distance between emitters (cm)	emitter's discharge (L h^{-1})	Emitter's runoff length (b) (cm)	runoff area	Total area of flux	Flux (cm min^{-1})	test
F30-4-1	30	4	55	11000	11471	-0,0194	No
F30-4-2	30	4	55	11000	11471	-0,0194	No
F30-4-3	30	4	55	11000	11471	-0,0194	No
F30-4-4	30	4	55	11000	11471	-0,0194	No
F30-4-5	30	4	55	11000	11471	-0,0194	No
F30-4-6	30	4	55	11000	11471	-0,0194	No
F30-4-7	30	4	55	11000	11471	-0,0194	No
F30-6-1	30	6	84	16800	17271	-0,0193	No
F30-6-2	30	6	84	16800	17271	-0,0193	No
F30-6-3	30	6	84	16800	17271	-0,0193	No
F30-6-4	30	6	84	16800	17271	-0,0193	No
F30-6-5	30	6	84	16800	17271	-0,0193	No
F30-6-6	30	6	84	16800	17271	-0,0193	No
F30-6-7	30	6	84	16800	17271	-0,0193	No
F30-8-1	30	8	113	22500	22971	-0,0193	No
F30-8-2	30	8	113	22500	22971	-0,0193	No
F30-8-3	30	8	113	22500	22971	-0,0193	No
F30-8-4	30	8	113	22500	22971	-0,0193	No
F30-8-5	30	8	113	22500	22971	-0,0193	No
F30-8-6	30	8	113	22500	22971	-0,0193	No
F30-8-7	30	8	113	22500	22971	-0,0193	No
F50-1-1	50	1	6,5	1300	1771	-0,0188	Ok

Proposed name	distance between emitters (cm)	emitter's discharge (L h^{-1})	Emitter's runoff length (b) (cm)	runoff area	Total area of flux	Flux (cm min^{-1})	test
F50-1-2	50	1	6,5	1300	1771	-0,0188	Ok
F50-1-3	50	1	6,5	1300	1771	-0,0188	Ok
F50-1-4	50	1	6,5	1300	1771	-0,0188	Ok
F50-1-5	50	1	6,5	1300	1771	-0,0188	Ok
F50-1-6	50	1	6,5	1300	1771	-0,0188	Ok
F50-1-7	50	1	6,5	1300	1771	-0,0188	Ok
F50-2-1	50	2	15	3000	3471	-0,0192	Ok
F50-2-2	50	2	15	3000	3471	-0,0192	Ok
F50-2-3	50	2	15	3000	3471	-0,0192	Ok
F50-2-4	50	2	15	3000	3471	-0,0192	Ok
F50-2-5	50	2	15	3000	3471	-0,0192	Ok
F50-2-6	50	2	15	3000	3471	-0,0192	Ok
F50-2-7	50	2	15	3000	3471	-0,0192	Ok
F50-3-1	50	3	24	4700	5171	-0,0193	Ok
F50-3-2	50	3	24	4700	5171	-0,0193	Ok
F50-3-3	50	3	24	4700	5171	-0,0193	Ok
F50-3-4	50	3	24	4700	5171	-0,0193	Ok
F50-3-5	50	3	24	4700	5171	-0,0193	Ok
F50-3-6	50	3	24	4700	5171	-0,0193	Ok
F50-3-7	50	3	24	4700	5171	-0,0193	Ok
F50-4-1	50	4	33	6500	6971	-0,0191	Ok
F50-4-2	50	4	33	6500	6971	-0,0191	Ok

Proposed name	distance between emitters (cm)	emitter's discharge (L h^{-1})	Emitter's runoff length (b) (cm)	runoff area	Total area of flux	Flux (cm min^{-1})	test
F50-4-3	50	4	33	6500	6971	-0,0191	Ok
F50-4-4	50	4	33	6500	6971	-0,0191	Ok
F50-4-5	50	4	33	6500	6971	-0,0191	Ok
F50-4-6	50	4	33	6500	6971	-0,0191	Ok
F50-4-7	50	4	33	6500	6971	-0,0191	Ok
F50-6-1	50	6	50	9900	10371	-0,0193	No
F50-6-2	50	6	50	9900	10371	-0,0193	No
F50-6-3	50	6	50	9900	10371	-0,0193	No
F50-6-4	50	6	50	9900	10371	-0,0193	No
F50-6-5	50	6	50	9900	10371	-0,0193	No
F50-6-6	50	6	50	9900	10371	-0,0193	No
F50-6-7	50	6	50	9900	10371	-0,0193	No
F50-8-1	50	8	67	13300	13771	-0,0194	No
F50-8-2	50	8	67	13300	13771	-0,0194	No
F50-8-3	50	8	67	13300	13771	-0,0194	No
F50-8-4	50	8	67	13300	13771	-0,0194	No
F50-8-5	50	8	67	13300	13771	-0,0194	No
F50-8-6	50	8	67	13300	13771	-0,0194	No
F50-8-7	50	8	67	13300	13771	-0,0194	No
F70-1-1	70	1	4	800	1271	-0,0187	No
F70-1-2	70	1	4	800	1271	-0,0187	No
F70-1-3	70	1	4	800	1271	-0,0187	No

Proposed name	distance between emitters (cm)	emitter's discharge (L h^{-1})	Emitter's runoff length (b) (cm)	runoff area	Total area of flux	Flux (cm min^{-1})	test
F70-1-4	70	1	4	800	1271	-0,0187	No
F70-1-5	70	1	4	800	1271	-0,0187	No
F70-1-6	70	1	4	800	1271	-0,0187	No
F70-1-7	70	1	4	800	1271	-0,0187	No
F70-2-1	70	2	10	2000	2471	-0,0193	No
F70-2-2	70	2	10	2000	2471	-0,0193	No
F70-2-3	70	2	10	2000	2471	-0,0193	No
F70-2-4	70	2	10	2000	2471	-0,0193	No
F70-2-5	70	2	10	2000	2471	-0,0193	No
F70-2-6	70	2	10	2000	2471	-0,0193	No
F70-2-7	70	2	10	2000	2471	-0,0193	No
F70-3-1	70	3	17	3300	3771	-0,0189	No
F70-3-2	70	3	17	3300	3771	-0,0189	No
F70-3-3	70	3	17	3300	3771	-0,0189	No
F70-3-4	70	3	17	3300	3771	-0,0189	No
F70-3-5	70	3	17	3300	3771	-0,0189	No
F70-3-6	70	3	17	3300	3771	-0,0189	No
F70-3-7	70	3	17	3300	3771	-0,0189	No
F70-4-1	70	4	23	4500	4971	-0,0192	No
F70-4-2	70	4	23	4500	4971	-0,0192	No
F70-4-3	70	4	23	4500	4971	-0,0192	No
F70-4-4	70	4	23	4500	4971	-0,0192	No

Proposed name	distance between emitters (cm)	emitter's discharge (L h^{-1})	Emitter's runoff length (b) (cm)	runoff area	Total area of flux	Flux (cm min^{-1})	test
F70-4-5	70	4	23	4500	4971	-0,0192	No
F70-4-6	70	4	23	4500	4971	-0,0192	No
F70-4-7	70	4	23	4500	4971	-0,0192	No
F70-6-1	70	6	35	6900	7371	-0,0194	No
F70-6-2	70	6	35	6900	7371	-0,0194	No
F70-6-3	70	6	35	6900	7371	-0,0194	No
F70-6-4	70	6	35	6900	7371	-0,0194	No
F70-6-5	70	6	35	6900	7371	-0,0194	No
F70-6-6	70	6	35	6900	7371	-0,0194	No
F70-6-7	70	6	35	6900	7371	-0,0194	No
F70-8-1	70	8	47	9400	9871	-0,0193	No
F70-8-2	70	8	47	9400	9871	-0,0193	No
F70-8-3	70	8	47	9400	9871	-0,0193	No
F70-8-4	70	8	47	9400	9871	-0,0193	No
F70-8-5	70	8	47	9400	9871	-0,0193	No
F70-8-6	70	8	47	9400	9871	-0,0193	No
F70-8-7	70	8	47	9400	9871	-0,0193	No

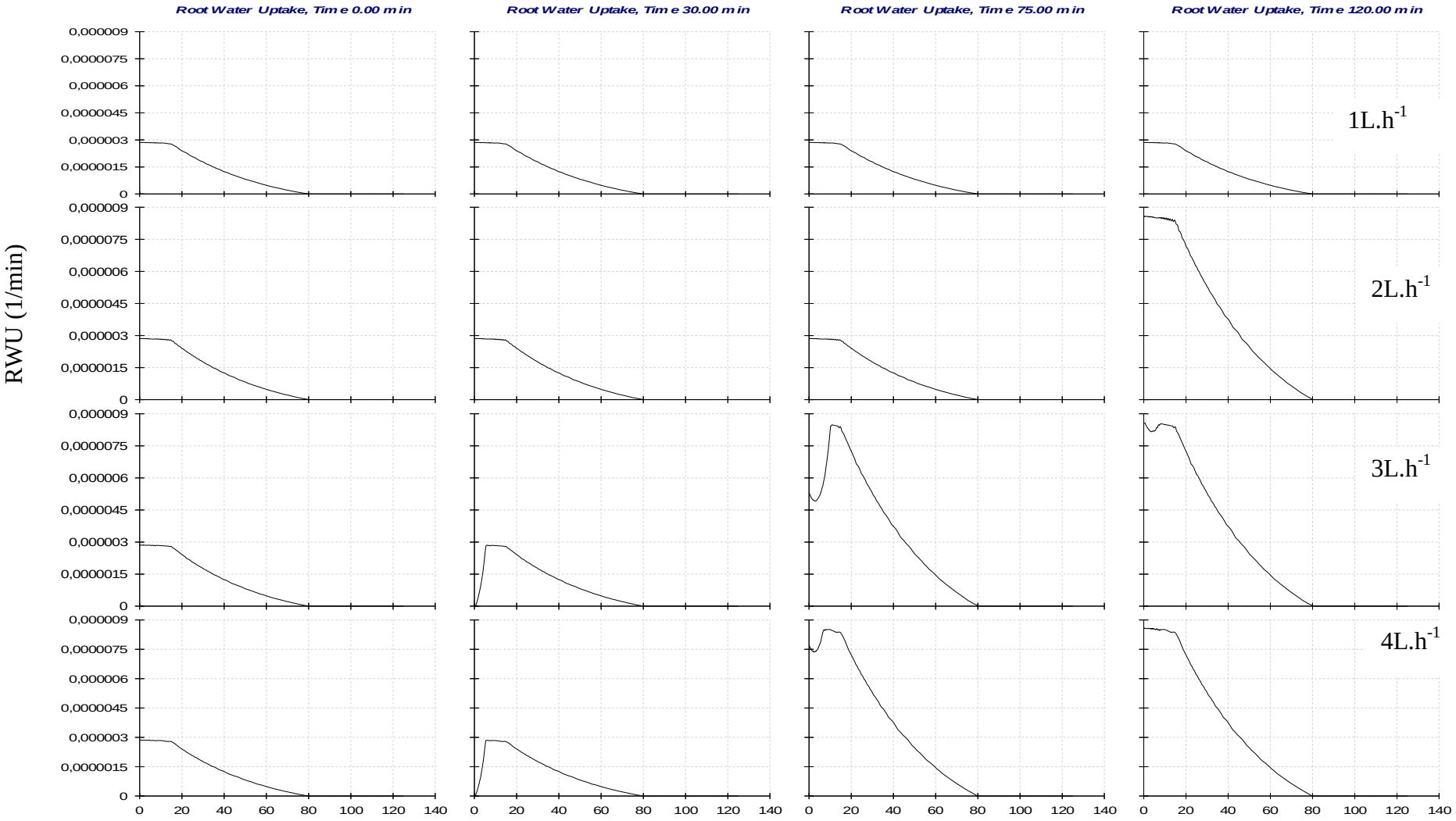
Root Water Uptake, Time 0.00 min
Root Water Uptake, Time 30.00 min
Root Water Uptake, Time 75.00 min
Root Water Uptake, Time 120.00 min
RWU (1/min)
0,000009
0,0000075
0,000006
0,0000045
0,000003
0,0000015
0
1L.h-1
2L.h-1
3L.h-1
4L.h-1
0 20 40 60 80 100 120 140
Length (cm)

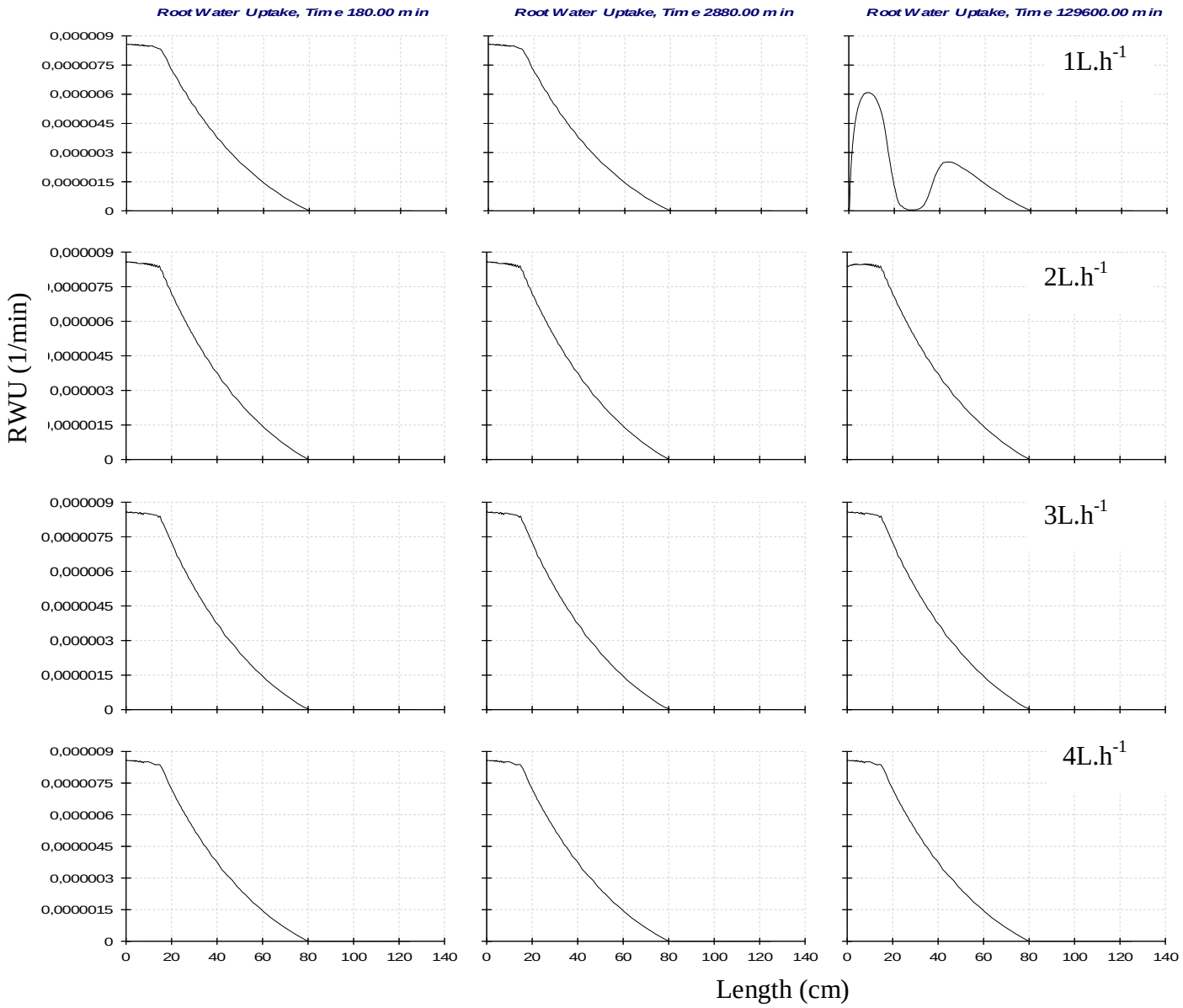

Fig..3.1 : Simulated root water uptake in the half distance from emitter at different times and different discharge during the experimental period.

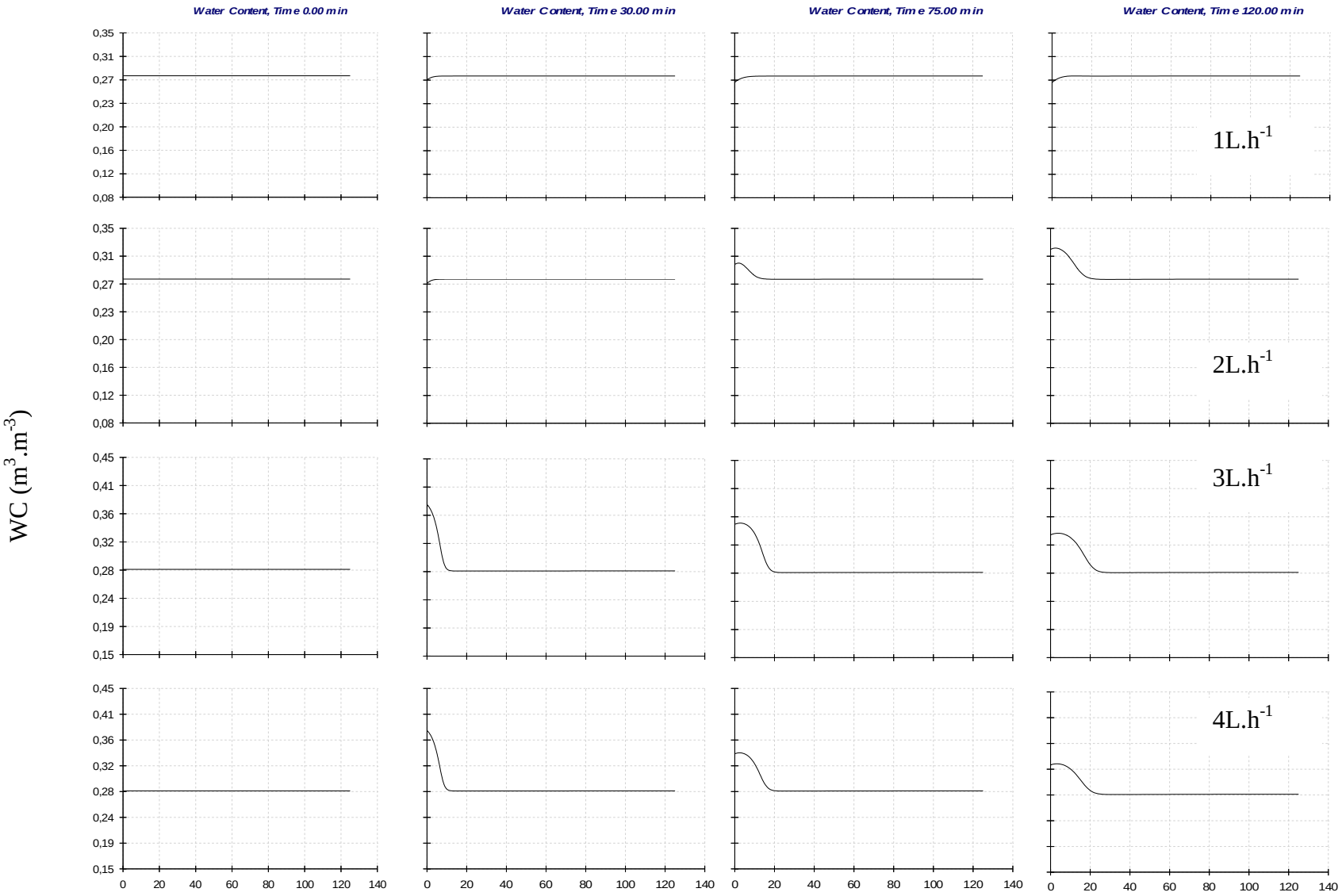
Water Content, Time 0.00 min
Water Content, Time 30.00 min
Water Content, Time 75.00 min
Water Content, Time 120.00 min
1L.h-1
2L.h-1
3L.h-1
4L.h-1
WC (m3.m-3)
Length (cm)

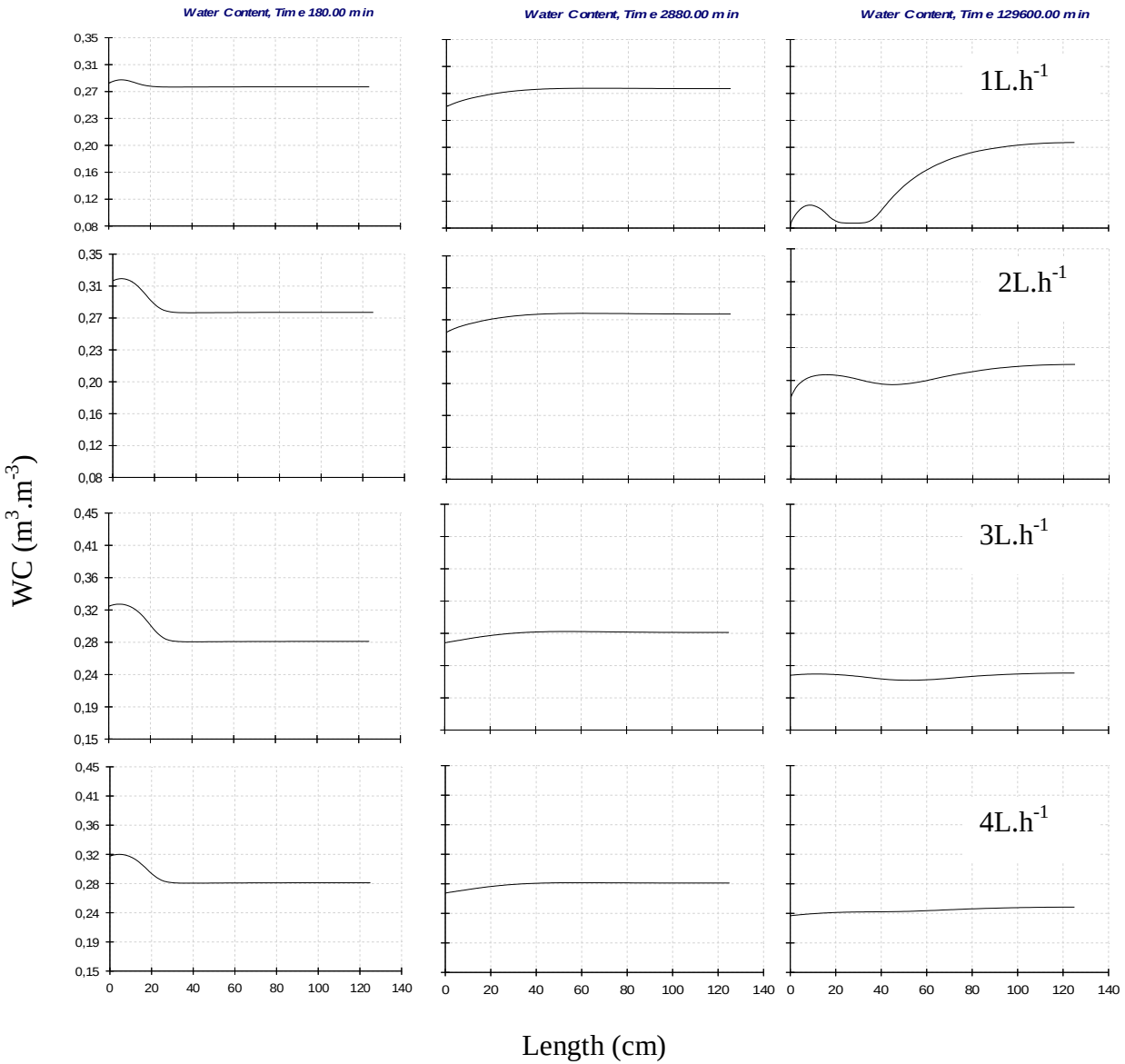

Fig.3.2: Simulated water content in the half distance from emitter at different times and different discharge during the experimental period.

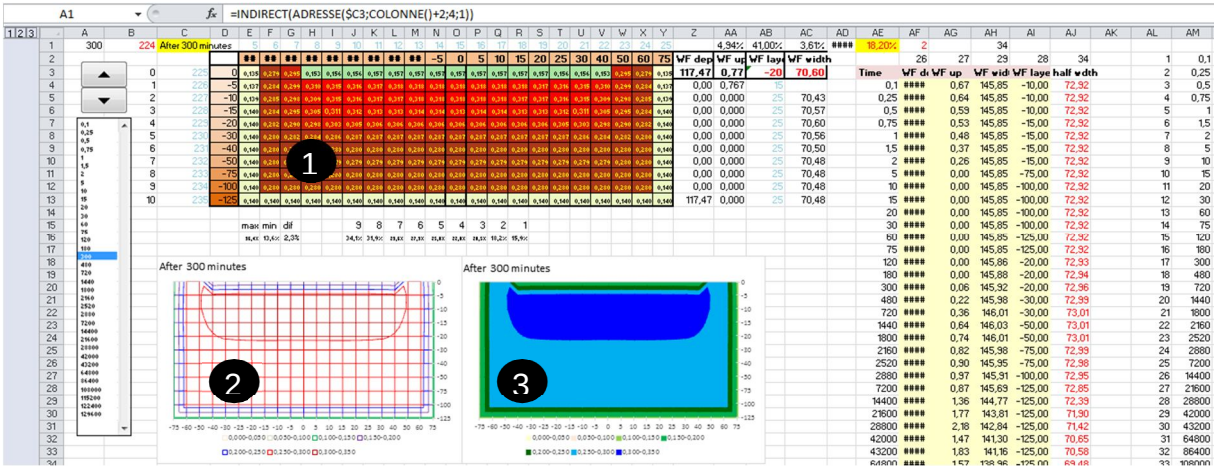

	-75	-60	-50	-40	-30	-25	-20	-15	-10	-5	0	5	10	15	20	25	30	40	50	60	75
0	0,135	0,279	0,295	0,153	0,156	0,156	0,157	0,157	0,157	0,157	0,157	0,157	0,157	0,157	0,157	0,156	0,156	0,153	0,295	0,279	0,135
-5	0,137	0,284	0,299	0,310	0,315	0,316	0,317	0,318	0,318	0,318	0,318	0,318	0,318	0,318	0,317	0,316	0,315	0,310	0,299	0,284	0,137
-10	0,139	0,285	0,298	0,309	0,315	0,316	0,317	0,317	0,318	0,318	0,318	0,318	0,318	0,317	0,317	0,316	0,315	0,309	0,298	0,285	0,139
-15	0,140	0,284	0,295	0,305	0,311	0,312	0,313	0,313	0,314	0,314	0,313	0,314	0,314	0,313	0,313	0,312	0,311	0,305	0,295	0,284	0,140
-20	0,140	0,282	0,290	0,298	0,303	0,305	0,306	0,306	0,306	0,306	0,306	0,306	0,306	0,306	0,306	0,305	0,303	0,298	0,290	0,282	0,140
-30	0,140	0,280	0,282	0,284	0,286	0,287	0,287	0,287	0,287	0,287	0,287	0,287	0,287	0,287	0,287	0,287	0,286	0,284	0,282	0,280	0,140
-40	0,140	0,280	0,280	0,280	0,280	0,280	0,280	0,280	0,280	0,280	0,280	0,280	0,280	0,280	0,280	0,280	0,280	0,280	0,280	0,280	0,140
-50	0,140	0,280	0,280	0,279	0,279	0,279	0,279	0,279	0,279	0,279	0,279	0,279	0,279	0,279	0,279	0,279	0,279	0,279	0,280	0,280	0,140
-75	0,140	0,280	0,280	0,280	0,280	0,280	0,280	0,280	0,280	0,280	0,280	0,280	0,280	0,280	0,280	0,280	0,280	0,280	0,280	0,280	0,140
-100	0,140	0,280	0,280	0,280	0,280	0,280	0,280	0,280	0,280	0,280	0,280	0,280	0,280	0,280	0,280	0,280	0,280	0,280	0,280	0,280	0,140
-125	0,140	0,140	0,140	0,140	0,140	0,140	0,140	0,140	0,140	0,140	0,140	0,140	0,140	0,140	0,140	0,140	0,140	0,140	0,140	0,140	0,140

1 Datasheet view of the full pattern each cell shows the moisture content of a node.

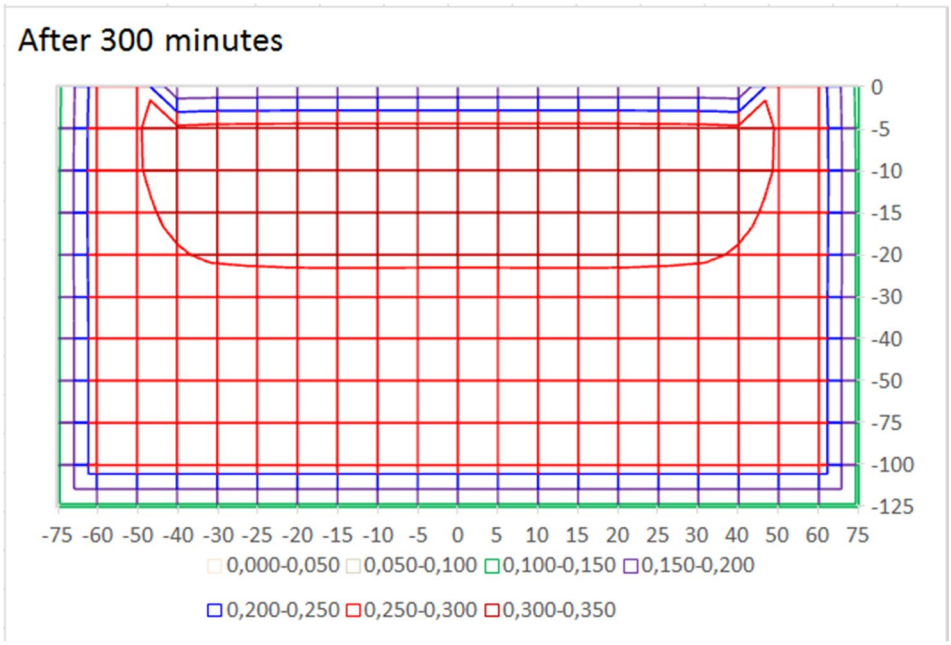

2 Wetting front advance step by 3l/h emitter after 300 minutes

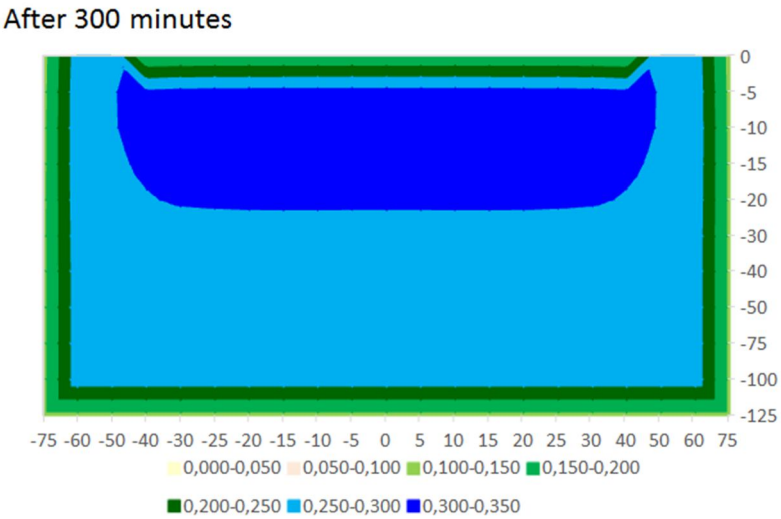

3 simple 2D view shows the wetting pattern, and drippers locations.

Fig 3. 3 Summary of output, as exported by the model.

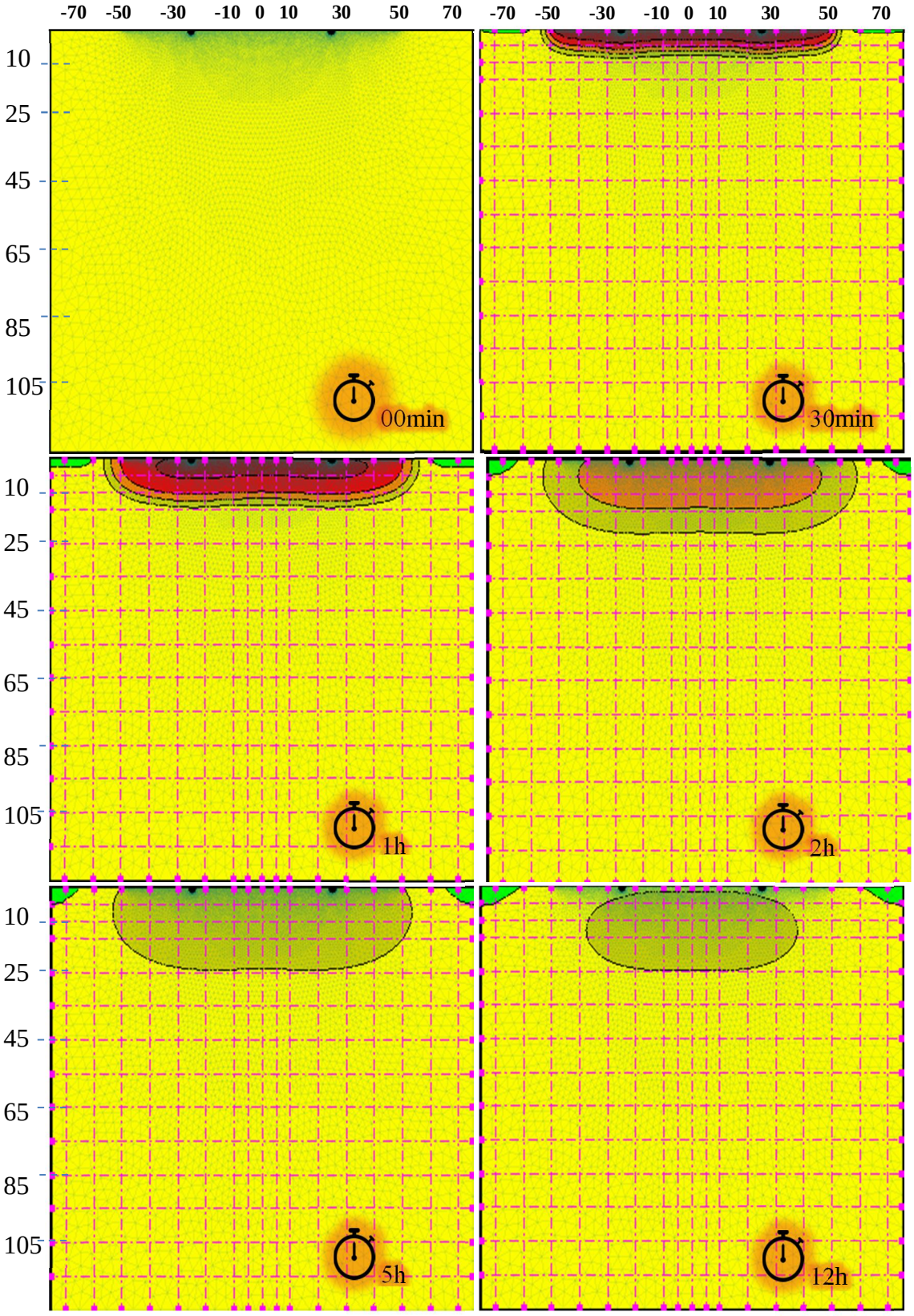
-70 -50 -30 -10 0 10 30 50 70
10
25
45
65
85
105
00min
30min
1h
2h
5h
12h

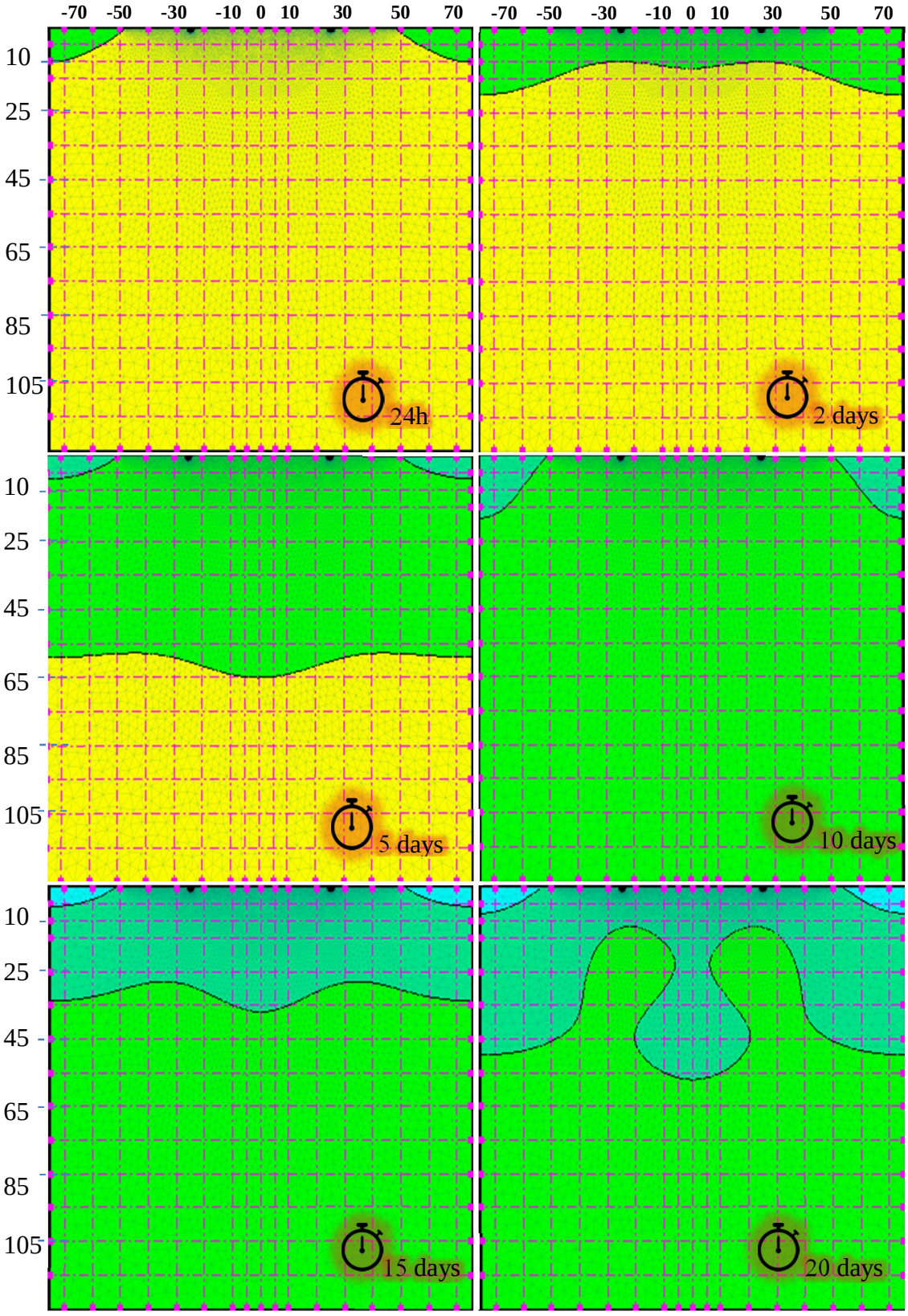
-70 -50 -30 -10 0 10 30 50 70
10
25
45
65
85
105
24h
2 days
5 days
10 days
15 days
20 days

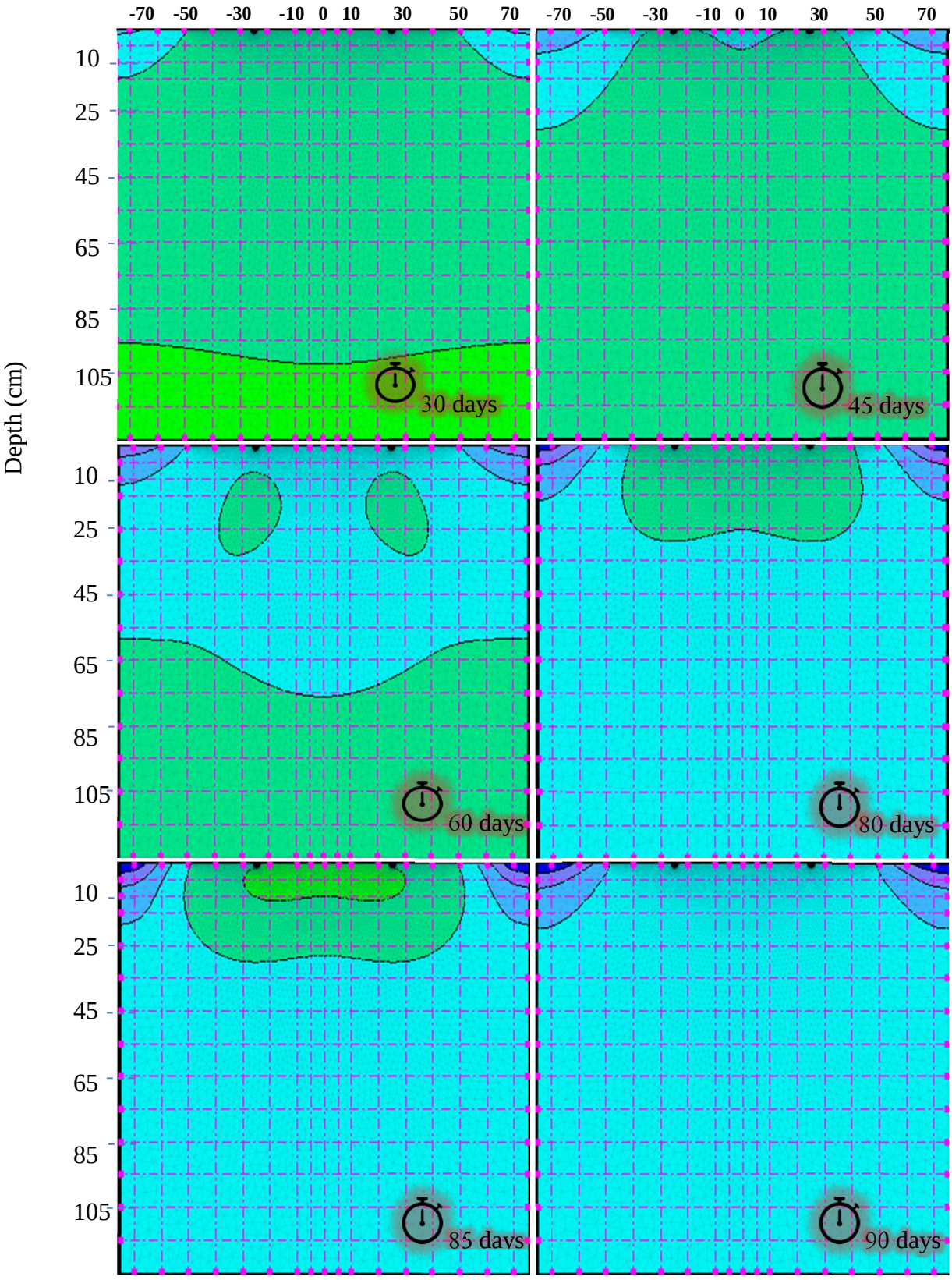

Fig 3.4 : Wet bulbs in two dimensions at different time for flow rate of $3Lh^{-1}$